DEMOCRATIC AND POPULAR REPUBLIC OF ALGERIA
MINISTRY OF HIGHER EDUCATION AND SCIENTIFIC RESEARCH
UNIVERSITY ABOU-BEKR BELKAID – TLEMCEN

LMD THESIS

Presented to :

FACULTY OF SCIENCES – DEPARTMENT OF MATHEMATICS

To obtain the

3rd cycle doctorate diploma

Speciality:*Applied Mathematics to Biology*

By:

Hammoum Amina

On the theme

Mathematical models in ecology: case of density-dependent mortality rates

---

Publicly defended on 04/12/2023 to the jury composed of :

Mr Bouguima Sidi-Mohammed	Professor	University of Tlemcen	Chairman
Mr Yadi Karim	Professor	University of Tlemcen	Supervisor
Mr Sari Tewfik	Professor	University of Montpellier, INRAE, Institut Agro, Montpellier, France	Co-supervisor
Mrs Abdellatif Nahla	Professor	ENSI- University of Manouba, Tunisia	Examiner
Mr Beroual Nabil	Lecturer A	University of Sétif	Examiner
Mr Moussaoui Ali	Professor	University of Tlemcen	Examiner

Dynamical Systems and Applications Laboratory

BP 119, 13000 Tlemcen - Algeria

Dedication

I dedicate this work to :

The memory of my father.

My dear mother.

My siblings Soumia, Meriem and Younes.

Acknowledgements

First of all, I would like to thank *Allah* for his greatness and for giving me the strength and courage to complete this thesis.

I would like to express my deepest gratitude to my supervisors for all their help and advice. I am very grateful to them for their support and their great contribution. I thank **Mr. Tewfik Sari** for his patience and invaluable guidance, which helped me to achieve the most important results of this thesis. I have benefited greatly from his wealth of knowledge and meticulous editing.
Words cannot express my gratitude to **Mr. Karim Yadi** for his motivation and immense knowledge. I have been extremely lucky to have a supervisor who cared so much about my work and who listened to my ideas and suggestions during all these years.

Thanks should also go to all members of my thesis committee : **Mr. Sidi Mohammed Bouguima** for agreeing to be the president of the jury, **Mrs. Nahla Abdellatif**, **Mr. Ali Moussaoui** and **Mr. Nabil Beroual**, for their agreeing to be the referees of this work.

I am also thankful to all my teachers of the Department of Mathematics at Tlemcen University.

Contents

Introduction 1

1 Some concepts of ecology 4
- 1.1 Some definitions . . . 4
- 1.2 Types of interaction . . . 5
  - 1.2.1 Some interspecific interaction examples . . . 5
  - 1.2.2 Some intraspecific interaction examples . . . 8

2 General modified Gause type model 11
- 2.1 About the growth rate function . . . 12
- 2.2 About the functional response . . . 13
- 2.3 Classical results . . . 17
- 2.4 Specific case (Rosenzweig-MacArthur model) . . . 18

3 Gause type model with variable disappearance rate 20
- 3.1 Hsu disappearance rate . . . 20
- 3.2 Bazykin's disappearance rate . . . 21
- 3.3 CF disappearance rate . . . 21
- 3.4 VT disappearance rate . . . 22
- 3.5 General variable disappearance rate . . . 23
  - 3.5.1 Positivity and boundedness . . . 24
  - 3.5.2 Existence and stability of equilibria . . . 24
  - 3.5.3 Poincaré-Andronov-Hopf bifurcation . . . 29
  - 3.5.4 Global asymptotic stability . . . 33
  - 3.5.5 Non-existence of limit cycles . . . 35

4 Applications from the ecological literature 37
- 4.1 Gause/RMA model . . . 40
  - 4.1.1 PAH bifurcation . . . 41
  - 4.1.2 Numerical simulations . . . 41
- 4.2 Hsu model . . . 43
  - 4.2.1 PAH bifurcation . . . 43

4.2.2 Numerical simulations . . . 45
4.3 Bazykin model . . . 47
4.3.1 PAH bifurcation . . . 47
4.3.2 Numerical simulations . . . 49
4.4 Cavani-Farkas (CF) model . . . 55
4.4.1 PAH bifurcation . . . 55
4.4.2 Numerical simulations . . . 57
4.5 Variable-Territory (VT) model . . . 62
4.5.1 PAH bifurcation . . . 62
4.5.2 Numerical simulations . . . 64

5 Further developments and remarks **69**
5.1 Singularly perturbed case . . . 69
5.1.1 Example of a slow-fast VT model . . . 73
5.1.2 Comparison with other models . . . 76
5.2 About the enrichment paradox . . . 78

Conclusion **84**

A Preliminary concepts from dynamical systems theory **85**
A.1 Some Definitions . . . 85
A.2 Lyapunov stability . . . 87
A.3 Classification of equilibria . . . 88
A.4 Two-dimensional system . . . 88
A.5 Bifurcation theory . . . 89
A.5.1 Types of bifurcations . . . 89
A.5.2 Some Local bifurcations of codimension-1 . . . 90
A.5.3 Some Global bifurcations of codimension-1 . . . 90

B Singular perturbation theory **91**

Bibliography **93**

Introduction

Individuals in non-isolated populations are considered always in interactions with each other. Ecology is the science that allows a better understanding of these interactions and the effect of the different environmental conditions (climatic variations, availability of resources, presence of enemies, ...) on the dynamics of each species. However, this purpose remains difficult to be realized in view of the complexity of the natural systems. Furthermore, the large time scale of some population dynamics and the differences in size between species can make many interesting experiments and conclusions difficult to be achieved. Mathematical modelling of population dynamics provides a better understanding of certain biological phenomena and behaviours in an ecosystem. It represents an important tool for interpreting different interactions. In particular, predation is one of the most important interactions in ecology. The first model describing the predator-prey interactions (consumer-resource relationship) is referred to Lotka and Volterra [42, 67]. It is the simplest and the easiest model to evaluate this relationship. The model is described by a system of two coupled ordinary differential equations, each equation represents the growth of one population. In this model, the so-called growth function of the prey and the functional response of the predator are both linear. Various biological and mathematical criticisms have motivated researchers to modify this model. Including additional factors and relationships can make the model more realistic, such as having a nonlinear functional response and growth function. For Gause [18], the purpose of having a nonlinear functional response is to obtain a saturation effect of predation when prey is abundant. Such a function is called prey-dependent functional response [4] since it depends only on the density of the prey. Holling [27] suggested three different functions of this type. A model with this function is called Gause model [17]. Similarly, incorporating a nonlinear growth function in Loteka-Voltera model is to avoid the non-boundedness of prey population growth in the absence of predators and to make a limited capacity of the prey. A model with the nonlinear functional response of predator and a growth function of prey is called the general Gause model or Gause-type model. Several propositions have been made to improve the prey-dependent functional response, for example by introducing a mutual interference with preda-

tors and making the functional response depend on both prey and predator densities. Such a function is called predator-dependent functional response. Arditi and Ginzuburg [3] proposed a more suitable general model with a functional response that depends on the ratio of prey to predator abundance. Other predator-dependent functional responses of this type have been introduced in [7, 13, 25]. On the other hand, all these models involve in their equations a constant mortality rate of the predator. In addition to the previous modifications that concerned only the growth function and the functional response, one can think about making the mortality rate non-constant. The experiments of Minter et al [46] on *ciliates Didinium nasutum* (the predator) show that their mortality rate decreases with increasing abundance of the prey (*ciliates Paramecium caudatum*) and a mathematical model has been proposed. Mathematically, the dependence of the mortality rate of the predator on the prey density has been considered before in Gause type model by Hsu [29]. The mortality rate can depend only on the predator density as indicated for instance in the rodent-vegetation model [64] where regulation of the number of herbivores by intraspecific mechanisms is considered. In the last reference, it is shown that the mortality rate can depend also on both densities by considering that the carrying capacity of the herbivores can be directly proportional to food availability. Note that the same consideration was introduced by Leslie [35, 36] for another type of Lotka Volterra modification. All these examples show that the consideration of a non-constant mortality rate can also undergo complex dynamic behaviour.

We present in this dissertation, with appropriate assumptions, a general Gause-type model with variable disappearance (mortality) rate of predators that contains also the natural mortality. Two important results are given: firstly, we determine a graphical criterion for the stability of positive hyperbolic equilibria that is an extension of the well-known *Rosenzweig–MacArthur graphical criterion* for the case of a constant predator mortality rate. The change in the stability of equilibria signifies the appearance of different types of bifurcations, in particular, the Poincaré-Andronov-Hopf bifurcation. Secondly, we give the formula of the first Lyapunov coefficient to determine the type of this bifurcation by using a suitable change of variable. Furthermore, some criteria on global stability and the non-existence of limit cycles are also given. To illustrate the relevance of our findings, we apply the above results to different predator-prey models. Typical phase portraits show the rich dynamics of the considered model especially the existence of some global bifurcations.

The dissertation is organized as follows: in Chapter 1, we give some important concepts and definitions in ecology including the different interactions between individuals. In Chapter 2, We recall some models used to describe the predator-prey interaction and the different results concerning the qualitative study of the general

Gause model. Chapter 3 contains the main results, we start by giving some biological reasons and mathematical models to show the dependence between the disappearance rate and densities of prey and predator. After that, we introduce the general Gause model with the variable disappearance rate. A qualitative analysis is made including the boundedness of solutions, local stability and Poincaré-Andronov-Hopf bifurcation. Some results on the global stability of the positive equilibrium and the non-existence of the limit cycle are also given. These results are extensions of what has been found before in the case of a constant disappearance rate. In Chapter 4, we present an application of results found in Chapter 3 to different models containing a non-constant disappearance rate. In Chapter 5, we describe two essential properties of our model which will be the goal of future articles. These properties concern the case of a slow-fast model and the enrichment paradox. This dissertation ends with a conclusion which contains some ecological interpretations of stability. We give also some appendices containing preliminary concepts from dynamical systems and an overview of the singular perturbation theory.

Chapter 1

Some concepts of ecology

The aim of this chapter is to introduce some important concepts and definitions in ecology derived from [1, 28, 50, 61] and chapter 1 of [62]. Different types of interactions between individuals are also given.

1.1 Some definitions

Ecology

The word ecology was first mentioned in 1866 by the German biologist Ernst Haeckel. This term comes from two Greek words: Oikos (meaning station, environment, habitat) and logos (science, knowledge). Ecology is defined as the science that studies conditions of existence of individuals and all kinds of interactions that exist between them. For more details about the history of ecology see [16].

Individual

An individual is the basic unit in ecology which is characterised by its size, weight, growth rate and reproduction rate. Its life contains birth, development, reproduction and death. During all these stages, the individual is always influenced by his environment.

Interaction

An interaction is defined by the reciprocal effect or the influence that can be established between individuals. Different types of interactions will be given in Section 1.2.

Population

A population is a group of individuals belonging to the same species, occupying the same geographical area and sharing one or more characteristics. Its growth usually depends on several factors: spatial heterogeneity, season, climate change, adaptation and selection processes, ...
Individuals in the same population may not share the same quantity of resources between them. It depends on their ages and strengths. Some individuals may have better access than others, this can produce interactions between them.

Ecosystem

An ecosystem is a group of populations of different species sharing the same place and interacting with each other. It is characterized by the dominance of certain species over others.

1.2 Types of interaction

There are two types of interaction : interspecific and intraspecific. An interspecific interaction is any interaction between individuals of different species. An intraspecific interaction is any competition that occurs between members of the same species.

1.2.1 Some interspecific interaction examples

Each individual can have either a positive (+), negative (-) or neutral (0) effect on another individual. The nature of the interaction established between two individuals is then a pair of these three elements as illustrated by the following examples.

Commensalism

Commensalism is a non-reciprocal biological interaction $(+, 0)$. One partner (the commensal) receives benefits and the other (the host) does not receive any benefits. The presence or absence of the commensal does not change the life of the host. For example, in *arum spathe*, *milichiids* live as commensals with *thomisa* spiders and they feed on the same prey of their host.

Mutualism

Mutualism is a mutually beneficial interaction $(+, +)$. Both species obtain a benefit related to protection, pollination, or food. For example, the pollination of plants by bees: plants offer nectar to bees and bees help plants to reproduce, Fig. 1.1.

Figure 1.1: The pollination of plants by bees. Image source : www.futura-sciences.com/planete/definitions/zoologie-mutualisme-11462

Amensalism

Amensalism is an interaction in which one population inhibits the development of other populations, it is neither affected nor benefits from this situation $(-, 0)$. For example, green plants release oxygen by photosynthesis, which is toxic to a certain type of bacteria called *anaerobic*.
Amensalism is also observed between bacteria. For example, the *fungus Penicillium notatum* can use antibiotic compounds such as *penicillin* to inhibit the growth of other type of bacteria, Fig.1.2.

Figure 1.2: *Penicillium notatum*. Image source : https://en.wikipedia.org/wiki/Penicillium_chrysogenum

Interspecific competition

Interspecific competition is a mutually unfavourable interaction $(-,-)$ between individuals of different species in which the same resources (food, water, light, ...) are not available in sufficient quantity. The more adapted species will take advantage which may lead to the exclusion of other species. For example, interspecific competition between *Laguncularia racemosa* and *Avicennia germinans* [34]. They are in competition with each other for access to light and sun. *Avicennia* has an advantage in accessing maximum light since it grows much faster than *Laguncularia*.

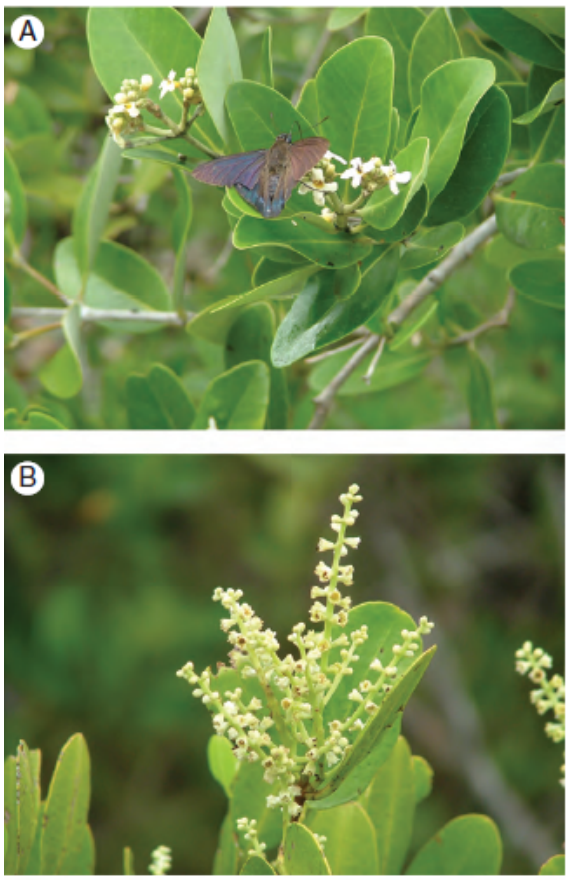

Figure 1.3: (A) *Avicennia germinans* (black *mangrove* with *Phocides pigmalion*). (B) *Laguncularia racemosa* (white *mangrove*). Image source : [34]

Predation

Predation is an interaction in which one species (the predator) consumes one or more species (the prey) totally or partially. It has a negative effect on the growth of the prey population and a positive effect on that of the predator $(-,+)$. The predation is also called consumer-resource interactions. A predator can be a carnivore, whose

preys are animals, a herbivore, whose resources are plants, or an omnivore, which is both a carnivore and a herbivore. For example, *Canadian lynx* is a carnivore whose main prey is the *Snowshoe hare*.

Parasitism

Parasitism [50] is an interaction where one species (the parasite) feeds and develops on another species (the host). At the same time, it can cause infection or disease of its host (-,+). An example of a parasite is the *caterpillar* which feeds on leaves of *oak* trees, weakening them but not killing them.

1.2.2 Some intraspecific interaction examples

Intraspecific interaction has an effect on the change in quantity (number of surviving individuals) and also on the change in quality (size, fecundity, weight, ...). Some of its types are given in the following.

Intraspecific competition for resources

This competition exists when individuals of the same species exploit the same limited resource as water, light and nutrients. For example, Fig. 1.4 illustrates the competition between two *Asian dogs* (*Cuon alpinus*) for prey.

Figure 1.4: Intraspecific competition between two dogs for prey. Image source : www.aquaportail.com/definition-1676-competition.html

There is no intraspecific competition in low densities. With increasing densities, a threshold is reached when density begins to influence mortality through resource

availability [19].
The distribution of resources in time and space plays a very important role as observed in the marine environment [70]. If resources are distributed more uniformly, competition is less likely than if they are separated.

Intraspecific competition for reproduction

It is a form of aggressive behaviour between individuals of the same population (males) when searching for a sexual partner (females). It can take the form of fighting in which one male chases the other. For example, *Cervus elaphus* often fight against each other and the winner will have access to reproduction, Fig. 1.5.

Figure 1.5: Intraspecific competition for reproduction in *Cervus elaphus* population. Image source: www.alloprof.qc.ca/fr/eleves/bv/sciences/les-relations-entre-les-individus-d-une-communaut-s1194

Intraspecific competition for a territory

It consists of defending and limiting a certain area against incursions by other individuals of the same species. For example, *Ruby-throated hummingbirds*, Fig. 1.6, are very territorial [57], one group of *hummingbirds* defends the territory that contains various food sources (small insects and nectar) against another group.

Figure 1.6: *Ruby-throated hummingbirds.* Image source : www.larousse.fr/encyclopedie/data/images/1309581-Colibri.jpg

Cannibalism

Cannibalism or intraspecific predation as indicated in [52] is a special case of predation that occurs within a species in which individuals eat each other. Cannibalism is caused either by ecological factors (insufficient resources, high densities of individuals, ...) or by social factors [2] (need for reproduction, parental care constraints in the face of too many offspring). For example, *Pseudomantis albofimbriata* female [53] becomes more aggressive and quick to attack when it is hungry, attracting males for consumption, Fig. 1.7.

Figure 1.7: *Pseudomantis albofimbriata.* Image source : https://en.wikipedia.org/wiki/False_garden_mantis

Chapter 2

General modified Gause type model

In the first half of the 20th century, the study of the dynamics of several interacting species appeared. During this period, known as the golden age of theoretical ecology, different models were constructed to study the interaction between a predator and its prey. To describe this phenomenon, a dynamic model can be formed by at least two coupled differential equations which represent the dynamics of prey and predator. Alfred J. Lotka in 1925 [42] and Vito Volterra in 1926 [67] proposed independently one of the first models describing the dynamics of biological systems in which a predator and its prey interact [68]. The Lotka-Volterra model (LV) is given by

$$\begin{cases} \dot{x} = r_1 x - axy, \\ \\ \dot{y} = [\tilde{a}x - m]\, y, \end{cases}$$

where the variables x and y are the densities of prey and predator species respectively, they are for biological reasons non-negative. The derivatives $\dot{x} = dx/dt$ and $\dot{y} = dy/dt$ are the growth of the two populations at time t. The parameters r_1, a, $\tilde{a}$ and m are positive, more precisely, the parameter r_1 is the natural growth rate of the prey, a is the per capita rate of the consumption of prey by predator population, $\tilde{a}$ is the rate of conversion of prey to predator and m is the mortality rate of the predator. This model is based on strong and unrealistic assumptions. For example, the exponential growth of the prey in the absence of the predator is rarely verified. However, populations are often limited by their environment and the effect of other factors. In addition, a mathematical study of LV model shows the existence of a nonlinear centre which makes the model structurally unstable. Accordingly, several models have been proposed with more consistent hypotheses and contain the main biological factors that should be taken into account in the predator-prey interaction.

In 1934, another model was given by the scientist Gause

$$\begin{cases} \dot{x} = r_1 x - p(x)y, \\ \\ \dot{y} = [ep(x) - m]\, y, \end{cases}$$

where p is the functional response of the predator with respect to prey. The positive parameter e is the conversion rate of the biomass of prey into the biomass of predator. In [17], the authors have considered a more general Gause model which can be presented by the following system

$$\begin{cases} \dot{x} = g(x) - p(x)y = p(x)\,[h(x) - y]\,, \\ \\ \dot{y} = [q(x) - m]\, y, \end{cases} \tag{2.1}$$

where g is the growth rate of the prey and the function q is the rate of conversion of prey to predator which have the same properties as the function p. For more detailed interpretations of these functions, we recommend the first two chapters in [40]. The function h is the prey isocline defined by $h(x) = g(x)/p(x)$. As some authors do, we call model (2.1) a *modified Gause-type* model.

In the following, we give a few words on the much used expressions of functions g, p and q in the literature.

2.1 About the growth rate function

In the absence of the predator, the growth rate of the prey can be described as

$$g(x) = (b_1(x) - d_1(x))x,$$

where $b_1(x)$ and $d_1(x)$ are the corresponding per capita reproduction and the death rates of the prey respectively [5].

Exponential growth equation

Assuming that $b_1(x)$ and $d_1(x)$ are both independent of population size, we obtain the classical historical Malthus equation [44] or the exponential growth equation for which

$$g(x) = (b_1 - d_1)x, \tag{2.2}$$

where $r_1 = b_1 - d_1$ is the population growth rate. In equation (2.2), reproduction and death rates of prey do not depend on the presence of other individuals. As a result, at least when $b_1 > d_1$, the prey population would increase exponentially.

Logistic function

In 1838, the biologist Pierre-François Verhulst proposed another growth function called the logistic function [65], depending on the size of the population. More precisely, b_1 and d_1 change with the population conditions and imply a limitation of population growth. For example, if resources become limited, individuals will use more energy to find them. Hence, the per capita reproduction rate b_1 may decrease. It is also possible that the death rate d_1 increases according to the growth of the population. These rates may depend on the population density and we obtain

$$b_1 = b_0 - b^* x, \quad d_1 = d_0 + d^* x, \tag{2.3}$$

where b_0 and d_0 are the reproduction and death rates when x is very small. The constants b^* and d^* correspond to the power of the density-dependence of reproduction and the death rates respectively.
Replacing the two rates b_1 and d_1 of (2.3) in (2.2), we get

$$g(x) = \left[r(1 - \frac{x}{K}) \right] x, \tag{2.4}$$

where $r = b_0 - d_0 > 0$ and $K = \dfrac{b_0 - d_0}{b^* + d^*}$ is the carrying capacity corresponding to the environment capacity to support population growth. We would like to draw attention to some very relevant comments on the logistic function that can be found, for example, in [40].

Definition 2.1. *A general growth rate function g is of the logistic type if it satisfies the following assumptions:*

- *g is a C^1 function such that $g(0) = 0$ and $g'(0) > 0$.*
- *There exists $K > 0$ such that $g(K) = 0$, $(x - K)g(x) < 0$ if $x \neq K$ and $g'(K) < 0$.*

2.2 About the functional response

The functional response corresponds to the number of prey killed per unit of time by a predator [27].

Lotka Volterra type functional response

In the model of Lotka and Volterra (LV), the function p is given by

$$p(x) = ax,$$

where a is the per capita rate consumption of prey by predator. In this case, predation is represented by the term

$$p(x)y = axy,$$

which is proportional to the rate of meeting between predator and prey.

Holling's functional responses

In 1959, Holling [27] proposed a functional response highlighting the fact that the predator can search the prey randomly. The time taken to search for and consume the prey is neglected. The number of prey killed is also proportional to their density until reaching a saturation level noted $\bar{x}$. This is the type I Holling function defined by :

$$p(x) = \begin{cases} ax & for \quad x < \bar{x} \\ \\ a\bar{x} & for \quad x \geq \bar{x}. \end{cases}$$

A second functional response is called the type II Holling function, or simply Holling II, in which the time taken by the predator to consume its prey is considered. It is given by

$$p(x) = \frac{ax}{c+x}, \tag{2.5}$$

where c is the half-saturation constant. This function was first used in 1913 by Michaelis and Menten [45], in the study of enzymatic reactions and also by Monod [49] in 1949 to describe the growth of microorganisms consuming substrates (the model of Monod).

Definition 2.2. *A general functional response p is of Holling II-type [40] if it satisfies the following assumptions:*

- *p is a C^1 bounded function from $\mathbb{R}_+$ to $\mathbb{R}$.*
- *$p(0) = 0$ and $p'(x) > 0$ for all $x \geq 0$.*

The type III Holling function [27] is a functional response in which the time taken by a predator to consume the prey is taken into account, as in the Holling II function. In addition, this type of functional response underlines the fact that, for a small density of prey, the effect of predation is low since the chance of finding prey individuals is low. This low predation can also be interpreted by the fact that the prey can prevent predators by taking refuge. Holling III functional response is given by the sigmoid function

$$p(x) = \frac{ax^2}{c+x^2}.$$

The three Holling's functional responses are represented in Fig. 2.1.

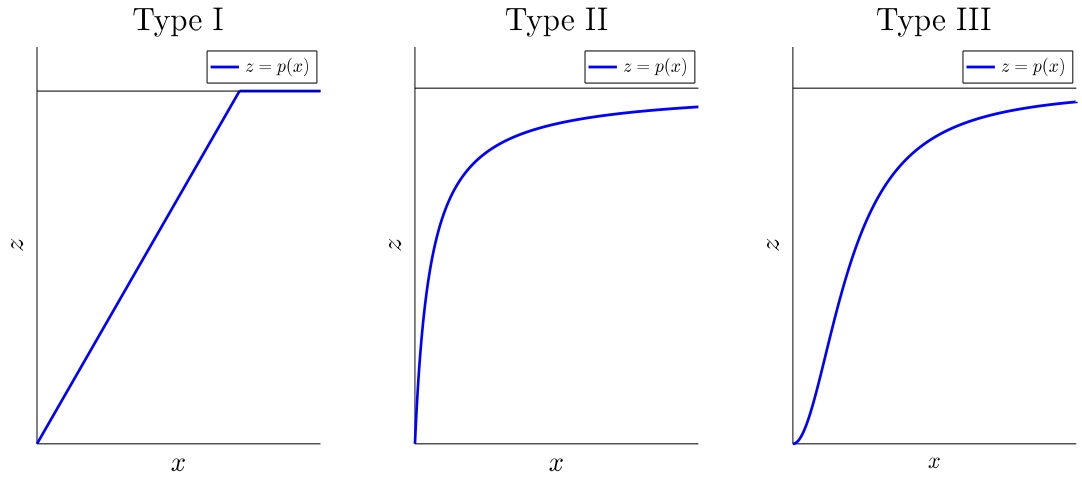

Figure 2.1: Holling's functional responses types.

Ratio-dependent functional response

All of the functional responses mentioned previously are called *prey-dependent* functional responses [4] since they depend on the density of the prey only. This characterization has been criticized by several biologists (see details in [4]). For instance, the interaction between *coyotes* and *jackrabbits* mentioned in [71] shows that if there are many predators for a fixed number of prey, the part of each one is reduced. Hence, the functional response should depend on the density of the prey and predator. Therefore, we can make the function p in (2.1) depending on x and y. In 1989, Arditi and Ginzburg (AG) proposed in their seminal article [3] a function of this type based on the Holling II functional response and depending on the ratio of both densities (x/y) given by

$$p_1\left(\frac{x}{y}\right) = \frac{a_1 \dfrac{x}{y}}{c + \dfrac{x}{y}} = \frac{a_1 x}{cy + x}, \tag{2.6}$$

where a_1 is the rate at which the prey is made available to the predator. In this case, the function p is called the ratio-dependent functional response. This function has been first used by Contois in microbiology in 1959 [11].

Predator-dependent functional response

Arditi and Ginzburg [3] called the functional responses of the form $p(x, y)$ *predator-dependent*. In these functions, the predator density y contributes also to determining the per capita kill rate. In this context, Hassel and Varley (HV) [25] had proposed in 1969 a functional response which indicates that the rate of consumption is low even if the density of the predator increases for a given prey quantity. It is given by

$$p_2(x, y) = \frac{a_1 x}{y^n},$$

where $n \geq 0$ is the mutual interference parameter. Note that for $n = 0$, we obtain the Lotka-Volterra response, and for $n = 1$, we obtain the Donor Control response (see Table 1.1 in [4]). Later, Beddington [7] and DeAngelis et al. [13] assumed that in addition to the time that a predator takes to search for and consume the prey it could also take time to interact with other predators. This functional response noted (BDA), is written as

$$p(x, y) = \frac{a_2 x}{1 + a_3 x + a_4 y},$$

where a_3 is the consumption rate, a_2 is the handling time, a_4 is the amplitude of the interference between predators.

Type	Model	Functional response
Prey-dependent	LV [42, 67]	$p(x) = ax$
	Holling II [27, 45, 49]	$p(x) = \frac{ax}{c + x}$
	Holling III [27]	$p(x) = \frac{ax^2}{c + x^2}$
Ratio-dependent	AG [4]	$p_1\left(\frac{x}{y}\right) = \frac{a_1 x}{cy + x}$
Predator-dependent	HV [25]	$p_2(x, y) = \frac{a_1 x}{y^n}$
	BDA [7, 13]	$p(x, y) = \frac{a_2 x}{1 + a_3 x + a_4 y}$

Table 2.1: Different functional responses existing in the literature.

In the literature, one also finds general functions of the type AG or HV (see Table 3.1 in [4]). The functional responses cited previously are summarised in Table 2.1.

2.3 Classical results

In this part, we give some mathematical issues concerning the model (2.1) in which the function g is considered to be of the logistic type (see Definition 2.1) and functions p and q are of Holling II-type (see Definition 2.2). We deduce by this choice about q that it has an inverse function q^{-1} such that

$$q^{-1}(0) = 0, \quad (q^{-1})' > 0. \tag{2.7}$$

In the following, some classical results concerning the qualitative study of (2.1) are given.

-Existence, uniqueness, positivity and boundedness: for each non-negative initial condition, there exists a unique solution of (2.1). Such a solution is non-negative and bounded.

-Existence of equilibria : the equilibria of (2.1) are $E_1(0,0)$ and $E_2(K,0)$ which always exist, where K is introduced in Definition 2.1. Moreover, there exists at least a positive equilibrium point $E^*(x^*, y^*)$ if and only if $q^{-1}(m) < K$ where $x^* = q^{-1}(m) > 0$ and $y^* = h(x^*)$.

- Stability : E_1 is always a saddle point, E_2 is locally exponentially stable (LES) if and only if $x^* > K$ and it is a saddle point if $x^* < K$. If $0 < x^* < K$, then E^* exists and it is LES if and only if $h'(x^*) < 0$. This condition is known in the literature as *the Rosenzweig-MacArthur graphical criterion* [17]. Therefore, if E^* lies on the ascending part of the prey isocline $y = h(x)$, then it is unstable. If it lies on the descending part, then it is LES.

- Poincaré-Andronov-Hopf bifurcation : under some assumptions, model (2.1) undergoes Poincaré-Andronov-Hopf bifurcation at $\tilde{E}(\tilde{x}, \tilde{y})$ when x^* crosses a critical value $\tilde{x}$ such that $h'(\tilde{x}) = 0$. Not that, $\tilde{E}(\tilde{x}, \tilde{y})$ can represent either a local maximum or a local minimum of h, see [59], Corollary 1. The nature of this bifurcation can be determined by the sign of the parameter ρ called the first Lyapunov exponent [59, 73] given by

$$\rho = \frac{1}{16}\left[2p'(\tilde{x})h''(\tilde{x}) + p(\tilde{x})h'''(\tilde{x}) - \frac{p(\tilde{x})q''(\tilde{x})}{q'(\tilde{x})}h''(\tilde{x})\right]. \tag{2.8}$$

See also [48] in which ρ is calculated for a generalized Gause-type model where g is a logistic growth function defined by (2.4).

If the parameter ρ is non-zero, then the bifurcation is non degenerate. If $\rho < 0$, then the bifurcation is supercritical while if $\rho > 0$, it is subcritical.

2.4 Specific case (Rosenzweig-MacArthur model)

When the predator growth function q is proportional to p in Gause-type model (2.1), that is $q(x) = ep(x)$, we obtain the Rosenzweig-MacArthur-type (RMA-type) model. The positive constant e is the conversion rate of the biomass of the prey into the biomass of the predator. Model (2.1) becomes

$$\begin{cases} \dot{x} = g(x) - p(x)y = p(x)\left[h(x) - y\right], \\ \\ \dot{y} = \left[ep(x) - m\right] y. \end{cases} \tag{2.9}$$

Several studies have investigated the dynamical behaviour of model (2.9), such as the local asymptotic stability, Hopf bifurcation and the existence of limit cycles [24, 26]. The sufficient and necessary global asymptotic stability conditions are also provided in [10, 12, 37]. If g is given by the logistic growth function and p is given by the Holling II functional response, then model (2.1) is called Rosenzweig-MacArthur (RMA) model [32]. It is given by

$$\begin{cases} \dot{x} = rx\left(1 - \dfrac{x}{K}\right) - \dfrac{axy}{c+x}, \\ \dot{y} = \left(\dfrac{eax}{c+x} - m\right) y. \end{cases} \tag{2.10}$$

It is well known that the condition of existence of a positive equilibrium $E^*(x^*, y^*)$ becomes $x_1 < K$, such that $x^* = x_1$ and $y^* = h(x^*)$, where

$$x_1 = \frac{mc}{ea - m}, \quad h(x) = \frac{r}{aK}(K - x)(c + x). \tag{2.11}$$

The stability condition of the equilibrium $E^*(x^*, y^*)$ becomes $\max(0, \hat{x}) < x^* < K$, where

$$\hat{x} = \frac{K - c}{2} \tag{2.12}$$

is the abscissa of the maximum of the function h. **Here, and in all that follows, we assume that** $\hat{x} > 0$. Therefore, if E^* lies on the ascending part of the prey isocline $y = h(x)$, then it is unstable (see Fig. 2.2, (a)). If it lies on the descending part, then it is asymptotically stable (see Fig. 2.2, (b)).
The Poincaré-Andronov-Hopf bifurcation occurs for $\tilde{x} = \hat{x}$ and the parameter ρ defined by (2.8) becomes

$$\rho = -\frac{r}{2K(c + K)} < 0, \tag{2.13}$$

which proves that the Hopf bifurcation in RMA model is always supercritical. It explains the presence of a stable limit cycle around the unstable positive equilibrium.

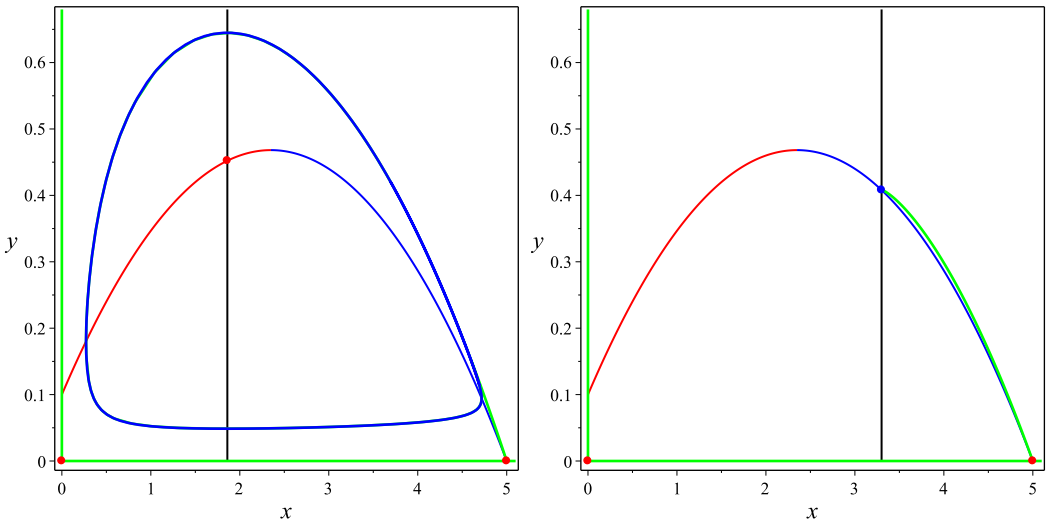

(a) $m = 0.31$ (b) $m = 0.33$

Figure 2.2: Some phase portraits of RMA model (2.10). $r = 0.2$, $K = 5$, $a = 0.6$, $c = 0.3$, $e = 0.6$. The value of m is depicted in each figure. Red dots indicate unstable equilibria and the blue dot indicates the stable equilibrium.

Chapter 3

Gause type model with variable disappearance rate

A number of modifications have been made to Gause type model (2.1) in order to answer some biological questions or to remove certain paradoxes inherent in this model. Among these modifications, we get interest to the case where the constant mortality rate m of the predator is replaced by a density-dependent function $d(x, y)$. In what follows, mathematical models are given from the literature where such a choice is made, together with biological justifications.

3.1 Hsu disappearance rate

Hsu [29] proposed an RMA type model in which the disappearance rate depends only on the prey population, this implies that $d(.)$ depends only on x. The predator equation in (2.9) becomes

$$\dot{y} = [ep(x) - d(x)]\, y.$$

The function d is assumed to satisfy

$$d(0) > 0; \quad d'(x) \leq 0, x \geq 0; \quad \lim_{x\to\infty} d(x) = d_\infty > 0. \tag{3.1}$$

Hsu did not mention in his article any biological justification of his model, but its ecological relevance can be illustrated for example in [46] where the authors studied the effect of the availability of the prey (*ciliates Paramecium caudatum*) at varying levels on the mortality rate of the predator (*ciliates Didinium nasutum*). Experimental data showed that the predator's mortality rate decreases with increasing prey abundance. This density-dependence of the mortality rate can also be justified by the fact that an abundance of prey implies a reduction in predator mortality.

Better still, we could consider $d(x)y$ as an emigration term, i.e. when prey density is rather low, predators are driven to leave the ecosystem in question.

3.2 Bazykin's disappearance rate

Bazykin [6] introduced a regulation by interspecific mechanisms, that is, a competition among predators for resources other than prey. For this, he subtracted a quantity αy^2 from the predator equation in (2.10) to have a predator disappearance rate $d(y) = \alpha y + m$. The predator equation in (2.10) becomes

$$\dot{y} = \left(\frac{eax}{c+x} - m - \alpha y\right) y.$$

With this simple modification, it turns out that Bazykin model exhibits new phase portraits such as multiple positive equilibria and many bifurcation types (see [5] and the detailed studies in [21] and [43]). A biological example where d depends only on y, is the *rodent-vegetation* model where regulation of herbivores is given by intraspecific mechanisms (see for example [64], model II in Table 1).

3.3 CF disappearance rate

Cavani and Farkas [9] proposed a modified RMA model (CF) for which the mortality of the predator in the absence of the prey is an increasing and bounded function which depends only on the density of the predator. It is given by

$$d(y) = \frac{\tilde{\gamma} + \tilde{\delta} y}{1+y} = \frac{(\tilde{\delta} - \tilde{\gamma})y}{1+y} + \tilde{\gamma}, \tag{3.2}$$

where $\tilde{\gamma}$ is the mortality at low density, $\tilde{\delta}$ is the maximal mortality with the natural assumption $0 < \tilde{\gamma} < \tilde{\delta}$. For technical reasons, we consider in the next that $\tilde{\gamma}$ is equal to the natural mortality rate m and we set $\alpha = \tilde{\delta} - m$. The predator equation in (2.9) becomes

$$\dot{y} = \left(\frac{eax}{c+x} - \frac{\alpha y}{1+y} - m\right) y.$$

We did not find a biological justification for the predator-dependent disappearance rate in [9] given by (3.2). However, in [47], such a rate is considered as the impact of cannibalism which depends only on the predator density and does not depend on the availability of food.

3.4 VT disappearance rate

From the Bazykin model, if the predator density-dependent parameter α is made inversely proportional to resource availability, the dynamics are described by the so-called variable-territory model of Turchin-Batzli [64]. One can see there the interpretations (model III, Table 1) that lead to the predator equation

$$\dot{y} = \left(\frac{eax}{c+x} - m\right) y - \frac{\alpha y^2}{x}.$$

The term $\alpha y^2/x$ represents the self-limitation of the predator. Nevertheless, self-limitation should be biologically limited when the concentration of the prey is small. It is not the case with Turchin-Batzli model where $\alpha y^2/x$ could become quite large in case of predators can subsist on few preys (i.e. $\alpha y^2/x \to \infty$ as $x \to 0$). This leads to the well-defined modified variable-territory (VT) model [31] for which

$$d(x, y) = m + \frac{\alpha y}{\delta + x},$$

where $\delta > 0$ is fixed. Hence, the self-limitation of the predator becomes less than $\alpha y^2/\delta$ and also the singularity in $x = 0$ is avoided. The predator equation in (2.9) becomes

$$\dot{y} = \left(\frac{eax}{c+x} - \frac{\alpha y}{\delta + x} - m\right) y.$$

All disappearance rates presented previously are summarised in Table 3.1.

Type	Model	Disappearance rate
Constant	Gause/RMA [17, 32, 40, 56, 59, 73]	$d = m$
Prey-dependent	Hsu [29]	$d(x)$
Predator-dependent	Bazykin [6, 5, 21, 43, 69]	$d(y) = \alpha y + m$
	CF [9, 15]	$d(y) = \frac{\alpha y}{1+y} + m$
Variable	V-T [31, 60, 64]	$d(x, y) = \frac{\alpha y}{\delta + x} + m$

Table 3.1: Different disappearance rates exist in the literature.

3.5 General variable disappearance rate

We consider model (2.1) with the general variable disappearance rate $d(x, y)$ which contains the natural mortality rate m. The complete model is therefore

$$\begin{cases} \dot{x} = g(x) - p(x)y, \\ \\ \dot{y} = [q(x) - d(x, y)]\, y. \end{cases} \tag{3.3}$$

Recall that, $\dot{x} = dx/dt$ and $\dot{y} = dy/dt$ represent the growth of the two populations at time t. The function g is the growth rate of the prey population and the function p is the functional response of the predator.
We note that $d(x, y)$ can have various interpretations such as intraspecific competition (for resources and territory) or cannibalism or emigration (see Section 1.2.2 of the first chapter). All models described above illustrate the dependence of the disappearance rate on prey and or predator densities. In view of examples given above, it is natural to consider that the predator mortality or disappearance rate is non-negative, decreasing with increasing prey density and increasing with increasing predator density, which will be specified in the assumptions on $d(x, y)$. In this section, we make the following assumptions :

- H_1 : The function g is of the logistic type (Definition 2.1).
- H_2 : The functions p and q are of the Holling II-type (Definition 2.2).
- H_3 : d is a positive C^1 function such that for all $(x, y) \in \mathbb{R}_+ \times \mathbb{R}_+$, $d(0, 0) > 0$, $d_x(x, y) := \frac{\partial d}{\partial x}(x, y) \leq 0$ and $d_y(x, y) := \frac{\partial d}{\partial y}(x, y) \geq 0$.

Since q is of Holling II-type, we have

$$\lim_{x \to +\infty} q(x) = q_\infty, \qquad 0 < q_\infty < +\infty, \tag{3.4}$$

the function q has an inverse function, such that

$$q^{-1} : [0, q_\infty) \to \mathbb{R}^+, \qquad q^{-1}(0) = 0, \qquad (q^{-1})' > 0. \tag{3.5}$$

The inequality $d_x(x, y) \leq 0$ signifies that the mortality rate decreases when the prey density increases for a fixed number of predators while the inequality $d_y(x, y) \geq 0$ indicates that the mortality rate increases when the density of predators increases for a fixed number of prey.

3.5.1 Positivity and boundedness

The positivity and boundedness of the solution of (3.3) are given in the following proposition.

Proposition 3.1. *[23] Under assumptions $H_1 - H_3$, solutions of (3.3) are non-negative and asymptotically bounded.*

Proof. For the model (3.3), the axes $x = 0$ and $y = 0$ are invariant and the positive cone is invariant. From H_1, the function g is of logistic type and from H_2 and the comparison lemma, it can be shown that

$$\limsup_{t \to +\infty} x(t) \leq K, \tag{3.6}$$

this means that the component $x(t)$ is asymptotically bounded above. To show the asymptotical boundedness of $y(t)$, a phase plane analysis can be used as given in [17], pp. 78-80. □

3.5.2 Existence and stability of equilibria

In this section, the existence and stability conditions of the equilibria are given. Note that, an equilibrium of (3.3) is defined by the intersection of the isoclines $\dot{x} = 0$ and $\dot{y} = 0$. The isocline $\dot{x} = 0$ is the union of the semi-axis $x = 0$ and the curve $y = h(x)$ where

$$h(x) := \frac{g(x)}{p(x)} \ \text{ if } \ x \neq 0, \quad h(0) = \frac{g'(0)}{p'(0)} > 0. \tag{3.7}$$

The isocline $\dot{y} = 0$ is the union of the semi-axis $y = 0$ and the curve of equation $U(x, y) = 0$, where U is defined by

$$U(x, y) := q(x) - d(x, y). \tag{3.8}$$

As a consequence of H_3, the limit

$$m := \lim_{x \to +\infty} d(x, 0) \geq 0$$

exists. Assume that $m < q_\infty$, Hence $x \mapsto d(x, 0)$ is decreasing from $d(0, 0) > 0$ to $m \in [0, q_\infty)$. Since q is strictly increasing from 0 to q_∞, the equation $q(x) = d(x, 0)$ has a unique solution denoted x_1 given by

$$x = x_1 \Longleftrightarrow q(x) = d(x, 0). \tag{3.9}$$

Under assumptions H_2 and H_3, the equation $U(x, y) = 0$ defines a function $x = \varphi(y)$, such that $x_1 = \varphi(0)$. More precisely, the following result is obtained.

Lemma 3.1. *[23] Assume that $m < q_\infty$. There exists a C^1 function*

$$\varphi : [0, y_\infty) \to \mathbb{R}+, \qquad 0 < y_\infty \leq +\infty, \qquad \varphi(0) = x_1, \tag{3.10}$$

such that, for all $y \in [0, y_\infty)$, we have $U(\varphi(y), y) = 0$, where U is defined by (3.8), and

$$\varphi'(y) = \frac{d_y(\varphi(y), y)}{[q'(\varphi(y)) - d_x(\varphi(y), y)]}. \tag{3.11}$$

Proof. Consider the set

$$I = \{y : \lim_{x \to +\infty} d(x, y) < q_\infty\},$$

where q_∞ is defined by (3.4). We have $0 \in I$ which implies that this set I is not empty. By considering $y_\infty = \sup I$, we have, for any $y \in [0, y_\infty)$,

$$d(\infty, y) := \lim_{x \to +\infty} d(x, y) < q_\infty.$$

Therefore, the function $x \mapsto d(x, y)$ is decreasing from $d(0, y) > 0$ to $d(\infty, y) < q_\infty$. Since q is increasing from $q(0) = 0$ to q_∞, for any $y \in [0, y_\infty)$, the equation $q(x) = d(x, y)$ has a unique solution denoted $x = \varphi(y)$. Using the Implicit Function Theorem, we prove that the function $y \mapsto \varphi(y)$ is C^1 and that its derivative is given by (3.11). □

Remark 3.1. *The isocline $U(x, y) = 0$ is the curve of equation $x = \varphi(y)$. If d does not depend on x, the function φ is given by*

$$\varphi(y) = q^{-1}(d(y)). \tag{3.12}$$

Furthermore, if $d_y(x, y) > 0$, the isocline $x = \varphi(y)$ can be considered as a curve with equation $y = \psi(x)$, where ψ is the inverse of the function φ such that

$$q(x) - d(x, \psi(x)) = 0, \tag{3.13}$$

with $\psi(x_1) = 0$ and $\psi'(x) = 1/\varphi'(y)$.

The following theorem determines the equilibria and the conditions of their existence.

Theorem 3.1. *[23] From assumptions H_1 to H_3, the model (3.3) has always the equilibria $E_1(0, 0)$ and $E_2(K, 0)$. In addition, there exists at least one positive equilibrium point if and only if*

$$x_1 < K \iff q(K) > d(K, 0), \tag{3.14}$$

where x_1 is defined by (3.9). Let $E^*(x^*, y^*)$ be a positive equilibrium, then $x^* \in [x_1, K)$ is a solution of equation $x = \varphi(h(x))$ and y^* is given by $y^* = h(x^*)$.

Proof. From H_1, the boundary equilibria are $E_1(0,0)$ and $E_2(K,0)$. From H_2, H_3 and (3.11), we have $\varphi'(y) \geq 0$. Consequently, $\varphi(y)$ is non-decreasing. To have at least one non-trivial intersection between isoclines $y = h(x)$ and $x = \varphi(y)$, it is necessary and sufficient that $x_1 < K$. Therefore, according to condition (3.14), there is at least one positive equilibrium point denoted $E^*(x^*, y^*)$. Thus $x^* = \varphi(y^*)$ and $y^* = h(x^*)$. Therefore, $x^* \in [x_1, K)$ and $x^* = \varphi(h(x^*))$. □

Some representative examples of isoclines of (3.3) are shown in Fig. 3.1 in which all equilibria are the intersections of blue and red curves.

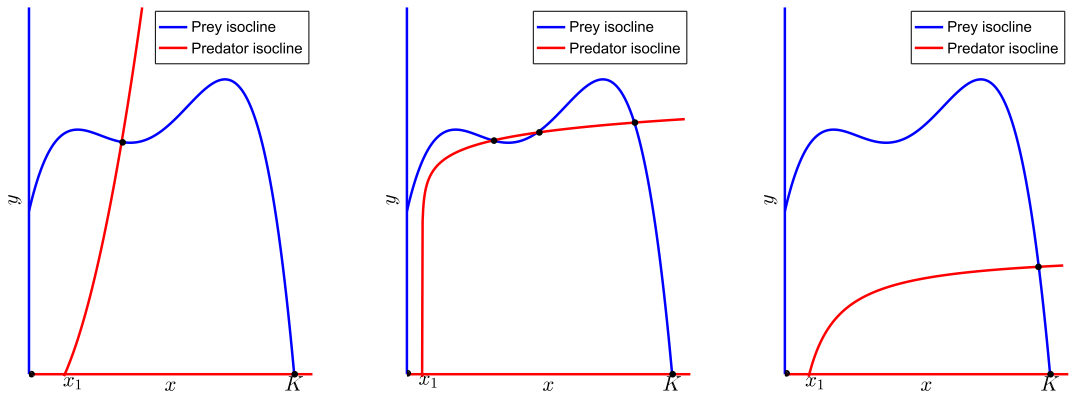

Figure 3.1: Schematic figures of isoclines of (3.3) and equilibria under condition (3.14).

The linearization method gives the stability properties of the equilibria in the following theorem.

Theorem 3.2. *[23] Under assumptions H_1, H_2, H_3, the equilibrium $E_1(0,0)$ is a saddle point whose stable separatrix is the y semi-axis and its unstable separatrix is the open segment $(0,K)$ of the x semi-axis. $E_2(K,0)$ is LES if and only if $x_1 > K$ and it is a saddle point if $x_1 < K$ the stable separatrix of which is the x semi-axis. When $E^*(x^*, y^*)$ exists, it is LES if and only if*

$$\varphi'(y^*)h'(x^*) < 1, \tag{3.15}$$

and

$$\frac{p(x^*)h'(x^*)}{h(x^*)} < d_y(x^*, h(x^*)). \tag{3.16}$$

Proof. The Jacobian matrix of system (3.3) at a point (x, y) is

$$A(x,y) = \begin{pmatrix} p(x)h'(x) + p'(x)\left[h(x) - y\right] & -p(x) \\ \left[q'(x) - d_x(x,y)\right] y & q(x) - d(x,y) - d_y(x,y)y \end{pmatrix}. \quad (3.17)$$

Using H_2 and H_3, the Jacobian matrix (3.17) at $E_1(0,0)$ is

$$A(E_1) = \begin{pmatrix} h(0)p'(0) & 0 \\ 0 & -d(0,0) \end{pmatrix},$$

the eigenvalues of which are $\lambda_1 = h(0)p'(0)$ and $\lambda_2 = -d(0,0)$. From H_2 and (3.7) we have $\lambda_1 > 0$. From H_3 we have $\lambda_2 < 0$. Then, $E_1(0,0)$ is a saddle point with separatrices indicated in the statement of the theorem.
Likewise, using H_1 and H_3, the Jacobian matrix (3.17) at $E_2(K,0)$ has the following form

$$A(E_2) = \begin{pmatrix} p(K)h'(K) & -P(K) \\ 0 & q(K) - d(K,0) \end{pmatrix}, \quad (3.18)$$

the eigenvalues of which are $\lambda_1 = p(K)h'(K)$ and $\lambda_2 = q(K) - d(K,0)$. From H_2, we have $\lambda_1 < 0$. Hence, $E_2(K,0)$ is LES if and only if $\lambda_2 < 0$, which means $q(K) < d(K,0)$, i.e. $x_1 > K$. If $x_1 < K$, it is a saddle point with the x semi-axis as the stable separatrix.
Consider now the stability of the positive equilibrium $E^*(x^*, y^*)$. The Jacobian matrix (3.17) at $E(x^*, y^*)$ is given by

$$A(x^*,y^*) = \begin{pmatrix} p(x^*)h'(x^*) & -p(x^*) \\ \left[q'(x^*) - d_x(x^*,y^*)\right] y^* & -d_y(x^*,y^*)y^* \end{pmatrix},$$

with $y^* = h(x^*)$. The stability of $E^*(x^*, y^*)$ is determined by the sign of the determinant and the trace given by

$$\det A(E^*) = h\left(x^*\right) p(x^*) \left[q'(x^*) - d_x\left(x^*, h\left(x^*\right)\right) - h'\left(x^*\right) d_y\left(x^*, h\left(x^*\right)\right)\right], \quad (3.19)$$

$$\operatorname{tr} A(E^*) = p(x^*)h'(x^*) - y^* d_y(x^*,y^*), \quad (3.20)$$

$$= p(x^*)h'(x^*) - h(x^*)d_y(x^*,h(x^*)), \quad (3.21)$$

Since $h\left(x^*\right) p(x^*) > 0$, we have

$$\det A(E^*) > 0 \Longleftrightarrow h'(x^*)d_y(x^*,y^*) < q'(x^*) - d_x(x^*,y^*).$$

Dividing by $q'(x^*) - d_x(x^*,y^*)$ which is positive, according to H_2 and H_3, we obtain

$$\det A(E^*(x^*,y^*)) > 0 \Longleftrightarrow \frac{d_y(x^*,y^*)}{q'(x^*) - d_x(x^*,y^*)} h'(x^*) < 1.$$

Using (3.11) and $x^* = \varphi(y^*)$, we obtain condition (3.15). We also have

$$\operatorname{tr} A(E^*) < 0 \Longleftrightarrow p(x^*)h'(x^*) < h(x^*)d_y(x^*,h(x^*)).$$

Dividing by $h(x^*)$ which is positive, we obtain condition (3.16) of the theorem. □

Remark 3.2. *From H_2 and H_3, the inequality (3.16) is verified when $h'(x^*)$ is negative and can be verified also for $h'(x^*)$ non-negative. It means that $E^*(x^*, y^*)$ can be LES even if it lies on an ascending branch of the prey isocline.*

The following conditions give an extension of the Rosenzweig-MacArthur graphical stability criterion [17]. The graphical description of the determinant condition is given first.

Proposition 3.2. *[23] Let $T_1 = (1, h'(x^*))$ and $T_2 = (\varphi'(y^*), 1)$ be the director vectors of the tangents of the prey and predator isoclines at $E^*(x^*, y^*)$, respectively. Condition (3.15) is equivalent to the condition $\det(T_1, T_2) > 0$, i.e. (T_1, T_2) is a basis with the same orientation as the canonical basis. Moreover, if $d_y(x^*, y^*) > 0$, the condition (3.15) becomes $\psi(x^*) > h'(x^*)$, where $y = \psi(x)$ is the equation of the predator isocline.*

Proof. Since $\det(T_1, T_2) = 1 - \varphi'(y^*)h'(x^*)$, condition (3.15) becomes equivalent to $\det(T_1, T_2) > 0$. In addition, if $d_y(x^*, y^*) > 0$, then in a neighbourhood of $E^*(x^*, y^*)$ the function φ has an inverse function ψ and $\psi'(x^*) = 1/\varphi'(y^*)$. Therefore, the condition $\varphi'(y^*)h'(x^*) < 1$ is equivalent to the condition $\psi'(x^*) > h'(x^*)$. □

Proposition 3.2 indicates that the determinant at the equilibrium point is positive if, and only if, the slope of the isocline of the prey is smaller than that of the predator.

In order to give the graphical description of the trace condition, we need to define the following functions H and G in $[0, K)$ with values in $\mathbb{R}$ by

$$H(x) = \frac{p(x)h'(x)}{h(x)}, \quad G(x) = d_y(x, h(x)). \tag{3.22}$$

Proposition 3.3. *[23] Let $\mathcal{A}$ be the closed subset of the prey isocline defined by*

$$\mathcal{A} = \{(x, h(x)) : x \in [0, K) \text{ and } H(x) \geq G(x)\}.$$

Condition (3.16) is satisfied if and only if $E^*(x^*, y^*) \notin \mathcal{A}$.

Proof. From definitions (3.22), the condition (3.16) can be written as $H(x^*) < G(x^*)$, which is equivalent to $E^*(x^*, y^*) \notin \mathcal{A}$. □

From H_2 and H_3, $\mathcal{A}$ is necessarily a subset of the ascending part of the prey isocline since $H(x) < 0$, for all x in $(\hat{x}, K)$ and $\varphi(x) > 0$, for all $x > 0$. It is confirmed by Proposition 3.3 that $\operatorname{tr} A(E^*(x^*, y^*))$ is positive if and only if the equilibrium point is located inside the subset $\mathcal{A}$.
The graphical criterion of a positive hyperbolic equilibrium point is obtained by the combination of Propositions 3.2 and 3.3.

Theorem 3.3. *[23] Let $E^*(x^*, y^*)$ be a positive equilibrium of (3.3).*

- *If, at $E^*(x^*, y^*)$, the slope of the prey isocline is larger than that of the predator isocline, then $E^*(x^*, y^*)$ is a saddle point.*
- *If, at $E^*(x^*, y^*)$, the slope of the prey isocline is smaller than that of the predator isocline and $E^*(x^*, y^*) \notin \mathcal{A}$, then $E^*(x^*, y^*)$ is LES.*
- *If, at E^*, the slope of the prey isocline is smaller than that of the predator isocline and $E^*(x^*, y^*) \in int\mathcal{A}$, then $E^*(x^*, y^*)$ is a repeller.*

Proof. In the case where the slope of the prey isocline is greater than that of the predator, Proposition 3.2 indicates that the determinant is negative, and this means that $E^*(x^*, y^*)$ is a saddle point.
In the case where the slope of the prey isocline is smaller than that of the predator isocline, Proposition 3.2 indicates that the determinant is positive and two sub-cases occur. If $E^*(x^*, y^*) \notin int\mathcal{A}$, Proposition 3.3 shows that the trace is negative which implies that $E^*(x^*, y^*)$ is LES. If $E^*(x^*, y^*)$ is in the interior of $\mathcal{A}$, Proposition 3.3 shows that the trace is positive which implies that $E^*(x^*, y^*)$ is a repeller. □

Remark 3.3. *At a positive equilibrium point where the isoclines of the prey and predator are tangent, the determinant is zero. This point corresponds to a saddle-node bifurcation.*
For a positive equilibrium point which is on the boundary of the arc $\mathcal{A}$, the trace is zero. In addition, if the determinant at this point is positive, then a Poincaré-Andronov-Hopf bifurcation can appear.

3.5.3 Poincaré-Andronov-Hopf bifurcation

In this section, we discuss an important phenomenon that allows stability to be transferred between a positive equilibrium point and a limit cycle. This is the Poincaré-Andronov-Hopf bifurcation (PAH) that occurs when the chosen parameter of (3.3) crosses a critical value. We simply choose x^* as the parameter bifurcation. For this reason, we consider that there exists a hyperbolic positive equilibrium point $\tilde{E}(\tilde{x}, \tilde{y})$ such that PAH occurs at $x^* = \tilde{x}$. By definition of $\tilde{E}(\tilde{x}, \tilde{y})$, $\tilde{x} \in [x_1, K)$ is a solution of the equation $\varphi(h(x)) = x$ and $\tilde{y} = h(\tilde{x})$. Assume that the following conditions are satisfied

$$\det A(\tilde{E}(\tilde{x}, \tilde{y})) > 0 \quad \text{and} \quad \operatorname{tr} A(\tilde{E}(\tilde{x}, \tilde{y})) = 0. \tag{3.23}$$

These conditions mean that the Jacobian matrix at $(\tilde{E}(\tilde{x},\tilde{y})$ has purely imaginary eigenvalues. We simplify the calculations by using the following notations

$$\begin{array}{l} p_0 = p(\tilde{x}), \quad p_1 = p'(\tilde{x}), \quad p_2 = p''(\tilde{x}), \\ q_0 = q(\tilde{x}), \quad q_1 = q'(\tilde{x}), \quad q_2 = q''(\tilde{x}), \\ h_0 = h(\tilde{x}), \quad h_1 = h'(\tilde{x}), \quad h_2 = h''(\tilde{x}), \quad h_3 = h'''(\tilde{x}), \\ d_1 = d_x(\tilde{x},\tilde{y}), \quad d_2 = d_y(\tilde{x},\tilde{y}), \\ d_{11} = d_{xx}(\tilde{x},\tilde{y}), \quad d_{12} = d_{xy}(\tilde{x},\tilde{y}), \quad d_{22} = d_{yy}(\tilde{x},\tilde{y}), \\ d_{112} = d_{xxy}(\tilde{x},\tilde{y}), \quad d_{122} = d_{xyy}(\tilde{x},\tilde{y}), \quad d_{222} = d_{yyy}(\tilde{x},\tilde{y}). \end{array} \tag{3.24}$$

Using these notations and (3.23) , $\det A(\tilde{E}(\tilde{x},\tilde{y}))$ can be denoted by ω^2. Then, we get from (3.19)

$$\omega^2 = \det A(\tilde{E}(\tilde{x},\tilde{y})) = p_0 h_0 (q_1 - d_1 - h_1 d_2). \tag{3.25}$$

The first Lyapunov coefficient is given by

$$\rho = \frac{1}{16 p_0 \omega^2} \left(p_0 h_0 b_0 + h_0 b_1 d_2 + h_0^2 b_2 d_2^2 + (2 h_0 d_{122} - p_2)\, h_0^3 d_2^3 \right), \tag{3.26}$$

where

$$\begin{aligned} b_0 &= 2p_0p_1q_1h_2 + p_0^2q_1h_3 - p_0^2q_2h_2 + \left(p_0^2h_2 - p_0h_0d_{12}\right) d_{11} \\ &\quad + (p_0q_2 - q_1h_0d_{22})\, h_0d_{12} - 2q_1^2h_0d_{22} - p_0q_1h_0d_{112} - q_1^2h_0^2d_{222} \\ &\quad - \left(p_0^2h_3 + 2p_0p_1h_2 - p_0h_0d_{112} - h_0^2d_{12}d_{22} - 2q_1h_0^2d_{222} - 4q_1h_0d_{22}\right) d_1 \\ &\quad - (h_0d_{222} + 2d_{22})\, h_0d_1^2, \\ b_1 &= p_0p_2q_1h_0 + p_0^3h_2^2 - p_0p_1q_2h_0 - p_0^2q_1h_2 + p_0p_1h_0d_{11} + p_0h_0(p_0h_2 - 2q_1)d_{12} \\ &\quad + (p_1q_1 + p_0q_2)h_0^2d_{22} - 2p_0h_0^2d_{12}^2 - q_1h_0^3d_{22}^2 - p_0h_0^2d_{11}d_{22} - 2p_0q_1h_0^2d_{122} \\ &\quad + \left(p_0^2h_2 - p_0p_2h_0 - p_1h_0^2d_{22} + h_0^3d_{22}^2 + 2p_0h_0d_{12} + 2p_0h_0^2d_{122}\right) d_1, \\ b_2 &= p_0q_2 - p_0p_1h_2 - p_0^2h_3 - p_0d_{11} + 2p_1h_0d_{12} + q_1h_0d_{22} - 2h_0^2d_{12}d_{22} \\ &\quad + q_1h_0^2d_{222} + p_0h_0d_{112} - (d_{22} + h_0d_{222})h_0d_1. \end{aligned}$$

Not that, ρ in (3.26) is expressed as a polynomial in d_2 of degree 3. The existence of a PAH bifurcation is shown in the next theorem.

Theorem 3.4. *[23] Let g, p, q and d be C^3. Suppose that assumptions H_1-H_3 are satisfied and condition (3.14) holds, so that system (3.3) has at least one positive equilibrium $\tilde{E}(\tilde{x},\tilde{y})$. Suppose that $\tilde{x}$ satisfies the following conditions*

$$\det A(\tilde{E}(\tilde{x},\tilde{y})) > 0 \Longleftrightarrow q'(\tilde{x}) - d_x(\tilde{x},\tilde{y}) - h'(\tilde{x}) d_y(\tilde{x},\tilde{y}) > 0, \tag{3.27}$$

$$\operatorname{tr} A(\tilde{E}(\tilde{x},\tilde{y})) = 0 \Longleftrightarrow H(\tilde{x}) = G(\tilde{x}), \tag{3.28}$$

and the transversality condition

$$H'(\tilde{x}) \neq G'(\tilde{x}), \tag{3.29}$$

where H and G are defined by (3.22). Then, the model (3.3) undergoes a PAH bifurcation when x^* crosses the value $\tilde{x}$. Moreover, if the parameter ρ defined by (3.26) is non-zero, then the bifurcation is non degenerate: if $\rho < 0$, then the bifurcation is supercritical, while if $\rho > 0$, it is subcritical.

Proof. First, by hypotheses (3.27) and (3.28), the necessary conditions (3.23) for a PAH Bifurcation are satisfied. Secondly, we prove the transversality condition

$$\frac{d}{dx^*} \operatorname{tr} A(E^*(x^*, y^*))\Big|_{x^*=\tilde{x}} \neq 0.$$

From the expression of the trace given in the proof of Theorem 3.2, we have

$$\operatorname{tr} A(E^*(x^*, y^*)) = h(x^*)\left(H(x^*) - G(x^*)\right).$$

Therefore,

$$\frac{d}{dx^*} \operatorname{tr} A(E^*(x^*, y^*)) = h'(x^*)\left(H(x^*) - G(x^*)\right) + h(x^*)\left(H'(x^*) - G'(x^*)\right).$$

By hypothesis (3.28), we obtain

$$\frac{d}{dx^*} \operatorname{tr} A(E^*(x^*, y^*))\Big|_{x^*=\tilde{x}} = h(\tilde{x})\left[H'(\tilde{x}) - G'(\tilde{x})\right].$$

From the assumption (3.29), the transversality condition is verified. Thirdly, in order to examine the non-degeneracy condition and to compute the number ρ given in [30] pg 169 or in [20] pg 152, the sign of which is that of the Lyapunov exponent, we introduce the following change of variables

$$x = N, \quad y = h'(\tilde{x})N + \frac{\omega}{p(\tilde{x})}P, \tag{3.30}$$

where $\omega = \sqrt{\det A(\tilde{E}(\tilde{x}, \tilde{y}))}$. The model (3.3) becomes

$$\begin{cases} \dot{N} = -\omega P + F(N, P), \\ \dot{P} = \omega N + G(N, P), \end{cases} \tag{3.31}$$

with

$$F(N, P) = p(N)\left[h(N) - h'(\tilde{x})N\right] - \omega P\left[\frac{p(N)}{p(\tilde{x})} - 1\right],$$

and

$$G(N,P) = \frac{1}{\omega}\Big[q(N) - D\big(N, h'(\tilde{x})N + \frac{\omega}{p(\tilde{x})}P\big) - m\Big]\left[p(\tilde{x})h'(\tilde{x})N + \omega P\right] - \frac{h'(\tilde{x})p(N)}{\omega}\Big[p(\tilde{x})h(N) - p(\tilde{x})h'(\tilde{x})N - \omega P\Big] - \omega N.$$

The parameter ρ is given by

$$\rho = \frac{1}{16}A_1 + \frac{1}{16\omega}\left[A_2 - A_3 - A_4\right], \tag{3.32}$$

where,

$$A_1 = F_{NNN} + F_{NPP} + G_{NNP} + G_{PPP}, \quad A_2 = F_{NP}(F_{NN} + F_{PP}),$$

$$A_3 = G_{NP}(G_{NN} + G_{PP}), \quad A_4 = F_{NN}G_{NN} - F_{PP}G_{PP}.$$

where F_{NN} denotes $\frac{\partial^2 F}{\partial N \partial N}(\tilde{N}, \tilde{P})$, F_{NP} denotes $\frac{\partial^2 F}{\partial N \partial P}(\tilde{N}, \tilde{P})$, and similarly for all other partial derivatives. Since F is linear in P, we have $F_{PP} = F_{NPP} = 0$. Notice that from the change of variables (3.30), we have $\tilde{N} = \tilde{x}$ and $\tilde{P} = \frac{p(\tilde{x})}{\omega}\left(\tilde{y} - h'\left(\tilde{x}\right)\tilde{x}\right)$.

After calculations, and using the notations (3.24), we find that A_i, $i = 1, \cdots, 4$ are given by the following expressions

$$\begin{aligned}
A_1 &= \frac{1}{p_0^2}\Big[p_0^2p_2h_1 + 3p_0^2p_1h_2 + p_0^3h_3 + p_0^2q_2 - p_0^2d_{11} - 4p_0^2h_1d_{12} \\
&\quad - 3\left(\omega^2 + p_0^2h_1^2\right)d_{22} - p_0^2h_0d_{112} - \left(\omega^2 + p_0^2h_1^2\right)h_0d_{222} - 2p_0^2h_0h_1d_{122}\Big], \\
A_2 &= -\omega p_1h_2, \\
A_3 &= \frac{1}{p_0\omega}\Big[p_1h_1 + q_1 - d_1 - 2h_1d_2 - h_0d_{12} - h_0h_1d_{22}\Big]\Big[p_0^2q_2h_0 - p_0^3h_1h_2 \\
&\quad + 2p_0^2q_1h_1 - 2p_0^2h_1d_1 - 2\left(\omega^2 + p_0^2h_1^2\right)d_2 - p_0^2h_0d_{11} - 2p_0^2h_0h_1d_{12} \\
&\quad - \left(\omega^2 + p_0^2h_1^2\right)h_0d_{22}\Big], \\
A_4 &= \frac{p_0^2h_2}{\omega}\Big[q_2h_0 - p_0h_1h_2 + 2q_1h_1 - 2h_1d_1 - 2h_1^2d_2 - h_0d_{11} - 2h_0h_1d_{12} \\
&\quad - h_0h_1^2d_{22}\Big].
\end{aligned}$$

Replacing these expressions in (3.32) we obtain the following formula for ρ

$$\rho = \frac{1}{16p_0^2\omega^2}\left(a_0 + a_2\omega^2 + a_4\omega^4\right),$$

where a_0, a_2 and a_4 do not depend on ω. Using MAPLE, we can replace ω^2 by its expression (3.25) and h_1 by $h_1 = d_2h_0/p_0$, which follows from the condition

$H(\tilde{x}) = G(\tilde{x})$. We obtain the expression of ρ given by (3.26). Under the assumption that $\rho \neq 0$ we conclude that (3.3) undergoes a non degenerate PAH bifurcation at $\tilde{E} = (\tilde{x}, \tilde{y})$, see Theorem 3.4.2 in [20]. □

Theorem 3.4 can also help to determine the existence of limit cycles for (3.3), This is a direct result of PAH bifurcation as explained in the following remark.

Remark 3.4. *If $H'(\tilde{x}) > G'(\tilde{x})$, then*

- *if $\rho < 0$, then there exists $\tilde{x}_1 > \tilde{x}$ such that if $x^* \in (\tilde{x}, \tilde{x}_1)$ then the corresponding equilibrium $E^*(x^*, h(x^*))$ is unstable and surrounded by a stable limit cycle,*
- *if $\rho > 0$, then there exists $\tilde{x}_1 < \tilde{x}$ such that if $x^* \in (\tilde{x}_1, \tilde{x})$ then the corresponding equilibrium $E^*(x^*, h(x^*))$ is stable and surrounded by a repelling limit cycle.*

Similarly if $H'(\tilde{x}) < G'(\tilde{x})$, then

- *if $\rho < 0$, then there exists $\tilde{x}_1 < \tilde{x}$ such that if $x^* \in (\tilde{x}_1, \tilde{x})$ then the corresponding equilibrium $E^*(x^*, h(x^*))$ is unstable and is surrounded by a stable limit cycle,*
- *while if $\rho > 0$, then there exists $\tilde{x}_1 > \tilde{x}$ such that if $x^* \in (\tilde{x}, \tilde{x}_1)$ then the corresponding equilibrium $E^*(x^*, h(x^*))$ is stable and is surrounded by a repelling limit cycle.*

3.5.4 Global asymptotic stability

In this section, the possibility of having a positive globally asymptotically stable (GAS) equilibrium is discussed. In the following theorem, we show that, if $E^*(x^*, y^*)$ lies on a descending branch of the prey isocline, then it can be GAS. More precisely, if graphically the horizontal line $y = y^*$ and the vertical line $x = x^*$ separate the isocline of the prey $h(x)$ into two disjoint portions, then $E^*(x^*, y^*)$ is GAS.

Theorem 3.5. *From assumptions $H_1 - H_3$, if (3.3) has a unique positive equilibrium E^* and the following condition holds*

$$(x - x^*)\,[h(x) - h(x^*)] \leq 0, \tag{3.33}$$

then, E^* is GAS.

Proof. Construct the following Lyapunov candidate function that is similar to that given [29]

$$V(x, y) = \int_{x^*}^{x} \frac{q(u) - d(u, y^*)}{p(u)} du + \int_{y^*}^{y} \frac{u - y^*}{u} du, \quad (x, y) \in \mathbb{R}_+ \times \mathbb{R}_+.$$

Then the time derivative of V along the solution of system (3.3) is given by

$$\begin{aligned}\frac{dV}{dt}(x,y) &= [q(x)-d(x,y^*)]\,[h(x)-y] + (y-y^*)\,[q(x)-d(x,y)] \\ &= [q(x)-d(x,y^*)]\,[h(x)-y^*] - (y-y^*)\,[d(x,y^*)-d(x,y)]\,.\end{aligned}$$

From the *mean value theorem*, we have

$$q(x)-d(x,y^*) = \left[q'(c_1)-d_x(c_1,y^*)\right](x-x^*),$$

and

$$d(x,y^*)-d(x,y) = -d_y(x,c_2)(y-y^*)^2,$$

where c_1 and c_2 are real constants such that c_1 is between x and x^* and c_2 is between y and y^*. Hence,

$$\frac{dV}{dt}(x,y) = \left[q'(c_1)-d_x(c_1,y^*)\right](x-x^*)\,[h(x)-y^*] - d_y(x,c_2)(y-y^*)^2.$$

From assumptions (3.33), H_1-H_3, we have

$$\frac{dV}{dt}(x,y) = \left[q'(c_1)-d_x(c_1,y^*)\right](x-x^*)\,[h(x)-y^*] - d_y(x,c_2)(y-y^*)^2 \leq 0.$$

Let S be the set defined by

$$S = \left\{(x,y)\in\mathbb{R}_+\times\mathbb{R}_+ : \frac{dV}{dt}(x,y) = 0\right\}.$$

Then, the largest invariant set M of system (3.3) in S is defined by $M=\{E^*(x^*,y^*)\}$. Hence, the global stability of E^* follows directly from LaSalle's Invariance Principle A.1. □

Fig.3.2 illustrates two possible situations where Theorem 3.5 applies. The arcs in orange indicate that $E^*(x^*,y^*)$ is GAS. Fig. 3.2 (a) shows the case where the function h has a minimum in $(0,K)$. Hence, condition (3.33) is verified if and only if $y^* < \min(h(x))$ on $(0,K)$. Fig. 3.2 (b) shows the case where the function h has not a minimum in $(0,K)$. In this situation, condition (3.33) is verified if and only if $y^* < h(0)$.
In general, condition (3.33) holds if and only if $y^* < \min(h(0), y_{min})$, where y_{min} is the global minimum of the function h in $(0,K)$.

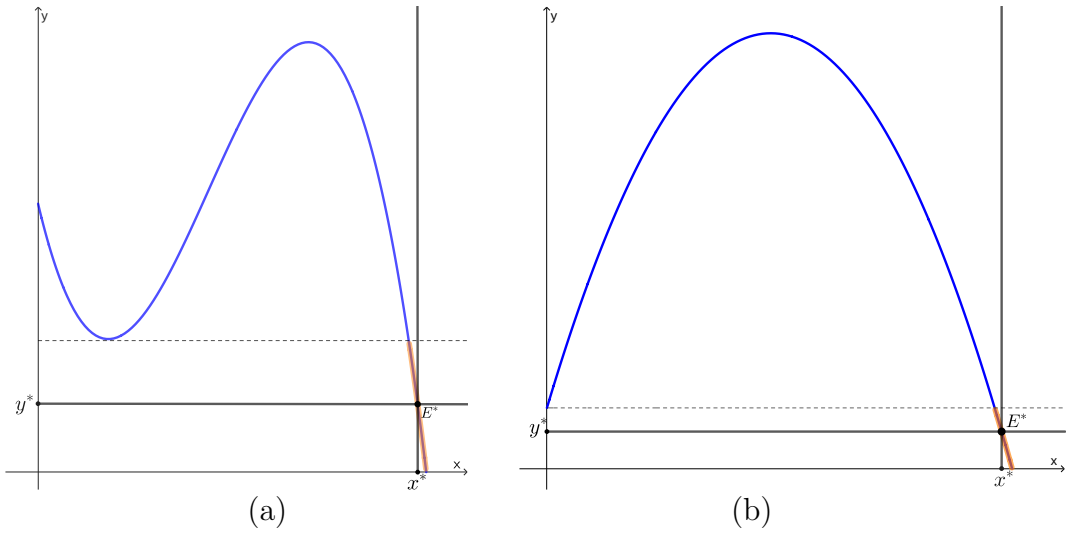

Figure 3.2: Schematic graphs of the prey isocline h in which $E^*(x^*, y^*)$ is GAS if it is on the part with orange colour.

Knowing that solutions are bounded, the global asymptotic stability of a unique positive equilibrium can be also established by showing the non-existence of a limit cycle around this point, which is the object of the following subsection.

3.5.5 Non-existence of limit cycles

The following theorems describe some situations where the non-existence of a limit cycle can be established. First, we give a graphical condition of the non-existence of a limit cycle when $d_y(x, y) = 0$.

Theorem 3.6. *Assume that* $d(x, y) = \tilde{d}(x) + m$ *and let*

$$\tilde{\phi}(x) := \frac{p'(x)h'(x) + p(x)h''(x)}{q'(x) - \tilde{d}'(x)}.$$

From assumptions H_1, H_2 *and* H_3, *if* $h'(x^*) < 0$ *and the following condition holds*

$$(x - x^*)\left[\tilde{\phi}(x) - \tilde{\phi}(x^*)\right] < 0, \quad \forall x \in (0, K), x \neq x^*, \tag{3.34}$$

then system (3.3) has no limit cycle.

Proof. Define the function $B(x, y) = p(x)^{-1}y^{\beta-1}$, where β is a real number to be determined. The divergence of the vector field $(Bdx/dt, Bdy/dt)$, noted Δ, is given by

$$\Delta = \frac{l(x)}{p(x)}y^{\beta-1},$$

where

$$l(x) = p(x)h'(x) + \beta \left[q(x) - \tilde{d}(x) - m\right].$$

Let $\beta = -\dfrac{p'(x^*)h'(x^*) + p(x^*)h''(x^*)}{q'(x^*) - \tilde{d}'(x^*)}$, then $l'(x)$ is given by

$$l'(x) = p'(x)h'(x) + p(x)h''(x) - \frac{p'(x^*)h'(x^*) + p(x^*)h''(x^*)}{q'(x^*) - \tilde{d}'(x^*)} \left[q'(x) - \tilde{d}'(x)\right]. \quad (3.35)$$

From H_2 and H_3, we rewrite $l'(x)$ as follows

$$l'(x) = \left[q'(x) - \tilde{d}'(x)\right] \left[\tilde{\phi}(x) - \tilde{\phi}(x^*)\right].$$

In addition, from (3.16), we have $l'(x^*) = 0$, $l'(x) > 0$ for $x < x^*$ and $l'(x) < 0$ for $x > x^*$, which indicates that $l(x^*) = p(x^*)h'(x^*)$ is the global maximum of $l(x)$. Hence, $\Delta < 0$ if and only if $h'(x^*) < 0$. Using Dulac criterion (see Theorem A.4), system (3.3) has no limit cycle provided that $h'(x^*) < 0$. □

The method of choosing an appropriate value of β in the proof of Theorem 3.6 to find the global maximum has been given in [39] for RMA type model (2.9) and in [38] for another type of the function p.

The following theorem gives a sufficient condition for the non-existence of a limit cycle when $d_y(x, y) \geq 0$.

Theorem 3.7. *From assumptions H_1 to H_3, if the following condition holds*

$$\forall (x, y) \in (0, K) \times \mathbb{R}^+, p(x)h'(x) - y d_y(x, y) < 0, \quad (3.36)$$

then, model (3.3) has no limit cycle.

Proof. Define $B(x, y) = [p(x)]^{-1} y^{-1}$, for all $x > 0$ and $y > 0$. The divergence Δ of the vector field $(B dx/dt, B dy/dt)$ is given by

$$\Delta = \frac{1}{y p(x)} \left[p(x)h'(x) - y d_y(x, y)\right].$$

Then, From H_1, H_2, H_3 and Condition (3.36), we have $\Delta < 0$. Using Dulac criterion (see Theorem A.4), model (3.3) has no limit cycle. □

Chapter 4

Applications from the ecological literature

In this chapter, we apply the main results obtained in Chapter 3 to different models with disappearance rates given in Table 3.1 which all verify conditions H_1–H_3. For All these models, we consider that g is the logistic growth function, p is the Holling II functional response and q is proportional to p. More exactly

$$g(x) = rx\left(1 - \tfrac{x}{K}\right), \qquad p(x) = \tfrac{ax}{c+x}, \qquad q(x) = ep(x) = \tfrac{eax}{c+x}, \tag{4.1}$$

where the parameters r, K, a, c and e are all positive biological parameters. Recall that r is the growth rate per capita of the prey, K is the carrying capacity of the prey, a is the maximum rate of prey consumption per unit of predator biomass, c is the half saturation constant for the prey and e is the rate of conversion of prey to predator.

With functions g and p given in (4.1), and according to (3.7), the prey isocline is the parabola $y = h(x)$ defined by

$$h(x) = \tfrac{r}{aK}(K - x)(c + x). \tag{4.2}$$

The top of the parabola is obtained for $x = \hat{x}$, where $\hat{x}$ is given by

$$\hat{x} := \tfrac{K-c}{2}. \tag{4.3}$$

Remember that we have assumed in Section 2.4 that $\hat{x}$ is positive. For the function q given in (4.1), a positive equilibrium exists if condition (3.14) of Theorem 3.1 is satisfied, that is

$$x_1 := q^{-1}(m) = \tfrac{mc}{ea-m} < K \iff \tfrac{eaK}{c+K} > m. \tag{4.4}$$

If $E^*(x^*, y^*)$ is a positive equilibrium, then $x_1 \leq x^* < K$, where x_1 is given in (4.4) such that $ea - m > 0$. The predator isocline is given implicitly according to Lemma 3.1 by

$$\frac{ea\varphi(y)}{c + \varphi(y)} - d(\varphi(y), y) = 0.$$

Except for RMA and Hsu models, $d_y(\varphi(y), y)$ is always positive in (3.11). Hence, the function $\psi = \varphi^{-1}$ exists and it can be obtained by solving in x the equation

$$\frac{eax}{c + x} = d(x, y).$$

The non-trivial predator isocline for each model is given by the following lemma.

Lemma 4.1. *For models of Table 3.1, the non-trivial predator isocline expression is given in Table 4.1.*

Proof. In RMA model, the predator isocline is given by

$$q(x) - m = 0 \iff \frac{eax}{c + x} - m = 0 \iff x = \varphi(y) = \frac{mc}{ea - m}.$$

For Hsu model, from (3.1), the predator isocline is given by

$$q(x) - d(x) = 0 \iff x = x_1.$$

For Bazykin model, the predator isocline is given by

$$q(x) - d(x, y) = 0 \iff \frac{eax}{c + x} - \alpha y - m = 0,$$

which leads to

$$y = \psi(x) = \frac{1}{\alpha}\left[\frac{(ea - m)x - mc}{c + x}\right].$$

In CF model, we have

$$q(x) - d(x, y) = 0 \iff \frac{eax}{c + x} - \frac{\alpha y}{1 + y} - m = 0,$$

hence,

$$y = \psi(x) = \frac{(ea - m)x - mc}{(\alpha - ea + m)x + (\alpha + m)c}.$$

For VT model, we have

$$q(x) - d(x, y) = 0 \iff \frac{eax}{c + x} - \frac{\alpha y}{\delta + x} - m = 0,$$

hence,

$$y = \psi(x) = \frac{\delta + x}{\alpha}\left[\frac{(ea - m)x - mc}{c + x}\right].$$

□

Table 4.1: Predator isocline of models in Table 3.1.

Model	Predator isocline
RMA model	$\varphi(y) = \dfrac{mc}{ea - m}$
Hsu model	$x = x_1$
Bazykin model	$\psi(x) = \dfrac{1}{\alpha}\left[\dfrac{(ea-m)x - mc}{c+x}\right]$
CF model	$\psi(x) = \dfrac{(ea-m)x - mc}{(\alpha - ea + m)x + (\alpha + m)c}$
VT model	$\psi(x) = \dfrac{\delta + x}{\alpha}\left[\dfrac{(ea-m)x - mc}{c+x}\right]$

The positive equilibria are the intersection points of the prey and predator isoclines.

The function H defined by (3.22) is written

$$H(x) = \frac{ax(K - c - 2x)}{(K - x)(c + x)^2}.$$

It should be noted that H is defined on $[0, K)$. It is positive for $x \in (0, \hat{x})$, negative for $x \in (\hat{x}, K)$ and satisfies $H(0) = 0$ and $H(\hat{x}) = 0$. It is increasing, then decreasing on the interval $[0, \hat{x}]$.

Table 4.2: The function G for each model in Table 3.1.

Model	$G(x) = d_y(x, h(x))$
RMA model	0
Hsu model	0
Bazykin model	α
CF model	$\dfrac{\alpha a^2 K^2}{[aK + r(K-x)(c+x)]^2}$
VT model	$\dfrac{\alpha}{\delta + x}$

The function G defined in (3.22) is non-negative, it depends only on the functions h and d. For each model in Table 3.1, the function G is given in Table 4.2.

In all figures of the following subsections, the non-trivial isoclines of the prey and predator are represented in blue and black colours respectively. The intersections of the non-trivial isoclines define the positive equilibria, which are plotted in blue dots when they are LES and in red dots when they are unstable, in addition to the two boundary equilibria, which are both saddle points.
The subset $\mathcal{A}$ of the ascending prey isocline branch in which the trace is non-negative, can be determined by solving the equation $H(x) = G(x)$. This equation can have at most two real roots noted x_L and x_R in $[0, \hat{x}]$. Therefore, the subset $\mathcal{A}$ is the closed arc

$$\mathcal{A} = \{(x, h(x)) : x_L \leq x \leq x_R\} \tag{4.5}$$

of the ascending branch of the prey isocline. This arc is plotted in red in all figures while the complementary arc is plotted in blue. If an equilibrium belongs to the red arc, then the trace is positive. If it belongs to the blue arc, the trace condition (3.16) holds.

Note that, the case $H(x) < G(x)$, for all x in $(0, K)$ corresponds to the non-existence of the arc $\mathcal{A}$ which means that the trace condition (3.16) is always verified for all positive equilibria.

We examine the change in phase portraits by increasing the value of m, which is chosen as the bifurcation parameter. It should be noted that, except the example in Fig. 4.11, the endpoints $(x_L, h(x_L))$ and $(x_R, h(x_R))$ of $\mathcal{A}$ do not change with m, since $H(x)$ and $G(x)$ do not.

4.1 Gause/RMA model

Recall that Gause type model is defined by the following system

$$\begin{cases} \dot{x} = g(x) - p(x)y = p(x)\left[h(x) - y\right], \\ \\ \dot{y} = \left[q(x) - m\right] y, \end{cases} \tag{4.6}$$

in which the disappearance rate $d(x, y) = m > 0$ does not depend on x nor on y. Hence, the function G is defined by $G(x) = 0$ and the closed arc becomes

$$\mathcal{A} = \{(x, h(x)) : 0 \leq x \leq \hat{x}\}.$$

4.1.1 PAH bifurcation

The only possibility to have a PAH bifurcation is for $\tilde{x} = \hat{x}$. Consequently, we have the following result which allows us to find the formula (2.8) of the Lyapunov coefficient in the literature from our general formula.

Proposition 4.1. *[23] For model (4.6), a PAH bifurcation can occur at $\tilde{x}$, if and only if $h_1 := h'(\tilde{x}) = 0$. Moreover, the first Lyapunov coefficient is given by*

$$\rho = \frac{1}{16}\left(2p_1h_2 + p_0h_3 - \frac{p_0q_2}{q_1}h_2\right), \tag{4.7}$$

with notations given in (3.24).

Proof. For (4.6), we have $\det A(\tilde{E}(\tilde{x},\tilde{y})) > 0$ and $\operatorname{tr} A(\tilde{E}(\tilde{x},\tilde{y})) = 0$, if and only if $h'(\tilde{x}) = 0$. Moreover, we have $d_2 = 0$, so only the first term $p_0h_0b_0$ in ρ given by (3.26) must be considered. Using the fact that all derivatives of d are equal to 0, the coefficient b_0 is given by

$$b_0 = 2p_0p_1q_1h_2 + p_0^2q_1h_3 - p_0^2q_2h_2.$$

Now, using (3.25) we have $\omega^2 = p_0h_0q_1$. Therefore, from (3.26), we have

$$\rho = \frac{1}{16p_0^2h_0q_1}p_0h_0b_0 = \frac{1}{16p_0q_1}b_0,$$

which is the expression given in the proposition. □

The formula (4.7) is the same as that given in equation (2.8). If we replace in (4.7) p, q and h by their expressions given in (4.1) and (4.2) respectively, we obtain

$$\rho = -\frac{r}{2K(c+K)},$$

which is always negative. Therefore, for RMA model (4.6), the PAH bifurcation is always supercritical. Note that, for other types of growth functions, it can be subcritical. This is the case, for instance, for the trigonometric growth function $q(x) = a\tanh(bx)$, as shown in [59].

4.1.2 Numerical simulations

In order to explain the stability results obtained for the RMA model with our graphical stability criterion, we choose the parameter values used in Fig. 2.2. The abscissa of the ends of the arc $\mathcal{A}$, are $x_L = 0$ and $x_R = \hat{x} = 2.35$, see Fig. 4.1.

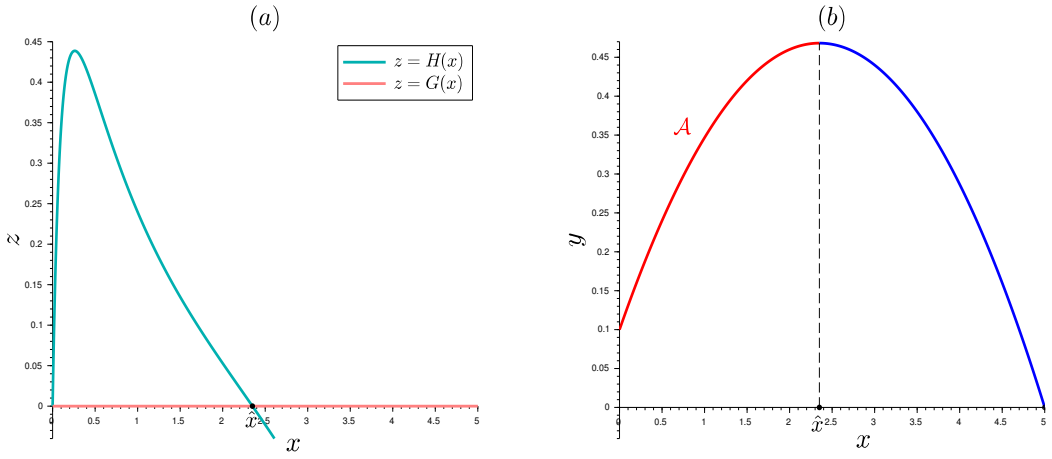

Figure 4.1: (a) : Graphs of functions H and G for RMA model with the parameter values of Fig. 2.2. (b) : The prey isocline and the corresponding arc $\mathcal{A}$.

The predator isocline passes through the maximum of the function h for $m = 0.3192$, that is to say for $\tilde{x} = \hat{x}$. The results on the existence and stability of the positive equilibrium are deduced from Theorem 3.3 and are summarized in Table 4.3. Moreover, for $m = 0.33$ in Fig. 2.2, the well known global asymptotic stability of the positive equilibrium $(x^*, h(x^*))$ can be re-obtained by Theorem 3.6 in which $\tilde{d}(x) = 0$. Indeed, $h'(x^*) < 0$ and the condition (3.34) is verified since the corresponding function $\tilde{\phi}$ is decreasing as shown by the graphical illustration of Fig. 4.2.

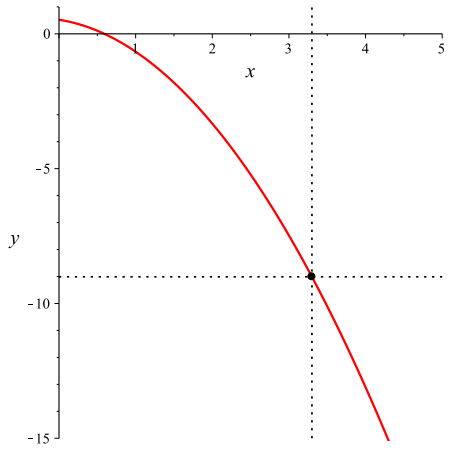

Figure 4.2: The function $\tilde{\phi}$ of Theorem 3.6 corresponding to Fig. 2.2, (b).

Table 4.3: The positive equilibrium of RMA model and its stability for the parameter values given in Fig. 2.2.

m	Behaviour of the system
$0 < m < 0.3192$	A unique positive unstable equilibrium
$m = 0.3192$	Supercritical PAH bifurcation ($\rho = -0.0037$)
$0.3192 < m$	At most one positive asymptotically stable equilibrium

4.2 Hsu model

The Hsu model is given by the following system

$$\begin{cases} \dot{x} = g(x) - yp(x), \\ \dot{y} = [q(x) - d(x)]\, y, \end{cases} \tag{4.8}$$

with the conditions (3.1). As in Gause model, the function G is defined by $G(x) = 0$ and the arc $\mathcal{A}$ becomes

$$\mathcal{A} = \{(x, h(x)) : 0 \leq x \leq \hat{x}\}.$$

4.2.1 PAH bifurcation

We have the following result.

Proposition 4.2. *[23] For model (4.8), a PAH bifurcation can occur at $\tilde{x}$, if and only if $h_1 := h'(\tilde{x}) = 0$. Moreover, the first Lyapunov coefficient is given by*

$$\rho = \frac{1}{16(q_1 - d_1)} \left(2p_1q_1h_2 + p_0q_1h_3 - p_0q_2h_2 - (p_0h_3 + 2p_1h_2)d_1 + p_0h_2d_{11}\right), \tag{4.9}$$

with notations given in (3.24).

Proof. For (4.8), we have $\det A(\tilde{E}(\tilde{x}, \tilde{y})) > 0$ and $\operatorname{tr} A(\tilde{E}(\tilde{x}, \tilde{y})) = 0$, if and only if $h'(\tilde{x}) = 0$. Moreover, we have $d_2 = 0$, so only the first term $p_0h_0b_0$ in ρ given by (3.26) must be considered. Using the fact that all derivatives of d are equal to 0, except for d_1 and d_{11}, the coefficient b_0 is given by

$$b_0 = 2p_0p_1q_1h_2 + p_0^2q_1h_3 - p_0^2q_2h_2 - (p_0^2h_3 + 2p_0p_1h_2)d_1 + p_0^2h_2d_{11}.$$

Using (3.25), we have $\omega^2 = p_0 h_0 (q_1 - d_1)$. Therefore, using (3.26), we have

$$\rho = \frac{1}{16 p_0^2 h_0 (q_1 - d_1)} p_0 h_0 b_0 = \frac{1}{16 p_0 (q_1 - d_1)} b_0,$$

which is the expression given in the proposition. □

To our knowledge, the formula (4.9) for ρ, is not known in the existing literature.

If we replace in (4.9) p, q and h by their expressions given in (4.1) and (4.2) respectively, the model (4.8) becomes

$$\begin{cases} \dot{x} = \left[r(1 - \dfrac{x}{K}) - \dfrac{ay}{c+x} \right] x, \\ \dot{y} = \left[\dfrac{eax}{c+x} - d(x) \right] y. \end{cases} \tag{4.10}$$

The next proposition gives a sufficient condition for the PAH bifurcation to be supercritical at $\tilde{x} = \hat{x} = (K - c)/2$.

Proposition 4.3. *Suppose that for (4.10) a PAH bifurcation occurs at $\tilde{x} = \hat{x}$. If the second derivative $d_{11} := d''(\tilde{x}) \geq 0$, then this bifurcation is supercritical.*

Proof. Using Proposition 4.2, replacing in (4.9) the functions p, q and h by their expressions given in (4.1) and (4.2) respectively, we obtain

$$\rho = -\frac{r\left[(K-c)(c+K)^2 d_{11} - 8c(c+K)d_1 + 16eac\right]}{\left[4eac - (c+K)^2 d_1\right](c+K)K}.$$

According to (3.1), we have $d_1 \leq 0$ and from the positiveness of $\hat{x}$, $K - c > 0$. Then, if $d_{11} \geq 0$, ρ is always negative. Therefore, the PAH is always supercritical. □

As an example, if we replace $d(x)$ in (4.10) by

$$d(x) = m + \frac{\alpha}{\delta + x}, \tag{4.11}$$

where α and δ are positive parameters, we have

$$d_{11} = d''(\tilde{x}) = \frac{2\alpha}{(\delta + \tilde{x})^3} > 0,$$

then, the PAH is supercritical.

4.2.2 Numerical simulations

We consider the disappearance rate given by (4.11) and the parameter values given in Table 4.4.

Table 4.4: Parameter values used in Hsu model. The value of m is depicted in each figure.

Figure	r	K	a	c	e	α	δ
Fig. 4.4	0.2	5	0.5	0.3	0.6	0.2	0.7

For these parameter values, the abscissa of the ends of the arc $\mathcal{A}$ are $x_L = 0$ and $x_R = \hat{x} = 2.35$, see Fig. 4.3.
The predator isocline passes through the maximum of the function h, at the point $(\hat{x}, h(\hat{x}))$, for $m_R = 0.20046$. This bifurcation value m_R of m is obtained by solving the equation $\hat{x} = \varphi(y)$, with respect to m, where φ is given in this example by

$$q(x) - d(x) = 0 \iff \frac{eax}{c+x} - \frac{\alpha}{\delta + x} - m = 0.$$

This leads to solving the following second algebraic equation

$$(ea - m)x^2 + (ea\delta - \delta m - cm - \alpha)x - c(\alpha + m\delta) = 0.$$

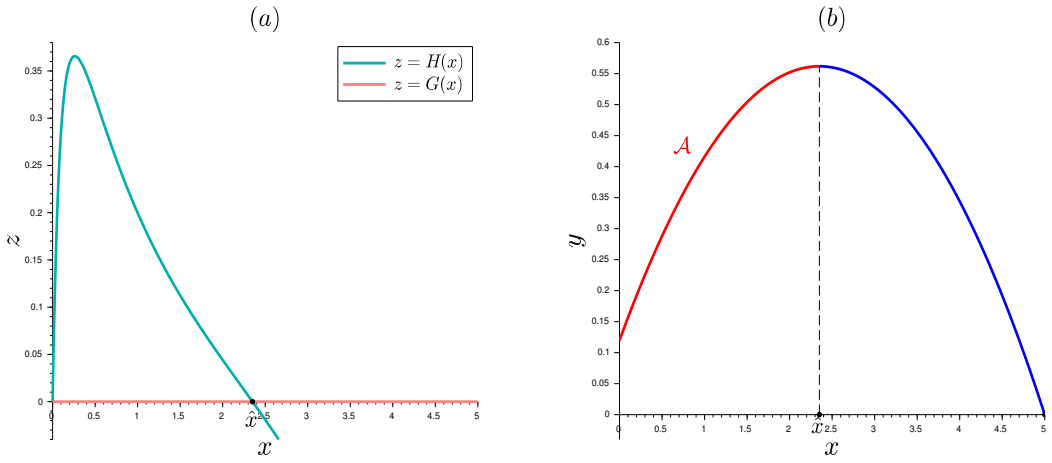

Figure 4.3: (a) : Graphs of functions H and G for Hsu model with parameter values given in Table 4.4. (b) : The corresponding arc $\mathcal{A}$ on the prey isocline.

We keep only its positive root $x = \varphi(y)$ given by

$$\varphi(y) = -\frac{\delta}{2} + \frac{cm + \alpha + \sqrt{(ea\delta - \delta m - cm - \alpha)^2 - 4c(ea - m)(\alpha + m\delta)}}{2(ea - m)}.$$

In Fig. 4.4, we give the main behaviours of (4.10) with the parameter values indicated in Table 4.4. They are similar to the RMA case.
The results on the existence and stability of the positive equilibrium are deduced from Theorem 3.3 and are summarized in Table 4.5.

Table 4.5: The positive equilibrium of Hsu model and its stability for the parameter values given in Table 4.4.

m	Behaviour of the system
$0 < m < 0.20046$	A unique positive unstable equilibrium
$m = 0.20046$	Supercritical PAH bifurcation ($\rho = -0.0034$)
$0.20046 < m$	At most one positive asymptotically stable equilibrium

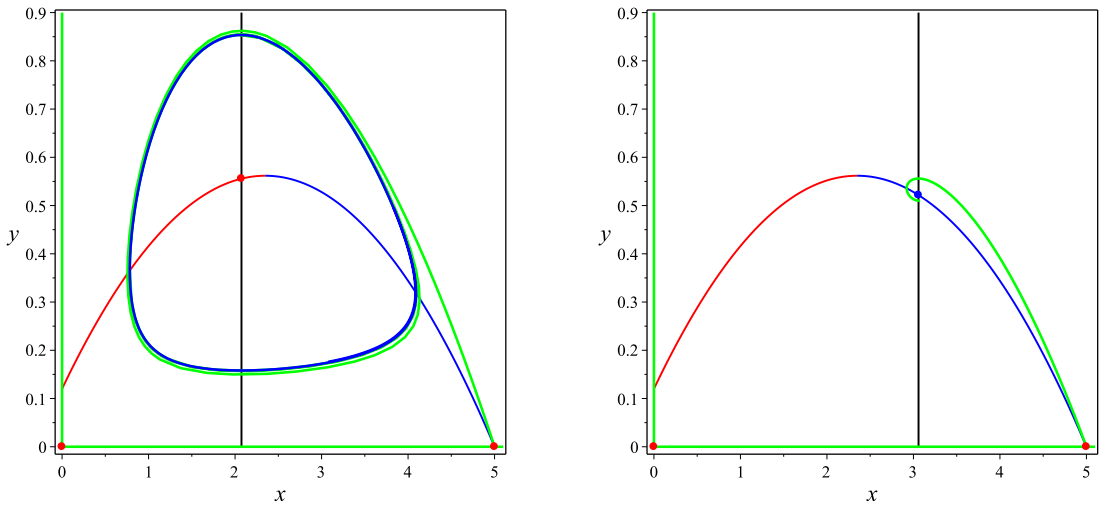

(a) $m = 0.19$ (b) $m = 0.22$

Figure 4.4: Some phase portraits of Hsu model with the parameter values given in Table 4.4.

Note that when $m < 0.20046$ the Poincaré-Bendixson theorem predicts that the system has at least one limit cycle which is stable in its exterior. Some of these behaviours are illustrated by numerical simulations.
For $m = 0.19$, the system has one positive equilibrium which is unstable, surrounded by a stable limit cycle (in blue). The unstable positive separatrix of $E_2(K, 0)$ (in green) converges towards this limit cycle, see Fig. 4.4(a).
For $m = 0.22$, the system has one positive equilibrium which is LES, the unstable positive separatrix of $E_2(K, 0)$ converges towards this equilibrium, see Fig. 4.4(b). The global asymptotic stability can be obtained by Theorem 3.6 in which $\tilde{d}(x) = \dfrac{\alpha}{\delta + x}$. Indeed, $h'(x^*) < 0$ and the Condition (3.34) is verified since the corresponding function $\tilde{\phi}$ is decreasing as shown by the graphical illustration of Fig. 4.5.

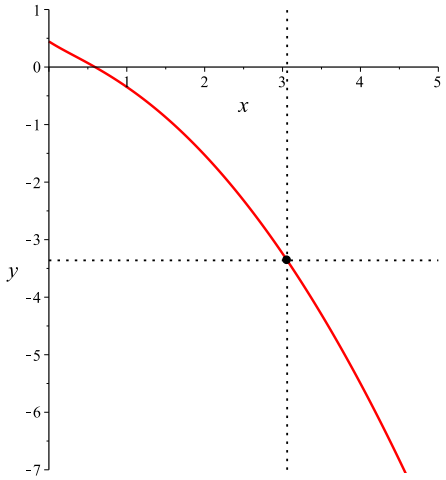

Figure 4.5: The function $\tilde{\phi}$ of Theorem 3.6 corresponding to Fig. 4.4, (b).

4.3 Bazykin model

Bazykin model is given by

$$\begin{cases} \dot{x} = g(x) - yp(x), \\ \dot{y} = [q(x) - \alpha y - m]\, y. \end{cases} \tag{4.12}$$

4.3.1 PAH bifurcation

Proposition 4.4. *[23] For model (4.12), a PAH bifurcation can occur at $\tilde{x}$, if and only if $q_1 - \alpha h_1 > 0$ and $p_0 h_1 / h_0 = \alpha$. Moreover, the first Lyapunov coefficient is given by*

$$\rho = \frac{1}{16(q_1 - \alpha h_1)} \left(c_0 + \frac{c_1}{p_0}\alpha + \frac{c_2}{p_0}\alpha^2 - \frac{p_2 h_0^2}{p_0^2}\alpha^3 \right), \tag{4.13}$$

where

$$\begin{aligned} c_0 &= 2p_1q_1h_2 + p_0q_1h_3 - p_0q_2h_2, \\ c_1 &= p_2q_1h_0 + p_0^2h_2^2 - p_1q_2h_0 - p_0q_1h_2, \\ c_2 &= q_2h_0 - p_1h_0h_2 - p_0h_0h_3, \end{aligned}$$

with notations given in (3.24).

Proof. For (4.12), we have

$$\det A(\tilde{E}(\tilde{x},\tilde{y})) = p(\tilde{x})h(\tilde{x})\left[q'(\tilde{x}) - \alpha h'(\tilde{x})\right].$$

Therefore $\det A(\tilde{E}(\tilde{x},\tilde{y})) > 0$ if and only if $q'(\tilde{x}) > \alpha h'(\tilde{x})$. On the other hand, we have

$$\operatorname{tr} A(\tilde{E}(\tilde{x},\tilde{y})) = p(\tilde{x})h'(\tilde{x}) - \alpha h(\tilde{x}).$$

Therefore $\operatorname{tr} A(\tilde{E}(\tilde{x},\tilde{y})) = 0$, if and only if $h'(\tilde{x}) = \alpha h(\tilde{x})/p(\tilde{x})$. Moreover, we have $d_2 = \alpha$. Using the fact that all other derivatives of d are equal to 0 we obtain

$$\begin{aligned} b_0 &= 2p_0p_1q_1h_2 + p_0^2q_1h_3 - p_0^2q_2h_2, \\ b_1 &= p_0p_2q_1h_0 + p_0^3h_2^2 - p_0p_1q_2h_0 - p_0^2q_1h_2, \\ b_2 &= p_0q_2 - p_0p_1h_2 - p_0^2h_3. \end{aligned}$$

Now, using (3.25) we have $\omega^2 = p_0h_0(q_1 - \alpha h_1)$. Therefore, using (3.26), we have

$$\rho = \frac{1}{16p_0^2(q_1 - \alpha h_1)}\left(p_0b_0 + b_1\alpha + h_0b_2\alpha^2 - p_2h_0^2\alpha^3\right),$$

which is the expression given in the proposition. □

To our knowledge, the formula (4.13) for ρ in Bazykin case, is known in the literature only for the specific case where g, p and q are of the form (4.1), see [43]. In what follows we give more details and information on this issue and we show how our formula (4.13) reduces in this special case to the formula of [43].
The Bazykin model, with g, p and q given by (4.1), is written

$$\begin{aligned} \dot{x} &= rx(1 - x/K) - \tfrac{ax}{c+x}y, \\ \dot{y} &= \left(e\tfrac{ax}{c+x} - \alpha y - m\right)y. \end{aligned} \tag{4.14}$$

The function G is defined by $G(x) = \alpha$ and the arc $\mathcal{A}$ becomes

$$\mathcal{A} = \{(x, h(x)) : x_L \le x \le x_R\}.$$

The difficulty in using formula (4.13) is that the value $\tilde{x}$ where the PAH bifurcation can occur is a solution of the equation $p_0 h_1/h_0 = \alpha$, i.e. $H(x) = G(x)$, which is written

$$\frac{ax(K-c-2x)}{(K-x)(c+x)^2} = \alpha. \tag{4.15}$$

This equation is equivalent to a third degree algebraic equation in x. To overcome this difficulty, and following [43], we parametrize Bazykin model (4.14) as follows

$$\begin{aligned} \dot{x} &= x(M-Nx) - \tfrac{B_1 x}{Q+x} y, \\ \dot{y} &= \left(\tfrac{B_2 x}{Q+x} - \tfrac{1}{N} y - P \right) y, \end{aligned} \tag{4.16}$$

where

$$B_1 = (M-N)(Q+1) \text{ and } B_2 = (P+1/N)(Q+1), \tag{4.17}$$

with $M > N > 0$, $P > 0$ and $Q > 0$, see the model (4.13) in [43]. There is a linear change of variable transforming system (4.14) in (4.16). The interest of the form (4.16) is that it has a positive equilibrium at $E(1,1)$. The study of the PAH bifurcation around $(1,1)$ in system (4.16), corresponds to the PAH bifurcation in (4.14) around a positive equilibrium where the determinant is positive and the trace is 0. This bifurcation occurs only if $H(1) = G(1) = 1/N$, which is equivalent to the following condition

$$M^* = \frac{N^2 Q + 2N^2 + Q + 1}{N}. \tag{4.18}$$

Now, we replace in (4.13), $\alpha = 1/N$, $\tilde{x} = 1$ and

$$g(x) = x(M-Nx), \quad p(x) = \frac{B_1 x}{Q+x}, \quad q(x) = \frac{B_2 x}{Q+x},$$

where B_1 and B_2 are defined by (4.17) and $M = M^*$ given by (4.18). We obtain the following expression for ρ,

$$\rho = -\frac{2(2N((N^2+1)Q^2+QN^2-N^2)+QP(1+N^2+2N^4+2N^2(N^2+1)Q))}{(Q+1)^2(Q+PNQ+QN^2+PN^3Q-1)},$$

which is the same, to a multiplicative positive factor, as the expression of the first Lyapunov coefficient σ_1 obtained by [43] on page 132.

4.3.2 Numerical simulations

In order to compare with some results in the literature, we choose the parameter values used in Figs. 4.5(a,d) of [43]. The parameters in (4.16), where B_1 and B_2 are given by (4.17), correspond to the following parameters in (4.14)

$$r = M, \quad K = \tfrac{M}{N}, \quad a = (M-N)(Q+1), \quad c = Q, \quad e = \tfrac{P+1/N}{M-N}, \quad \alpha = \tfrac{1}{N}, \tag{4.19}$$

and $m = P$. We use the values of M, N, P and Q given in Table 4.6. The value of m is depicted in each figure.
These values are chosen such that Fig. 4.7(d), where $m = P = 0.25$, corresponds to Fig. 4.5(a) of [43] and Fig. 4.8(b), where $m = P = 4/3 - 0.07$, corresponds to Fig. 4.5(d) of [43].

Table 4.6: Values of parameters M, N, P and Q .

Figure	M	N	P	Q
Figs. 4.6, 4.7	$5 - 0.03$	2	$1/4$	$1/5$
Fig. 4.8	$5 - 0.0015$	2	$4/3 - 0.07$	$1/5$

Recall that the abscissa x_L and x_R of the ends of the arc $\mathcal{A}$ are the roots of the third degree algebraic equation (4.15), which lay between 0 and $\hat{x}$, where $\hat{x}$ is given by (4.3).

First simulation

We give in Fig. 4.7 the plots corresponding to the values of the parameter r, K, a, c, e and α defined in Line 1 of Table 4.6 and various values of m, chosen such that the principal behaviours of (4.14) are illustrated.
For these parameter values, the abscissa x_L and x_R are given by $x_L = 0.0065$ and $x_R = 0.9924$, see Fig. 4.6 and 4.7.

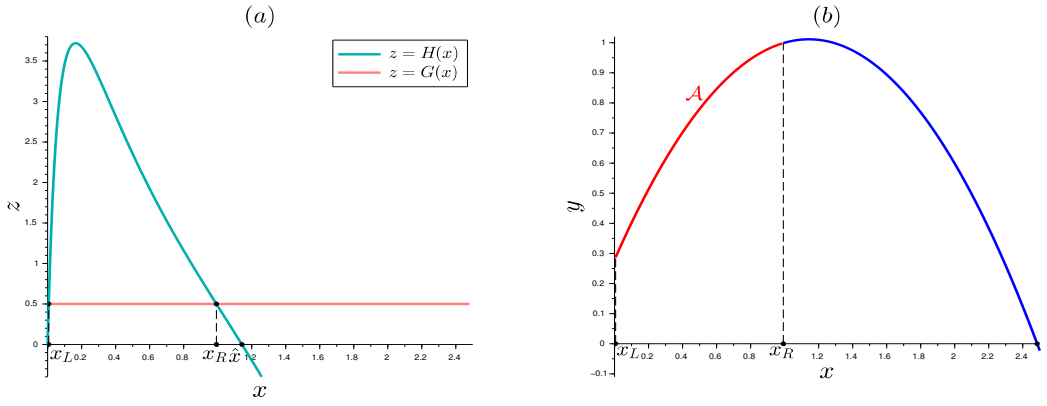

Figure 4.6: (a) : Graphs of the functions H and G for Bazykin model with parameter values given in Table 4.6. (b) : the corresponding arc $\mathcal{A}$ on the prey isocline.

The corresponding bifurcation values m_L and m_R of m are obtained by solving equation $\psi(x_i) = h(x_i)$, $i = L, R$, with respect to m, where ψ is given in Table 4.1. For these parameter values, $m_L = -0.1151$ and $m_R = 0.2496$. The first value corresponds to the passage of the predator isocline through the point $(x_L, h(x_L))$. This means that for $m = 0$, the positive equilibrium is on the arc $\mathcal{A}$. The second value corresponds to the passage of the predator isocline through the point $(x_R, h(x_R))$. Furthermore, the predator and prey isoclines are tangent when $m = 0.2468$ or $m = 0.2530$, which corresponds to saddle-node bifurcations. These two values are obtained firstly by solving the equation $h'(x) = \psi'(x)$, with respect to x. This leads to solving a third degree algebraic equation. We keep only its positive roots noted by x_1^{SN} and x_2^{SN}. For these parameter values, $x_1^{SN} = 0.5149$ and $x_2^{SN} = 0.8534$. Then, by solving the equation $\psi(x_i^{SN}) = h(x_i^{SN})$, $i = 1, 2$, with respect to m, we obtain the two values of m stated above. The results on the existence and stability of the positive equilibria are deduced from Theorem 3.3 and are summarized in Table 4.7.

Table 4.7: Positive equilibria of Bazykin model and their stability for the parameter values given in Line 1 of Table 4.6.

m	Behaviour of the system
$0 \leq m < 0.2468$	A unique positive (unstable) equilibrium
$m = 0.2468$	Saddle-node bifurcation
$0.2468 < m < 0.2496$	Three positive unstable equilibria
$m = 0.2496$	Subcritical PAH bifurcation ($\rho = 1.6678$)
$0.2496 < m < 0.2530$	Three positive equilibria, two unstable and one asymptotically stable
$m = 0.2530$	Saddle-node bifurcation
$0.2530 < m$	At most one positive asymptotically stable equilibrium

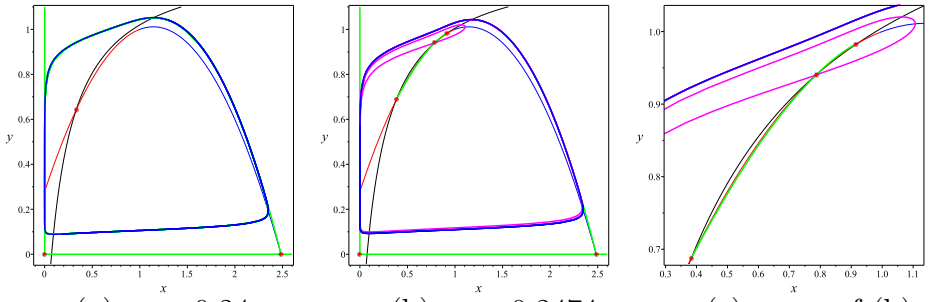

(a) $m = 0.24$ (b) $m = 0.2474$ (c) zoom of (b)

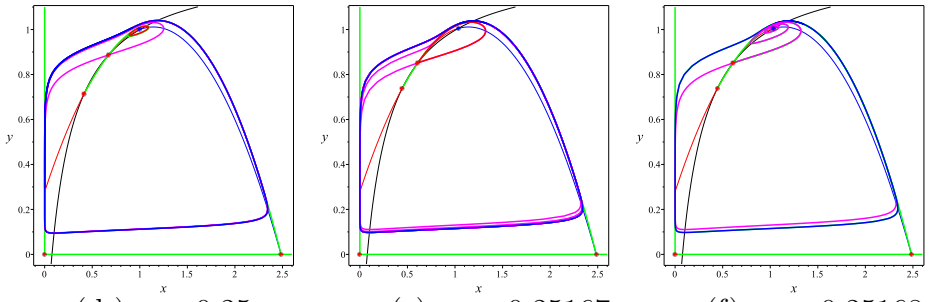

(d) $m = 0.25$ (e) $m = 0.25167$ (f) $m = 0.25168$

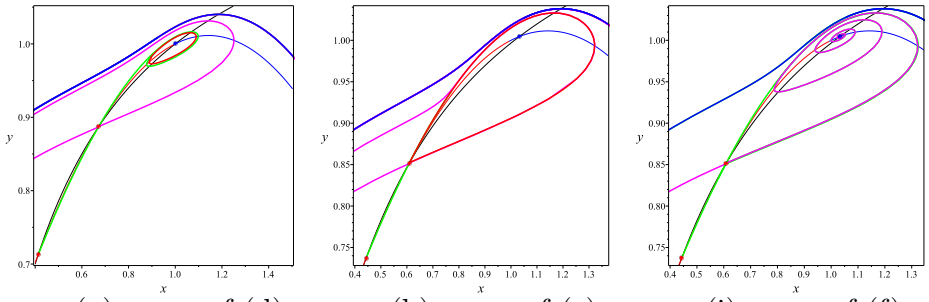

(g) zoom of (d) (h) zoom of (e) (i) zoom of (f)

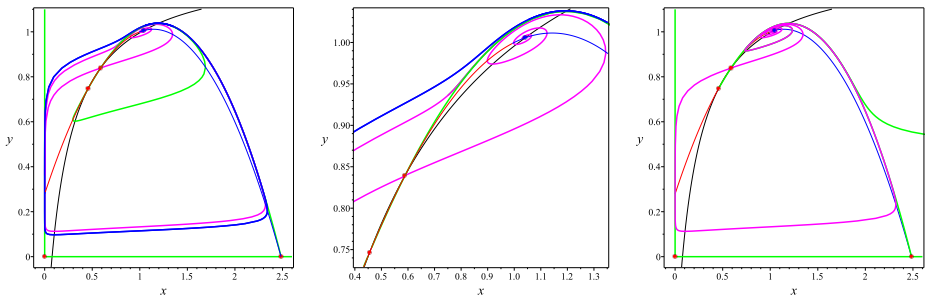

(j) $m = 0.25214$ (k) zoom of (j) (l) $m = 0.25215$

Figure 4.7: Some phase portraits of Bazykin model with the parameter values given in Line 1 of Table 4.6.

Note that when $m < 0.2496$, the Poincaré-Bendixson theorem predicts that the system has at least one limit cycle that is stable in the exterior. Indeed, in this case,

the system has only unstable equilibria.
The behaviours of (4.14) are illustrated by numerical simulations, which will also highlight homoclinic bifurcations.

For $m = 0.24$, the system has one positive equilibrium which is unstable, surrounded by a stable limit cycle (in blue). The unstable positive separatrix of $E_2(K, 0)$ (in green) converges towards this limit cycle, see Fig. 4.7 (a).

For $m = 0.2474$, the system has three positive equilibria. The left and right points are unstable, the middle one is a saddle. These equilibria are surrounded by the blue stable limit cycle, see Fig. 4.7 (b and c). Note that the unstable positive separatrix of $E_2(K, 0)$ and the unstable separatrices (in magenta) of the interior saddle point converge towards the limit cycle, while the stable separatrices (in green) of the interior saddle point each converge towards one of the two unstable equilibria when $t \to -\infty$.

For $m = 0.25$, which corresponds to Fig. 4.5(a) in [43], the system has three positive equilibria. The left one is unstable, the middle one is a saddle point and the right one is LES. These equilibria are surrounded by a big stable limit cycle (in blue). The right equilibrium is surrounded by a small unstable limit cycle (in red) which has been created by a subcritical PAH bifurcation for $m = 0.2496$, see Fig. 4.7 (d and g). Note that the unstable positive separatix of $E_2(K, 0)$ and the unstable separatrices of the interior saddle point converge towards the big limit cycle, while a stable separatrix of the interior saddle point converges towards the small cycle when $t \to -\infty$.

When the value of m increases, the unstable limit cycle grows and approaches the unstable separatrix of the positive saddle point.
When m crosses a value between 0.25167 and 0.25168 (see Fig. 4.7 (e and f) and their zooms), the unstable limit cycle disappears when meeting the saddle point by a homoclinic bifurcation.

For $m = 0.25167$, the stable separatrix is trapped between the unstable separatrix (magenta) and the small cycle.

For $m = 0.25168$, the unstable separatrix converges to the positive LES equilibrium and is surrounded by the stable separatrix. There has been a crossing of separatrices, leading to the destruction of the unstable cycle. The stable big cycle also disappears through a homoclinic bifurcation which occurs for a value of m between 0.25214 and 0.25215, see Fig. 4.7 (j and l).

Second simulation

In Fig. 4.8, we consider the parameter values indicated in Line 2 of Table 4.6. For these parameter values, the abscissa of the ends of the arc $\mathcal{A}$, are given by

$x_L = 0.0064$ and $x_R = 0.9996$. Note that the predator isocline passes through the ends of the arc $\mathcal{A}$ for $m = m_L = -0.0768$ or $m = m_R = 1.2632$. The first value corresponds to the passage of the predator isocline through point $(x_L, h(x_L))$. The second value corresponds to the passage of the predator isocline through point $(x_R, h(x_R))$.

Table 4.8: The positive equilibrium of Bazykin model and its stability for the parameter values given in Line 2 of Table 4.6.

m	Behaviour of the system
$0 \leq m < 1.2632$	A unique positive (unstable) equilibrium
$m = 1.2632$	Subcritical PAH bifurcation ($\rho = 0.0213$)
$1.2632 < m$	At most one positive asymptotically stable equilibrium

The results on the existence and stability of the positive equilibrium are deduced from Theorem 3.3 and are summarized in Table 4.8.

When $m < 1.2632$, the Poincaré-Bendixson theorem predicts that the system has at least one limit cycle that is stable in the exterior and surrounding the unique unstable positive equilibrium. Numerical simulations in Fig. 4.8 illustrate these behaviours and also highlight a saddle node bifurcation of cycles.

For $m = 1.217$, the system has one positive equilibrium which is unstable and surrounded by a stable limit cycle (in blue). The unstable positive separatrix of $E_2(K, 0)$ (in green) converges towards this limit cycle, see Fig. 4.8 (a).

For $m = 4/3 - 0.07$, which corresponds to Fig. 4.5 (d) in [43], the system has one positive equilibrium which is LES and is surrounded by two limit cycles, a big stable one (in blue) and a small unstable one (in red). The small limit cycle has been created by a subcritical PAH bifurcation for $m = 1.2632$, see Fig. 4.8 (b and c). Note that the unstable positive separatix of $E_2(K, 0)$ still converges towards the big limit cycle.

For $m = 1.2636$, the cycles approach each other, the stable one getting smaller, and the unstable one getting bigger. The two cycles disappear through a saddle node bifurcation of cycles which occurs for a value of m between 1.2636 and 1.2637, see Fig. 4.8 (d, e and f).

For $m = 1.2637$, the unstable separatrix of $E_2(K, 0)$ converges to the positive LES equilibrium, see Fig. 4.8 (f).

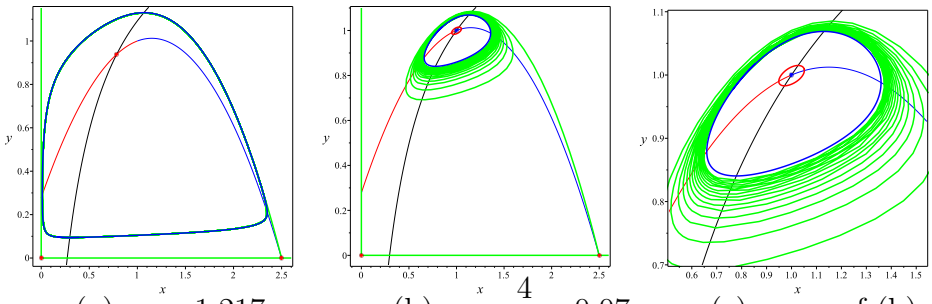

(a) $m = 1.217$ (b) $m = \frac{4}{3} - 0.07$ (c) zoom of (b)

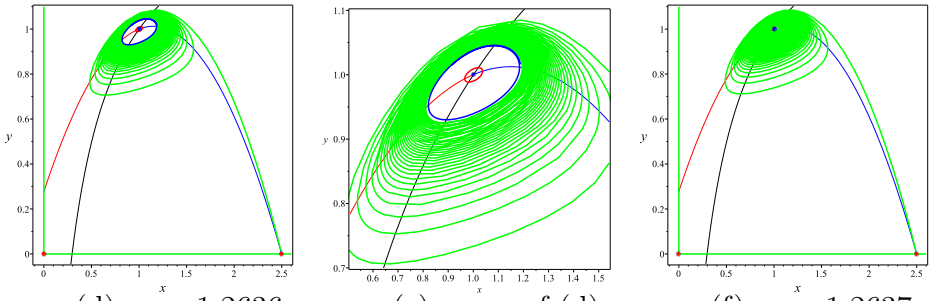

(d) $m = 1.2636$ (e) zoom of (d) (f) $m = 1.2637$

Figure 4.8: Some phase portraits of Bazykin model with the parameter values given in Line 2 of Table 4.6.

4.4 Cavani-Farkas (CF) model

In Cavani-Farkas model, system (3.3) is written

$$\begin{cases} \dot{x} = g(x) - yp(x), \\ \dot{y} = \left[q(x) - \frac{\alpha y}{1+y} - m\right] y. \end{cases} \tag{4.20}$$

The equation $H(x) = G(x)$ becomes, with g, p and q given by (4.1),

$$\frac{ax(K - c - 2x)}{(K - x)(c + x)^2} = \frac{\alpha}{(1 + h(x))^2}, \tag{4.21}$$

where h is given by (4.2). It is a sixth degree algebraic equation in x. The values x_L and x_R are the roots that lay between 0 and $\hat{x}$, where $\hat{x}$ is given by (4.3).

4.4.1 PAH bifurcation

The exponent ρ is given by the following proposition.

Proposition 4.5. *For model (4.20), a PAH bifurcation can occur at $\tilde{x}$, if and only if $q_1 - \alpha h_1/(1+h_0)^2 > 0$ and $p_0 h_1/h_0 = \alpha/(1+h_0)^2$. In addition, we have*

$$\rho = \frac{1}{16p_0(1+h_0)^4\left[p_0q_1(1+h_0)^4 - \alpha^2 h_0\right]}\left(e_0 + e_1\alpha + e_2\alpha^2 + e_3\alpha^3\right), \tag{4.22}$$

where

$$\begin{aligned}
e_0 &= p_0^2(1+h_0)^8(p_0q_2h_2 - 2p_1q_1h_2 - p_0q_1h_3^2),\\
e_1 &= p_0(1+h_0)^4\left[(1+h_0)^2(-p_0^2h_2^2 + p_1q_2h_0 - p_2q_1h_0 + p_0q_1h_2) + 2q_1^2h_0(h_0-2)\right],\\
e_2 &= h_0(1+h_0)^3\left[p_0(1+h_0)(p_1h_2 + p_0h_3) + p_0q_2h_0 + 2p_1q_1h_0 - p_0q_2\right],\\
e_3 &= h_0^2\left[p_2(1+h_0)^2 + 2q_1\right].
\end{aligned}$$

Proof. For (4.20), we have

$$detA(\tilde{E}(\tilde{x},\tilde{y})) = p(\tilde{x})h(\tilde{x})\left[q'(\tilde{x}) - \frac{\alpha}{(1+h(\tilde{x}))^2}h'(\tilde{x})\right].$$

Therefore $\det A(\tilde{E}(\tilde{x},\tilde{y})) > 0$ if and only if $q'(\tilde{x}) > \alpha/((1+h(\tilde{x}))^2)h'(\tilde{x})$. On the other hand, we have

$$trA(\tilde{E}(\tilde{x},\tilde{y})) = p(\tilde{x})h'(\tilde{x}) - \alpha h(\tilde{x})/(1+h(\tilde{x}))^2.$$

Therefore $trA(\tilde{E}(\tilde{x},\tilde{y})) = 0$, if and only if $h'(\tilde{x}) = \alpha h(\tilde{x})/\left[(1+h(\tilde{x}))^2 p(\tilde{x})\right]$. Moreover, all derivatives of d with respect to x are equal to 0 and we have

$$d_2 = \frac{\alpha}{(1+h_0)^2}, \quad d_{22} = -\frac{2\alpha}{(1+h_0)^3}, \quad d_{222} = \frac{6\alpha}{(1+h_0)^4},$$

$$w^2 = \frac{h_0}{(1+h_0)^4}\left[q_1p_0(1+h_0)^4 - \alpha^2h_0\right].$$

We obtain

$$\begin{aligned}
b_0 &= 2p_0p_1q_1h_2 + p_0^2q_1h_3 - p_0^2q_2h_2 + \frac{2(2-h_0)q_1^2h_0\alpha}{(1+h_0)^3},\\
b_1 &= p_0p_2q_1h_0 + p_0^3h_2^2 - p_0p_1q_2h_0 - p_0^2q_1h_2 - \frac{2(p_1q_1+p_0q_2)h_0^2\alpha}{(1+h_0)^3} - \frac{4q_1h_0^3\alpha^2}{(1+h_0)^6},\\
b_2 &= p_0q_2 - p_0p_1h_2 - p_0^2h_3 - (1-2h_0)\frac{2q_1h_0\alpha}{(1+h_0)^4}.
\end{aligned}$$

Therefore

$$\rho = \frac{1}{16p_0\left[q_1p_0(1+h_0)^4 - \alpha^2h_0\right]}\left(p_0b_0 + \frac{b_1\alpha}{(1+h_0)^2} + \frac{h_0b_2\alpha^2}{(1+h_0)^4} - \frac{p_2h_0^2\alpha^3}{(1+h_0)^6}\right).$$

Hence, writing the numerator of ρ as a polynomial in α, we obtain the expression given in the proposition. □

4.4.2 Numerical simulations

First simulation

In Fig. 4.10, we give the main behaviours of (4.20) with the values of the parameters indicated in Line 1 of Table 4.11. These values were chosen to show the possibility of having homoclinic bifurcation in CF model. For these parameter values, the abscissa of the ends of the arc $\mathcal{A}$ are given by $x_L = 0.1365$ and $x_R = 0.4717$, see Fig. 4.9 and Fig. 4.10.

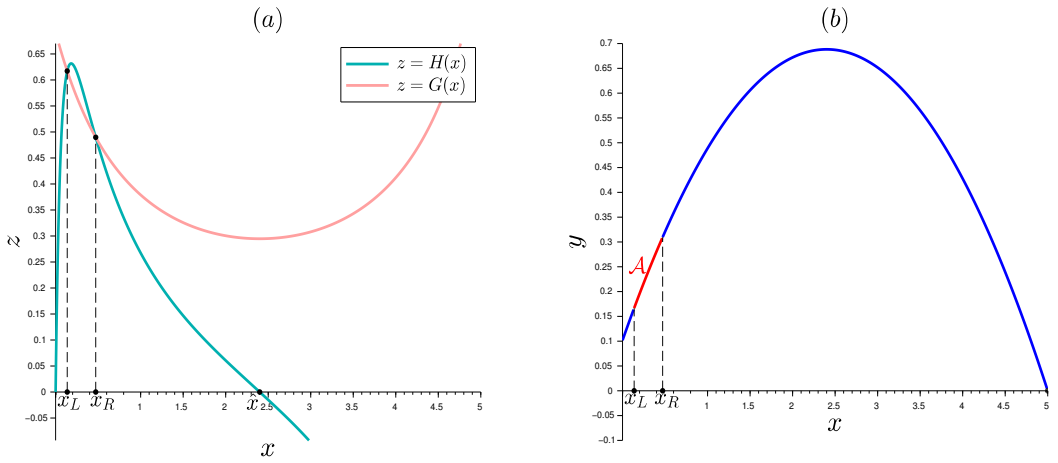

Figure 4.9: (a) : Graphs of the functions H and G for CF model with parameter values given in Line 1 of Table 4.11. (b) : the corresponding arc $\mathcal{A}$ on the prey isocline.

Note that the predator isocline passes through the ends of the arc $\mathcal{A}$ if $m = m_L = 0.0473$ and $m = m_R = 0.0910$. The first value corresponds to the passage of the predator isocline through the point $(x_L, h(x_L))$. The second value corresponds to the passage of the predator isocline through the point $(x_R, h(x_R))$. The bifurcation values m_L and m_R are obtained by solving equation $\psi(x_i) = h(x_i)$, $i = L, R$, with respect to m. For the second value, $E^*(x_R, h(x_R))$ is a saddle point since $\det A(E^*(x^*, y^*)) < 0$. Hence, Condition (3.23) is not verified and the PAH bifurcation does not occur at $m = m_R$.
Furthermore, the isocline of the predator is tangent to the isocline of the prey, which corresponds to a saddle-node bifurcation, when $m = 0.0368$ or $m = 0.0911$. These two values are obtained firstly by solving the equation $h'(x) = \psi'(x)$, with respect to m. We find a value of $m = m(x)$ that depends on x. Substituting $m(x)$ in ψ and solving the equation $h(x) = \psi(x)$ with respect to x, we only keep the positive

roots, noted by x_1^{SN} and x_2^{SN}. With our parameter values, we find $x_1^{SN} = 2.1536$ and $x_2^{SN} = 0.4454$. Then, by solving the equation $\psi(x_i^{SN}) = h(x_i^{SN})$, $i = 1, 2$, with respect to m, we obtain the two values of m stated above.

Table 4.9: Positive equilibria of CF model and their stability for the parameter values given in Line 1 of Table 4.11.

m	Behaviour of the system
$0 < m < 0.0368$	A unique positive asymptotically stable equilibrium
$m = 0.0368$	Saddle-node bifurcation
$0.0368 < m < 0.0473$	Three positive equilibria, two asymptotically stable and one unstable
$m = 0.0473$	Supercritical PAH bifurcation ($\rho = -0.0272$)
$0.0473 < m < 0.0911$	Three positive equilibria, two unstable and one asymptotically stable
$m = 0.0911$	Saddle-node bifurcation
$0.0911 < m$	At most one positive equilibrium which is stable

The results on the existence and stability of the positive equilibria are deduced from Theorem 3.3 and are summarized in Table 4.9.

Some behaviours of (4.20) are given by numerical simulations in Fig.. 4.10 which will also highlight homoclinic bifurcation.

For $m = 0.02$, the system has one positive equilibrium, which is LES and the unstable positive separatrix of $E_2(K, 0)$ (in green) converges towards this equilibrium, see Fig. 4.10 (a).

For $m = 0.038$, the system has three positive equilibria. The left and the right point are LES, the middle is a saddle, see Fig. 4.10 (b). Note that the unstable positive separatrix of $E_2(K, 0)$ converges towards the right LES point. The unstable separatrices (in magenta) each converge to one of the two LES equilibria.

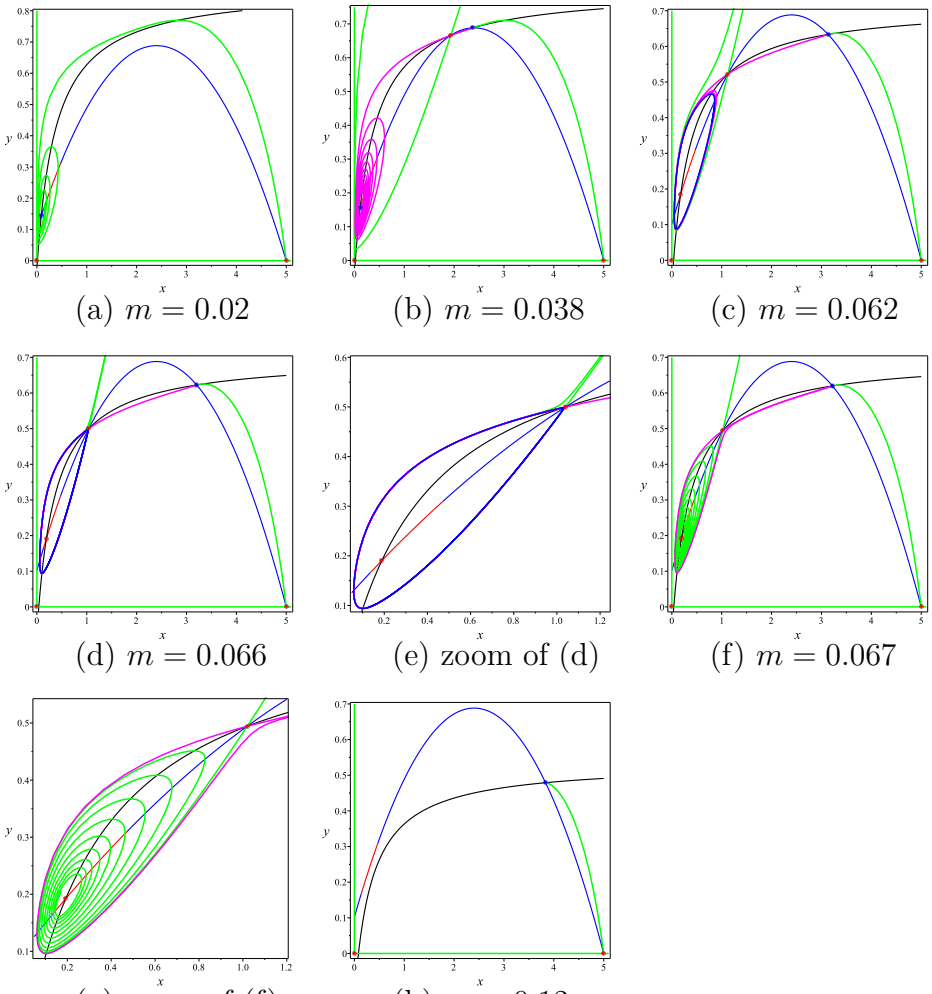

(a) $m = 0.02$ (b) $m = 0.038$ (c) $m = 0.062$

(d) $m = 0.066$ (e) zoom of (d) (f) $m = 0.067$

(g) zoom of (f) (h) $m = 0.12$

Figure 4.10: Some phase portraits of CF model with the parameter values given in Line 1 of Table 4.11.

For $m = 0.062$, the system has three positive equilibria. The left one is unstable, the middle one is a saddle point and the right one is LES. The left equilibrium is surrounded by a stable limit cycle (in blue) which has been created by a supercritical PAH bifurcation for $m = 0.0473$, see Fig. 4.10 (c). The unstable positive separatrix of $E_2(K, 0)$ converges towards the right equilibrium while unstable separatrices converge one towards the limit cycle, the other towards the LES equilibrium. When the value of m increases, the stable limit cycle grows and approaches the unstable separatrix of the positive saddle point.

When m crosses a value between 0.066 and 0.067, (see Fig. 4.10 (d and f) and their zooms), the stable limit cycle disappears when meeting the saddle point by a

homoclinic bifurcation. There has been a crossing of stable and unstable separatrices.

For $m = 0.12$, the system has one positive equilibrium which is LES, the unstable positive separatrix of $E_2(K, 0)$ converges towards this equilibrium, see Fig. 4.10 (h).

Second simulation

Actually, for the CF model, as written for example in [15], $\alpha = \delta - m$, where δ is a constant, and thus depends on m. It is the case of the parameter values indicated in Line 2 of Table 4.11, for which the bifurcation diagram of Fig. 3 (a) was dressed in [15]. The authors gave there the bifurcation values $m_1 = 0.5806$ and $m_2 = 2.265$. Note that in this case, the arc $\mathcal{A}$ varies with m, since it depends on α which varies with m. We can predict the existence and stability of the positive equilibrium by the use of Theorem 3.3 (see Table 4.10).

Table 4.10: The positive equilibrium of CF model and its stability for the parameter values given in Line 2 of Table 4.11 .

m	Behaviour of the system
$0 \leq m < 0.5806$	A unique positive asymptotically stable equilibrium
$m = 0.5806$	Supercritical PAH bifurcation ($\rho = -0.3565$)
$0.5806 < m < 2.265$	A unique positive (unstable) equilibrium
$m = 2.265$	Supercritical PAH ($\rho = -0.4177$)
$2.265 < m$	At most one positive equilibrium which is stable

Numerical simulations are reproduced in Fig. 4.11. Note that, when $0.5806 < m < 2.265$, the Poincaré-Bendixson theorem predicts that the system has at least one limit cycle that is stable in the exterior.

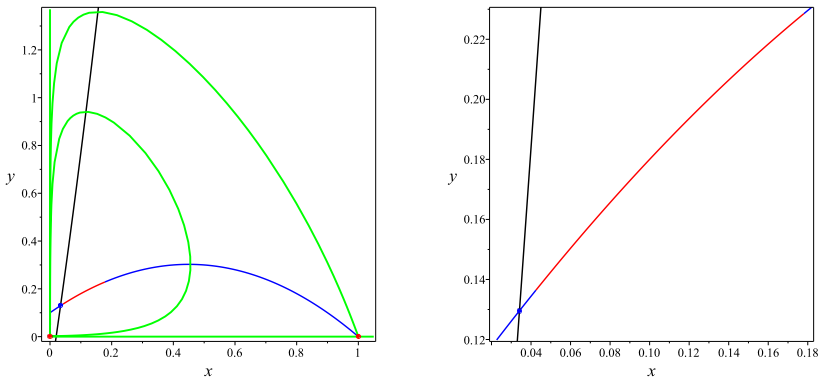

(a) $m = 0.5$ (b) zoom of (a)

(c) $m = 1.5$ (d) $m = 2.288$

Figure 4.11: Some phase portraits of CF model with the parameter values given in Line 2 of Table 4.11. The red arc $\mathcal{A}$ depends on m.

For $m = 0.5$, the system has one positive equilibrium which is LES. The unstable positive separatrix of $E_2(K, 0)$ (in green) converges towards this equilibrium, see Fig. 4.11 (a and b).

For $m = 1.5$, the system has one positive equilibrium which is unstable and surrounded by a stable limit cycle (in blue) which has been created by a supercritical PAH bifurcation for $m = 0.5806$, see Fig. 4.11 (c). Note that the unstable positive separatrix of $E_2(K, 0)$ converges towards this stable limit cycle.

For $m = 2.288$, the unstable positive separatrix of $E_2(K, 0)$ converges to the unique positive LES equilibrium, see Fig. 4.11 (d).

For $m = 2.265$, the cycle disappears through a supercritical PAH bifurcation and not subcritical, as claimed in [15].

Here is briefly the procedure that allows us to find the bifurcation values : the PAH bifurcation values m_1 and m_2 are given by solving the equation (4.21) where $\alpha = \delta - m$, with respect to m. We find a value of $m = m(x)$ that depends on x.

We substitute $m(x)$ in ψ, where ψ is given in Table 4.1, and solve the equation $h(x) = \psi(x)$ with respect to x. We only keep the positive roots which are smaller than K, noted by x_1 and x_2. With our parameter values, we find $x_1 = 0.0390$ and $x_2 = 0.3905$. Then, by solving the equation $\psi(x_i)) = h(x_i)$, $i = 1, 2$, with respect to m, we obtain the two same values of m given in [15].

Table 4.11: Parameter values used in the CF model. The value of m is depicted in each figure.

Figure	r	K	a	c	e	α
Figs. 4.9, 4.10	0.28	5	0.55	0.2	0.75	0.84
Fig. 4.11	1	1	1	0.1	3	$2.8 - m$

4.5 Variable-Territory (VT) model

VT model is given by

$$\begin{cases} \dot{x} = g(x) - yp(x), \\ \dot{y} = \left[q(x) - \dfrac{\alpha y}{\delta + x} - m\right] y. \end{cases} \tag{4.23}$$

The equation $H(x) = G(x)$ becomes now, with g, p and q given by (4.1),

$$\frac{ax(K - c - 2x)}{(K - x)(c + x)^2} = \frac{\alpha}{\delta + x}.$$

It is a third degree algebraic equation in x. The values x_L and x_R are the roots that lay between 0 and $\hat{x}$.

4.5.1 PAH bifurcation

The coefficient ρ is given by the following proposition.

Proposition 4.6. *For model (4.23), a PAH bifurcation can occur at $\tilde{x}$, if and only if $q_1 + \alpha h_0/(\delta + \tilde{x})^2 - \alpha h_1/(\delta + \tilde{x}) > 0$ and $p_0 h_1/h_0 = \alpha/(\delta + \tilde{x})$. In addition, we have*

$$\rho = \frac{f_0 + f_1\alpha + f_2\alpha^2 + f_3\alpha^3}{16(\delta + \tilde{x})^2 p_0 \left[-p_0 q_1 (\delta + \tilde{x})^2 + \alpha h_0(\alpha - p_0)\right]}, \tag{4.24}$$

where

$$
\begin{aligned}
f_0 &= p_0^2(\delta+\tilde{x})^4(p_0q_2h_2 - 2p_1q_1h_2 - p_0q_1h_3),\\
f_1 &= p_0(\delta+\tilde{x})\Big[(\delta+\tilde{x})^2(-p_0^2h_2^2 + p_1q_2h_0 - p_2q_1h_0 + p_0q_1h_2)\\
&\quad + p_0h_0(\delta+\tilde{x})(-2p_1h_2 - p_0h_3 + q_2) + 2p_0h_0(-p_0h_2 + q_1)\Big],\\
f_2 &= p_0h_0\left[(\delta+\tilde{x})^2(p_1h_2 + p_0h_3 - q_2) + (\delta+\tilde{x})(-p_2h_0 + 2p_0h_2 - 2q_1) - 2p_1h_0\right],\\
f_3 &= h_0^2\left[p_2(\delta+\tilde{x}) + 2p_1\right].
\end{aligned}
$$

Proof. For (4.23), we have

$$
\det A(\tilde{E}(\tilde{x},\tilde{y})) = p(\tilde{x})h(\tilde{x})\left[q'(\tilde{x}) + \frac{\alpha h(\tilde{x})}{(\delta+\tilde{x})^2} - \frac{\alpha h'(\tilde{x})}{\delta+\tilde{x}}\right].
$$

Therefore $\det A(\tilde{E}(\tilde{x},\tilde{y})) > 0$ if and only if $q'(\tilde{x}) > -\alpha h(\tilde{x})/(\delta+\tilde{x})^2 + \alpha h'(\tilde{x})/(\delta+\tilde{x})$. On the other hand, we have

$$
trA(\tilde{E}(\tilde{x},\tilde{y})) = p(\tilde{x})h'(\tilde{x}) - \alpha h(\tilde{x})/(\delta+\tilde{x}).
$$

Therefore $trA(\tilde{E}(\tilde{x},\tilde{y})) = 0$, if and only if $h'(\tilde{x}) = \alpha h(\tilde{x})/\left[(\delta+\tilde{x})p(\tilde{x})\right]$. Moreover, using the fact that $d_{22} = d_{222} = d_{122} = 0$,

$$
\begin{aligned}
d_1 &= -\frac{\alpha h_0}{(\delta+\tilde{x})^2}, \quad d_2 = \frac{\alpha}{\delta+\tilde{x}}, \quad d_{11} = \frac{2\alpha h_0}{(\delta+\tilde{x})^3}, \quad d_{12} = -\frac{\alpha}{(\delta+\tilde{x})^2},\\
d_{112} &= \frac{2\alpha}{(\delta+\tilde{x})^3}, \quad w^2 = \frac{h_0}{(\delta+\tilde{x})^2}\left[p_0q_1(\delta+\tilde{x})^2 + \alpha p_0h_0 - \alpha^2h_0\right],
\end{aligned}
$$

we obtain

$$
\begin{aligned}
b_0 &= 2p_0p_1q_1h_2 + p_0^2q_1h_3 - p_0^2q_2h_2 + \frac{2p_0^2h_0h_2\alpha}{(\delta+\tilde{x})^3} - \frac{p_0q_2h_0\alpha}{(\delta+\tilde{x})^2} - \frac{2p_0q_1h_0\alpha}{(\delta+\tilde{x})^3}\\
&\quad + \left(p_0^2h_3 + 2p_0p_1h_2\right)h_0\frac{\alpha}{(\delta+\tilde{x})^2},\\
b_1 &= p_0p_2q_1h_0 + p_0^3h_2^2 - p_0p_1q_2h_0 - p_0^2q_1h_2 + \frac{2p_0p_1h_0^2\alpha}{(\delta+\tilde{x})^3}\\
&\quad - (2p_0h_2 - 2q_1 - p_2h_0)\frac{p_0h_0\alpha}{(\delta+\tilde{x})^2},\\
b_2 &= p_0q_2 - p_0p_1h_2 - p_0^2h_3 - \frac{2p_1h_0\alpha}{(\delta+\tilde{x})^2}.
\end{aligned}
$$

Therefore

$$
\rho = \frac{(\delta+\tilde{x})^2}{16p_0\left[p_0q_1(\delta+\tilde{x})^2 + \alpha p_0h_0 - \alpha^2h_0\right]}\left(p_0b_0 + \frac{b_1\alpha}{\delta+\tilde{x}} + \frac{b_2h_0\alpha^2}{(\delta+\tilde{x})^2} - \frac{p_2h_0^2\alpha^3}{(\delta+\tilde{x})^3}\right).
$$

Hence, writing the numerator of ρ as a polynomial in α, we obtain the expression given in the proposition. □

4.5.2 Numerical simulations

First simulation

We first consider the parameter values indicated in Line 1 of Table 4.14. These values were chosen to reproduce, for $m = 2.4$ and $\delta = 0$, the case of Fig.1 (phase plot VT) in [60]. To compare with this reference and in order to use our results, we have taken a value of $\delta = 10^{-6}$ close to zero. For these parameter values, the abscissa of the ends of the arc $\mathcal{A}$ are given by $x_L = 0.2753$ and $x_R = 3.2491$, see Fig. 4.12.

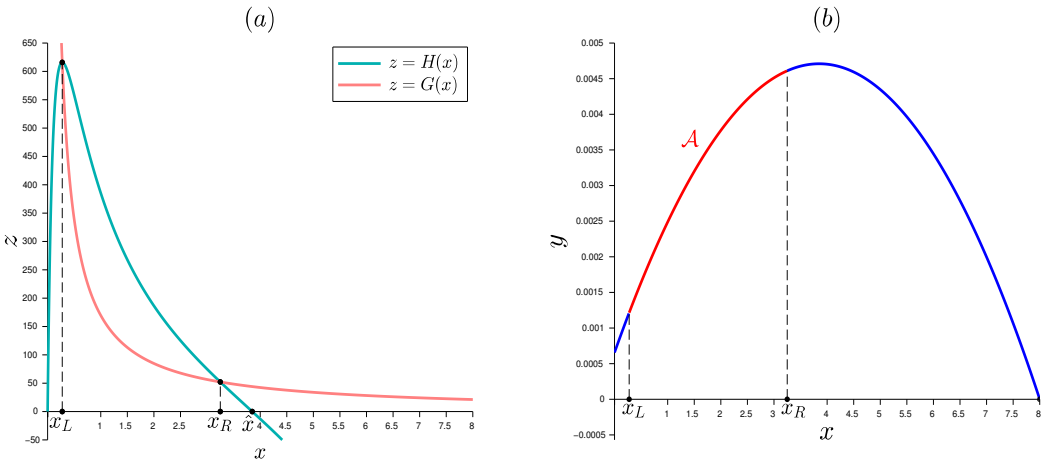

Figure 4.12: (a) : Graphs of the functions H and G for VT model with the parameter values given in Line 1 of Table 4.14. (b) : the corresponding arc $\mathcal{A}$ on the prey isocline.

Note that the predator isocline passes through the ends of the arc $\mathcal{A}$ if $m = m_L = 0.7830$ and $m = m_R = 2.6888$. The first value corresponds to the passage of the predator isocline through the point $(x_L, h(x_L))$. The second value corresponds to the passage of the predator isocline through the point $(x_R, h(x_R))$.
The bifurcation values m_L and m_R are obtained by solving equation $\psi(x_i) = h(x_i)$, $i = L, R$ with respect to m, where ψ is given in Table 4.1.

The results on the existence and stability of the positive equilibrium are deduced from Theorem 3.3 and are summarized in Table 4.12. Numerical simulations are reproduced in Fig. 4.13.

Table 4.12: The positive equilibrium of VT model and its stability for the parameter values given in Line 1 of Table 4.14.

m	Behaviour of the system
$0 < m < 0.7830$	A unique positive asymptotically stable equilibrium
$m = 0.7830$	Supercritical PAH bifurcation ($\rho = -0.2243$)
$0.7830 < m < 2.6888$	A unique positive (unstable) equilibrium
$m = 2.6888$	Supercritical PAH bifurcation ($\rho = -0.0097$)
$2.6888 < m$	At most one positive equilibrium which is stable

Note that when $0.7830 < m < 2.6888$, the Poincaré-Bendixson theorem predicts that the system has at least one limit cycle that is stable in its exterior.

We see numerically that for $m = 0.7$, model (4.23) has one positive equilibrium which is LES. The unstable positive separatrix of $E_2(K, 0)$ (in green) converges towards this equilibrium, see Fig. 4.13 (a and b).

For $m = 2.4$, the system has one positive equilibrium which is unstable and surrounded by a stable limit cycle (in blue) which has been created by a supercritical PAH bifurcation for $m = 0.7830$, see Fig. 4.13 (c). The unstable positive separatrix of $E_2(K, 0)$ converges towards this stable limit cycle.

For $m = 2.8$, the unstable separatrix of $E_2(K, 0)$ converges to the positive LES equilibrium, see Fig. 4.13 (d). The stable limit cycle has been destroyed through a supercritical PAH bifurcation for $m = 2.6888$.

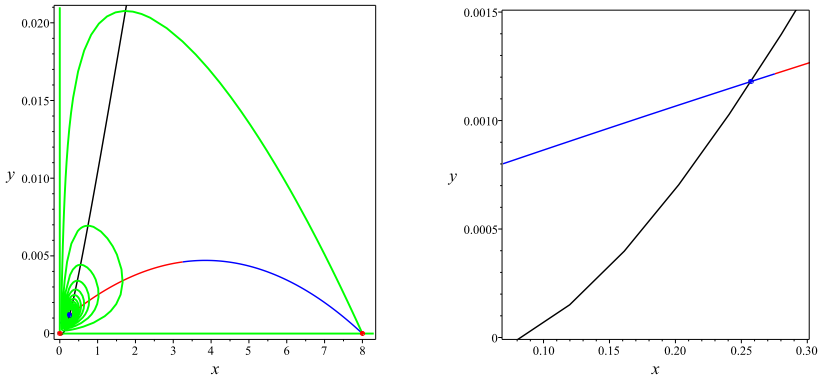

(a) $m = 0.7$ (b) zoom of (a)

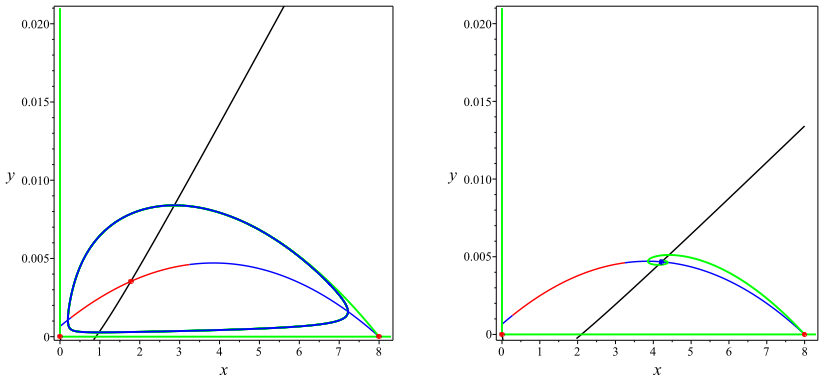

(c) $m = 2.4$ (d) $m = 2.8$

Figure 4.13: Some phase portraits of VT model with the parameter values given in Line 1 of Table 4.14.

Second simulation

In Fig. 4.14, we consider the parameter values indicated in Line 2 of Table 4.14. For these parameter values, the abscissa of the ends of the arc $\mathcal{A}$, are given by $x_L = 0.0065$ and $x_R = 0.9943$. Note that the predator isocline passes through the ends of the arc $\mathcal{A}$ if $m = m_L = -0.1151$ or $m = m_R = 0.2558$. The first value corresponds to the passage of the predator isocline through the point $(x_L, h(x_L))$. The second value corresponds to the passage of the predator isocline through the point $(x_R, h(x_R))$.

Furthermore, the isocline of the predator is tangent to the one of the prey, which corresponds to a saddle-node bifurcation, when $m = 0.2518$ or $m = 0.2556$. The bifurcation values m_L and m_R are obtained by solving equation $\psi(x_i) = h(x_i)$, $i = L, R$ with respect to m.

The results on the existence and stability of the positive equilibria are deduced from

Theorem 3.3 and are summarized in Table 4.13.

Table 4.13: Positive equilibria of VT model and their stability for the parameter values given in Line 2 of Table 4.14.

m	Behaviour of the system
$0 \leq m < 0.2518$	A unique positive (unstable) equilibrium
$m = 0.2518$	Saddle-node bifurcation
$0.2518 < m < 0.2556$	Three positive unstable equilibria
$m = 0.2556$	Saddle-node bifurcation
$0.2556 < m < 0.2558$	A unique positive (unstable) equilibrium
$m = 0.2558$	Subcritical PAH bifurcation ($\rho = 1.3839$)
$0.2558 < m$	At most one positive equilibrium which is stable

Note that when $m < 0.2556$ the Poincaré-Bendixson theorem predicts that the system has at least one limit cycle that is stable in its exterior. Indeed, in this case, the system has only unstable equilibria.
The principal behaviours of model (4.23) are given by numerical simulations, which will also highlight a saddle node bifurcation of cycles.

For $m = 0.1$, the system has one positive equilibrium which is unstable, surrounded by a stable limit cycle (in blue). The unstable positive separatrix of $E_2(K, 0)$ (in green) converges towards this limit cycle, see Fig. 4.14 (a).

For $m = 0.2528$, the system has three positive equilibria. The left and right points are unstable, the middle one is a saddle. These equilibria are surrounded by the blue stable limit cycle, see Fig. 4.14 (b). Note that the unstable positive separatrix of $E_2(K, 0)$ and unstable separatrices (in magenta) of the interior saddle point converge towards the limit cycle, while stable separatrices (in green) of the interior saddle point each converge towards one of the two unstable equilibria when $t \to -\infty$.

For $m = 0.2557$, the system has one positive equilibrium which is unstable, see Fig. 4.14 (c).

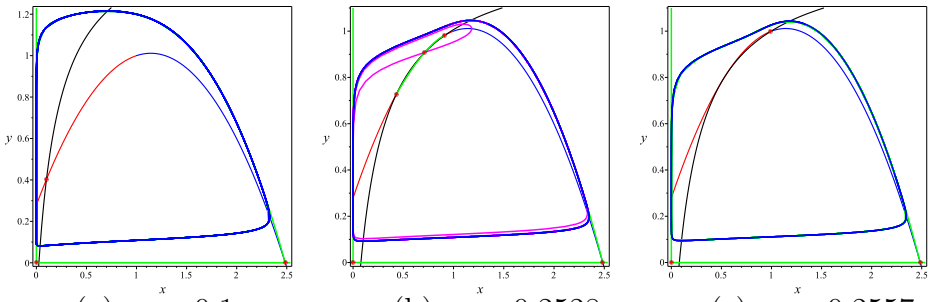

(a) $m = 0.1$ (b) $m = 0.2528$ (c) $m = 0.2557$

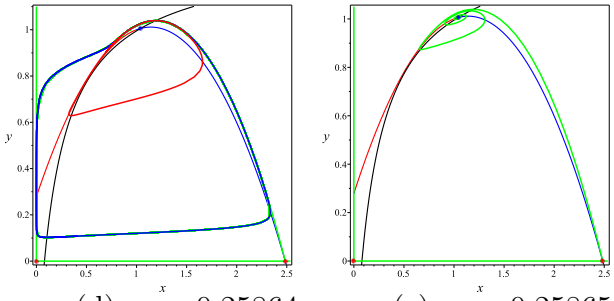

(d) $m = 0.25864$ (e) $m = 0.25865$

Figure 4.14: Some phase portraits of VT model with the parameter values given in Line 2 of Table 4.14.

For $m = 0.25864$, the system has one positive equilibrium which is LES, in addition to the big blue stable limit cycle. It is surrounded also by a small unstable limit cycle (in red) which has been created by a subcritical PAH bifurcation for $m = 0.2558$, see Fig. 4.14 (d).

When the value of m increases, the unstable limit cycle grows and approaches the stable one. When m crosses a value between 0.25864 and 0.25865, see Fig. 4.14 (d and e), the two limit cycles disappeared when both meat each other by a saddle node bifurcation of cycles.

For $m = 0.25167$, the system has one positive equilibrium which is LES. The unstable positive separatrix of $E_2(K, 0)$ converges towards this equilibrium.

Table 4.14: Parameter values used for the VT model. The value of m is depicted in each figure.

Figure	r	K	a	c	e	α	δ
Figs. 4.12 and 4.13	1.75	8	800	0.3	0.004	169.6	10^{-6}
Fig. 4.14	4.97	2.4850	3.564	0.2	0.2525	40	80

Chapter 5

Further developments and remarks

In this chapter, we want to discuss two remarkable properties of our model, namely *a singularly perturbed case* and the question of the *enrichment paradox*. A more detailed write-up will be the subject of a future research article.

5.1 Singularly perturbed case

We assume that the prey multiplies much faster than the predator. This hierarchical structure of time scales can be justified as follows, for example : we first write in the general model (3.3) $q(x) = aq_0(x)$ and $d(x, y) = bd_0(x, y)$. Then, we assume that the growth and mortality rates of the predator are relatively small, which means that $a = \varepsilon a^*$, and $b = \varepsilon b^*$, where ε is a positive small parameter. With these assumptions, the prey growth is much faster than the predator one, which is frequently observed in nature. After omitting the stars, model (3.3) becomes

$$\begin{cases} \dot{x} = g(x) - yp(x), \\ \dot{y} = \varepsilon \left[q(x) - d(x, y)\right] y. \end{cases}$$

By changing the time scale (we conserve the same notation t), we get interest to the following initial value problem (IVP)

$$\begin{cases} \varepsilon \dfrac{dx}{dt} = g(x) - yp(x), & x(0) = x_0, \\ \dfrac{dy}{dt} = \left[q(x) - d(x, y)\right] y, & y(0) = y_0. \end{cases} \tag{5.1}$$

This system is called a *slow-fast model*. To study this problem we will use the *singular perturbations theory* given in Appendix B. The so-called *fast equation* is given by

$$\frac{dx}{d\tau} = g(x) - yp(x) =: \phi(x, y), \tag{5.2}$$

where $\tau = t/\varepsilon$ and y is considered as a parameter. This equation gives an approximation of the fast dynamics of (5.1), for fixed y. The so-called *slow manifold* of (5.1) is formed by the union $\mathcal{V}_1 \cup \mathcal{V}_2$ where

$$\mathcal{V}_1 := \{(x, y) \in \mathbb{R}_+ \times \mathbb{R}_+ : x = 0\},$$
$$\mathcal{V}_2 := \{(x, y) \in \mathbb{R}_+ \times \mathbb{R}_+ : y = h(x)\}.$$

The slow manifold is the set of equilibrium points of the fast equation, parametrized by the slow variable y. In this case, it is rather a slow curve. Let's study the attractivity of the slow manifold, by deriving the function $\phi(x, y)$ with respect to x. By attractivity, we mean, according to *Tikhonov's theory* for the slow-fast systems, the (uniform) asymptotic stability of equilibria of the fast equation. We get

$$\frac{\partial \phi(x, y)}{\partial x} = g'(x) - yp'(x).$$

Then we have

$$\frac{\partial \phi(0, y)}{\partial x} = g'(0) - yp'(0)$$

which is negative if and only if $y > \dfrac{g'(0)}{p'(0)}$, and

$$\frac{\partial \phi(x, h(x))}{\partial x} = g'(x) - h(x)p'(x)$$

which is negative if and only if $h'(x) < 0$ (recall that $h = g/p$). Hence, the attractive part of the slow manifold is given by the union of the half straight-line

$$\mathcal{C}_1 := \left\{(x, y) \in \mathcal{V}_1 : y > \frac{g'(0)}{p'(0)}\right\},$$

and the curve

$$\mathcal{C}_2 := \left\{(x, y) \in \mathcal{V}_2 : h'(x) < 0\right\}.$$

If the initial condition (x_0, y_0) of (5.1) is such that $y_0 > g'(0)/p'(0)$ and x_0 is in the basin of attraction of the asymptotically stable equilibrium $x = 0$ of the fast equation (5.2) then the corresponding so-called *reduced problem* is given by

$$\frac{dy}{dt} = -d(0, y)y, \quad y(0) = y_0, \tag{5.3}$$

where y is in an arbitrary open interval $]\delta_1, \delta_2[$ such that $\delta_1 > \dfrac{g'(0)}{p'(0)}$. The equation (5.3) describes the slow part of the dynamics of (5.1), along the slow curve $\mathcal{C}_1$. The following proposition gives a $\mathcal{C}^0$ approximation of this slow motion on the slow curve $\mathcal{C}_1$.

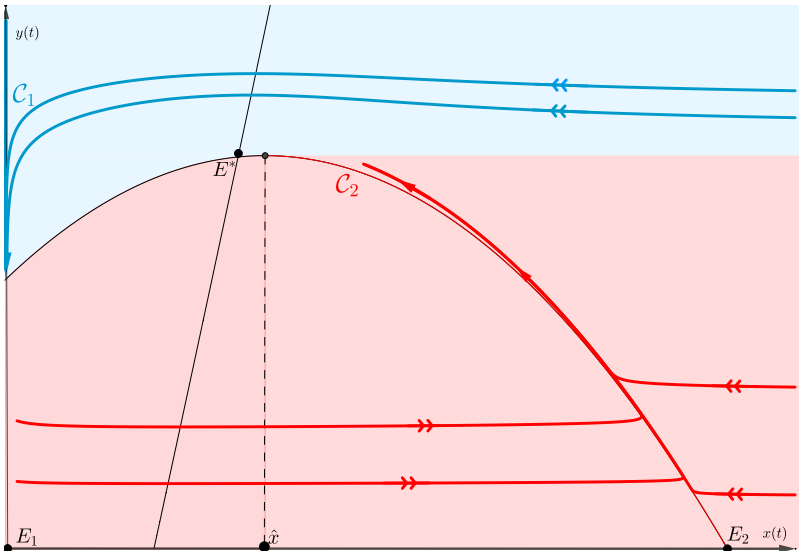

Figure 5.1: An example of an attractive part of the slow manifold ($\mathcal{C}_1$ and $\mathcal{C}_2$). The "basin of attraction"of $\mathcal{C}_1$ is the region colored with light blue and the "basin of attraction"of $\mathcal{C}_2$ is the region colored with light red.

Proposition 5.1. *Let $t \mapsto y_1(t)$ be the solution of (5.3) defined in $[0, T_1]$ such that $y(t)$ is in $]\delta_1, \delta_2[$. Then the solution $(x(t,\varepsilon), y(t,\varepsilon))$ of (5.1) is defined at least on $[0, T_1]$ and verifies the limits*

$$\lim_{\varepsilon \longrightarrow 0} x(t,\varepsilon) = 0, \quad \forall t \in]0, T_1],$$

$$\lim_{\varepsilon \longrightarrow 0} y(t,\varepsilon) = y_1(t), \quad \forall t \in [0, T_1].$$

Proof. It is a straightforward application of *Tikhonov's Theorem* (see Fig. 5.1, the region with light blue). □

Now, let $\hat{x}$ such that $h'(\hat{x}) = 0$ [1]. For x in $[\eta_4, \eta_3]$, where $\max(0, \hat{x}) < \eta_4 < \eta_3 < K$, the function h is decreasing then invertible. The inverse of the restriction of h to $[\eta_4, \eta_3]$ is denoted by $y \longrightarrow x = j(y)$ and is defined on $[\delta_3, \delta_4] = [h(\eta_3), h(\eta_4)]$. If the initial condition (x_0, y_0) of (5.1) is such that $\delta_3 < y_0 < \delta_4$ and x_0 is in the basin of attraction of the asymptotically stable equilibrium $x = j(y_0)$ of (5.1), then, the corresponding reduced problem is given by

$$\frac{dy}{dt} = [q\,(j(y)) - d(j(y), y)]\, y, \quad y(0) = y_0, \tag{5.4}$$

[1] In this case, we have implicitly assumed that $\hat{x}$ is unique. This condition is not necessary and one can imagine a result with a slow manifold with several bumps.

where y is in the open interval $]\delta_3, \delta_4[$. The equation (5.4) describes the slow part of the dynamics of (5.1), along the slow curve $\mathcal{C}_2$. The following proposition gives an C^0 approximation of the slow dynamics on $\mathcal{C}_2$.

Proposition 5.2. *Let $t \mapsto y_2(t)$ be the solution of (5.4) defined in $[0, T_2]$ such that $y_2(t)$ is in $]\delta_3, \delta_4[$. Then the solution $(x(t,\varepsilon), y(t,\varepsilon))$ of (5.1) is defined at least on $[0, T_2]$ and verifies the limits*

$$\lim_{\varepsilon \longrightarrow 0} x(t,\varepsilon) = j(y_2(t)), \quad \forall t \in]0, T_2],$$

$$\lim_{\varepsilon \longrightarrow 0} y(t,\varepsilon) = y_2(t), \quad \forall t \in [0, T_2].$$

Proof. It is a straightforward application of *Tikhonov's Theorem* (see Fig. 5.1, the region with light red). □

Now, for the whole model (5.1) without initial conditions, where ε is just a positive parameter (not necessarily small), the equilibria are the same than those of model (3.3) and they do not depend on ε. In particular, the necessary and sufficient conditions (3.15) and (3.16) of the exponential stability of the interior equilibrium $E^*(x^*, h(x^*))$ become

$$\varphi'(h(x^*))h'(x^*) < 1$$

and

$$h'(x^*) < \varepsilon \frac{d_y(x^*, h(x^*))h(x^*)}{p(x^*)}.$$

These conditions are obviously satisfied when $h'(x^*)$ is negative, that is when E^* is on a decreasing branch of the graph of h which is nothing else than the attractive slow manifold $\mathcal{C}_2$. However, when $h'(x^*)$ is positive and the determinant condition $\varphi'(h(x^*))h'(x^*) < 1$ is satisfied, the equilibrium E^* is on an ascending branch and the trace condition is verified if and only if $\varepsilon > \tilde{\varepsilon}$, with

$$\tilde{\varepsilon} = \frac{p(x^*)h'(x^*)}{d_y(x^*, h(x^*))h(x^*)}. \tag{5.5}$$

In other words, when ε is smaller than the threshold $\tilde{\varepsilon}$, the equilibrium E^* loses its stability. In particular, when the system is a slow-fast one (ε very small), such an equilibrium will be necessarily unstable. This sensitivity with respect to the deformation parameter ε is, for our knowledge, an interesting fact. A better description is illustrated in the next example.

5.1.1 Example of a slow-fast VT model

In view of the slow-fast case, we consider the VT model written as follows where $\varepsilon \in (0, 1]$.

$$\begin{cases} \dfrac{dx}{dt} = \dfrac{1}{\varepsilon}\left[g(x) - yp(x)\right], \\ \dfrac{dy}{dt} = \left[q(x) - \dfrac{\alpha y}{\delta + x} - m\right] y. \end{cases} \tag{5.6}$$

The functions g, p and q are given by (4.1). We choose the parameter values given in Line 1 of Table 4.14 with $m = 0.24$. The different phase portraits are given in Fig. 5.2. This figure illustrates the effect of the parameter ε on the arc $\mathcal{A}$. By decreasing the value of ε from 1 to 0.01, the abscissa x_L and x_R of the ends of the arc $\mathcal{A}$ approach 0 and $\hat{x}$ respectively. Consequently, when ε goes to zero, the arc $\mathcal{A}$ will cover all the ascending branch of the prey isocline, see Fig. 5.2, Column 1, where we plotted the graphs of the functions H (red) and G (blue) given by (3.22). In the same figure, for the chosen values of ε, we plotted the phase portrait to illustrate the stability of the equilibria by the graphical method discussed previously. The enlargement of the arc $\mathcal{A}$ leads to a destabilization of the positive equilibrium $E^*(x^*, y^*)$ by a PAH bifurcation for $\tilde{\varepsilon} = 0.6265$ calculated using (5.5). For $\varepsilon > \tilde{\varepsilon}$, the unstable separatrix of $E_2(K, 0)$ converges to the positive equilibrium (see Fig 5.2 (b), (e) and their zooms). For $\varepsilon < \tilde{\varepsilon}$, the unstable positive separatrix of $E_2(K, 0)$ converges towards a stable limit cycle which has been created by a PAH bifurcation at $\varepsilon = \tilde{\varepsilon}$ (see Fig 5.2 (h), (k) and their zooms). For decreasing values of ε after the emergence of the limit cycle, the shape and size of the latter vary significantly. For infinitely small ε, the resulting cycle is a slow-fast cycle, with the quasi-horizontal parts travelling faster than the other parts that coincide with the slow curves. Those are relaxation oscillations [14, 74]. The closed shape formed by the concatenation of horizontal lines and parts of the slow curve is sometimes called *singular cycle* [54].

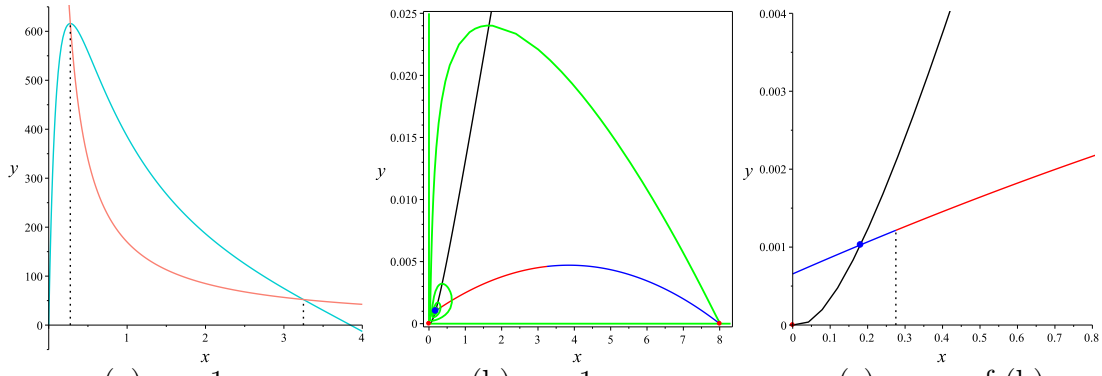

(a) $\varepsilon = 1$ (b) $\varepsilon = 1$ (c) zoom of (b)

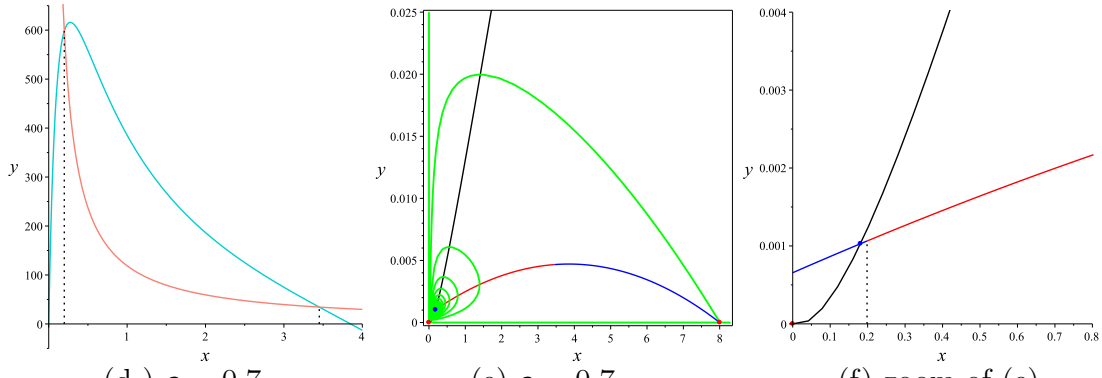

(d) $\varepsilon = 0.7$ (e) $\varepsilon = 0.7$ (f) zoom of (e)

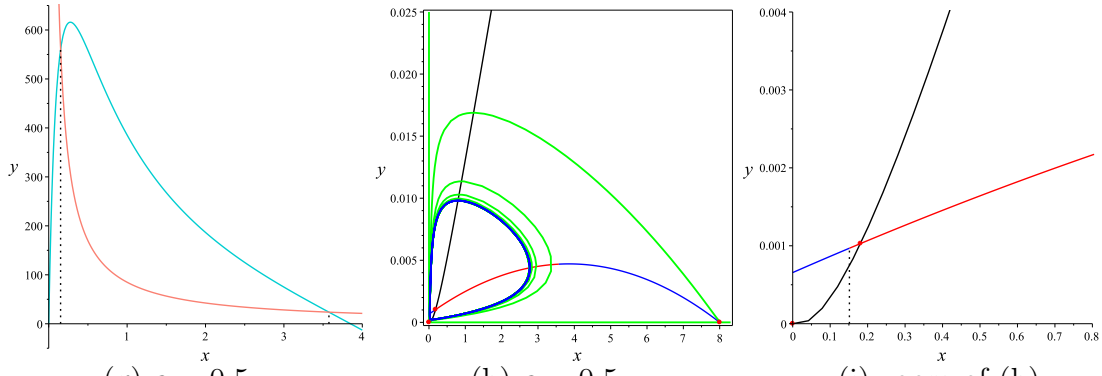

(g) $\varepsilon = 0.5$ (h) $\varepsilon = 0.5$ (i) zoom of (h)

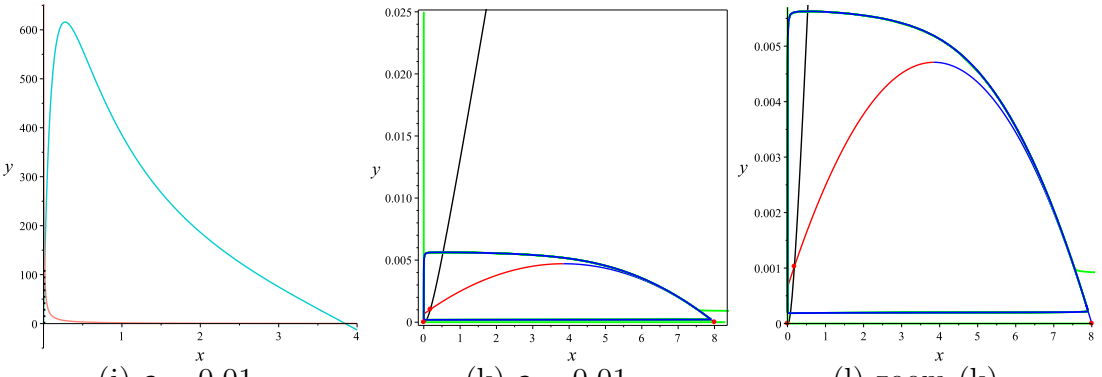

(j) $\varepsilon = 0.01$ (k) $\varepsilon = 0.01$ (l) zoom (k)

Figure 5.2: Effect of the variation of ε on phase portraits of VT model (5.6) with the parameter values given in Line 1 of Table 4.14 and $m = 0.24$.

Description of a trajectory of model (5.6) for $\varepsilon = 0.001$

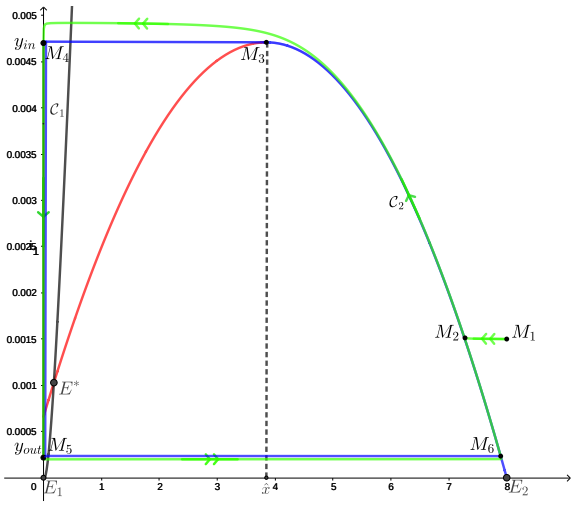

Figure 5.3: Phase portraits of the slow-fast VT model with parameter values given in Line 1 of Table 4.14, $m = 0.24$ and $\varepsilon = 0.001$.

We propose to give a qualitative description of a trajectory with parameters of Fig. 5.3. For this purpose, we consider in Fig. 5.3 the case when $\varepsilon = 0.001$. The double arrows represent the fast motion and the single arrows represent the slow motion. The considered trajectory of (5.6) starting at the point $M_1(x_0, y_0)$ such that $y_0 < h(\hat{x})$ reaches fastly and quasi-horizontally an ε-neighborhood of the attractive slow manifold $\mathcal{C}_2$ arround the point M_2. It moves up slowly along $\mathcal{C}_2$ until it reaches a neighborhood of the point $M_3 = (\hat{x}, h(\hat{x}))$. Then, it jumps quasi-horizontally to a small neighbourhood of the slow axis $\mathcal{C}_1$ near the point $M_4(0, y_{in} = h(\hat{x}))$. It evolves along the vertical slow curve $\mathcal{C}_1$ and reaches slowly an ε-neighborhood of a point $M_5 = (0, y_{out})$ that will be determined further down. This point will be located on the repulsive part of the vertical slow curve. Then, the trajectory jumps again quasi-horizontally to an ε-neighbourhood of $\mathcal{C}_2$ near the point M_6. It evolves slowly along $\mathcal{C}_2$ until it reaches again an ε-neighbourhood of M_3. For later times, the trajectory rolls up around the closed curve $(M_3M_4M_5M_6)$ forming a singular limit cycle. Using fixed-point techniques, we can show the existence of a real slow-fast cycle in an ε-neighborhood of this singular cycle. The relationship between the two points $(0, y_{in})$ and $(0, y_{out})$ is called the *input-output* (or, *entry-exit*) relationship. It is used to find implicitly y_{out} if we know y_{in} by the following equation

$$\int_{y_{out}}^{y_{in}} \frac{\tilde{F}(0,y)}{\tilde{G}(0,y)y} dy = 0, \tag{5.7}$$

where

$$\tilde{F}(x,y) = r\left(1-\frac{x}{K}\right) - \frac{ay}{c+x}, \quad \tilde{G}(x,y) = \frac{eax}{c+x} - \frac{\alpha y}{\delta+x} - m.$$

Hence,

$$\int_{y_{out}}^{y_{in}} \frac{\delta(ay-rc)}{cy(\alpha y+\delta m)} = 0.$$

This relationship explains why the point $(0, y_{in})$ lies on the repulsive part of the y-axis, which may seem counter-intuitive. This is known as the superstability or canard phenomenon. The way to obtain formula (5.7) is similar to the well-known case of RMA type models (see for example [8, 54]). It can also be established for the general model with a variable mortality rate.

The transition of the solution between $\mathcal{C}_1$ and $\mathcal{C}_2$ under the input-output relationship defines the relaxation oscillation cycle of system (5.6).

5.1.2 Comparison with other models

A brief comparison of model (5.6) with RMA and AG slow-fast predation models is discussed when the positive equilibrium point is on the ascending branch of the isocline of the prey. This comparison involves the sensitivity of the positive equilibrium stability with respect to ε and the existence of a slow-fast limit cycle.

Comparison with RMA model

Consider the RMA model (2.10) and assume that the growth of the prey is much faster than the predator one; this leads to the following slow-fast RMA model

$$\begin{cases} \dfrac{dx}{dt} = \dfrac{1}{\varepsilon}\left[g(x) - yp(x)\right], \\ \dfrac{dy}{dt} = \left[q(x) - m\right] y. \end{cases} \tag{5.8}$$

The functions g, p and q are given by (4.1). We choose the parameter values given in Fig. 2.2 with $m = 0.31$. In model (5.8), the sensitivity with respect to ε does not appear since if the interior equilibrium point is on the ascending branch it remains unstable surrounded by an attractive limit cycle (see Figure 5.4). That is to say that the phase portraits of RMA models are topologically equivalent for all positive values of ε.

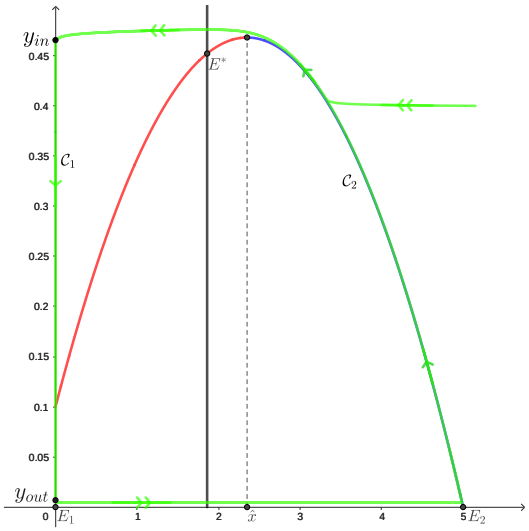

Figure 5.4: Phase portrait of the slow-fast RMA model with parameter values given in Fig. 2.2, $m = 0.31$ and $\varepsilon = 0.001$.

Comparison with AG model

We consider the following AG model with the ratio-dependent functional response given by (2.6)

$$\begin{cases} \dfrac{dx}{dt} = \left[r\left(1 - \dfrac{x}{K}\right) - \dfrac{a_1 y}{cy + x} \right] N \\ \dfrac{dy}{dt} = \left[\dfrac{ea_1 x}{cy + x} - m \right] y. \end{cases} \tag{5.9}$$

The prey isocline is the parabola $y = h(x)$ defined by

$$h(x) = rx\left(\frac{x - K}{cr(K - x) - a_1 K}\right).$$

The predator isocline is given by the straight line defined by the following equation

$$y = \frac{ea_1 - m}{mc} x.$$

The singularly perturbed AG model (5.9) is given by

$$\begin{cases} \dfrac{dx}{dt} = \dfrac{1}{\varepsilon}\left[r\left(1 - \dfrac{x}{K}\right) - \dfrac{a_1 y}{cy + x} \right] N \\ \dfrac{dy}{dt} = \left[\dfrac{ea_1 x}{cy + x} - m \right] y. \end{cases} \tag{5.10}$$

An interesting discussion on model (5.10) was made by C. Lobry in [40] and we want to develop it from another direction in further works.

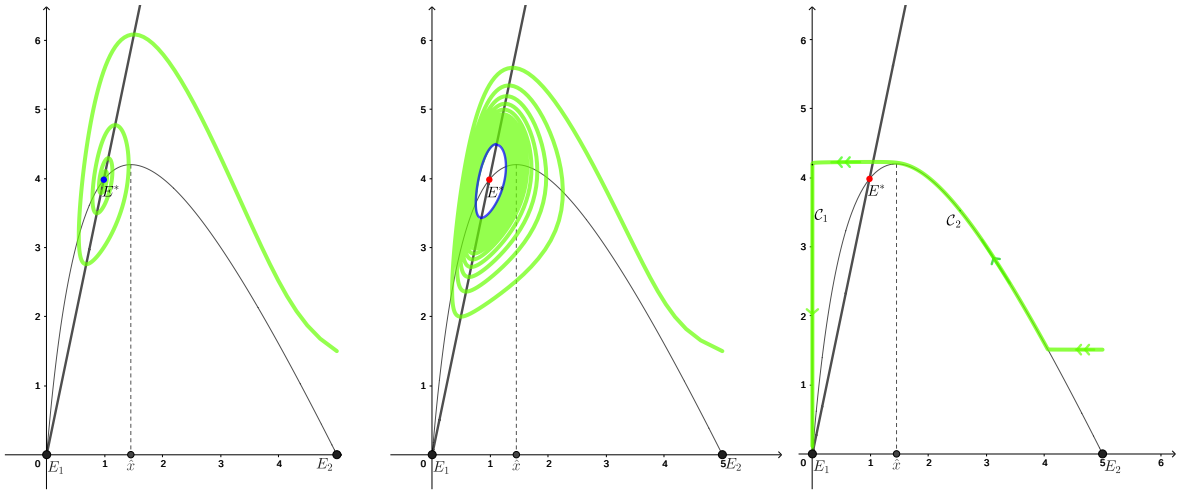

(a) $\varepsilon = 1$ (b) $\varepsilon = 0.62$ (c) $\varepsilon = 0.001$

Figure 5.5: Some phase portraits of the slow-fast AG model. $r = 0.6$, $K = 5$, $a_1 = 0.36$, $c = 0.5$, $e = 0.84$, $m = 0.1$. The value of ε is depicted in each figure.

Fig. 5.5 is given to illustrate the sensitivity of the positive equilibrium stability with respect to ε in AG model. In this figure, the isoclines of the prey and the predator are represented with the black curve and the black straight line respectively. For $\varepsilon = 1$, the positive equilibrium on the ascending branch is asymptotically stable (Fig. 5.5, a). For $\varepsilon = 0.62$, the positive equilibrium has lost its stability by a PAH bifurcation and is surrounded by a stable limit cycle (Fig. 5.5, b). For $\varepsilon = 0.001$, the cycle disappeared (Fig.5.5, c). Therefore, the relaxation phenomenon observed in the slow-fast VT model is not available for model (5.10) and one have an extinction of the two populations. This is due to the nature of the origin as a non-hyperbolic equilibrium of the AG model. This time, the phase portraits of the three simulations in Fig.5.5. are totally different.

5.2 About the enrichment paradox

When RMA model was first proposed, it highlighted a paradox that Rosenzweig described as a natural phenomenon [55]: enrichment of the environment by increasing the carrying capacity K can destabilize a coexistence equilibrium and give rise to a stable limit cycle. For higher values of K, the cycle approaches the axes more

and more, which in practice can mean the extinction of the prey first, then of the predator, or of the predator first, and then the stabilization of the prey at its carrying capacity. In fact, as some authors have pointed out, this only has to do with the relative relevance of the mathematical RMA's prey-dependent model (see the well-documented discussion in [4], chapter 5). This paradox and other problems such as the response of a trophic chain and the paradox of the plankton are given in C. Lobry's monograph [40] and the book of Arditi and Ginzburg. Mathematically, the PAH bifurcation is considered to be the main reason for the destabilization of the equilibrium. Several studies have suggested solutions to avoid this paradox. For example, the incorporation of a ratio-dependent functional response or introduction of a density-dependent mortality term in the predator-prey model can prevent the destabilization of the equilibrium [58]. With this in view, we have started to develop results giving necessary and/or sufficient conditions to lift the aforementioned paradox for our model (3.3) with a variable disappearance rate. In this section, we will simply present and discuss a few examples based on numerical simulations.

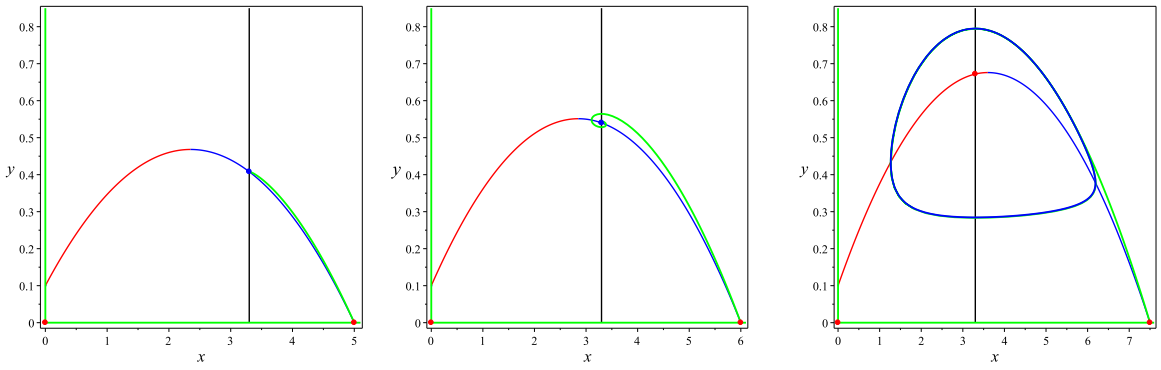

(a) $K = 5$ (b) $K = 6$ (c) $K = 7.5$

Figure 5.6: Environmental enrichment response in terms of prey density in RMA model (2.10). $r = 4.97$, $a = 0.6$, $c = 0.3$, $e = 0.6$, $m = 0.33$. The value of K is depicted in each figure.

Figure 5.6 illustrates the paradox of enrichment as historically observed for the RMA model (2.10).

For $K = 5$, the coexistence equilibrium (asymptotically stable) is located at the intersection of the descending branch of the prey isocline and the vertical predator isocline. When K is increased to 7.5, for example, the top of the parabola has moved to the right of the predator's isocline, which does not depend on K, and the positive equilibrium has moved to the increasing branch and has therefore lost its

attractivity. It is surrounded by a stable limit cycle, created by a PAH bifurcation. In fact, the paradox was already visible for $K = 6$ on the figure : the increase in carrying capacity had an effect on the density of the predator at the equilibrium, but none on that of the prey, even though this is a parameter specific to the latter's growth!

Figure 5.7 shows a simple configuration of VT model (4.23), with g, p and q given by (4.1), for which the paradox of enrichment is clearly lifted: both equilibrium densities of prey and predator have increased with K. Moreover, coexistence equilibrium is maintained outside the red arc of instability. The shape of the predator isocline is essential. Here, it is no longer vertical, but increasing in x. The concavity of this isocline is propitious to the lifting of the paradox and deserves a mathematical study in terms of its necessity and/or sufficiency, including the general model (3.3).

It should be noted that the ratio-dependent Arditi-Ginzburg model (5.9), an example of which is shown in Figure 5.8, also lifts the paradox, the predator isocline being a straight line with a positive slope. We also intend to study the effect of K on the stability of the coexistence equilibrium lying on an ascending branch of the prey isocline, both for our model with variable disappearance rate and for ratio-dependent models.

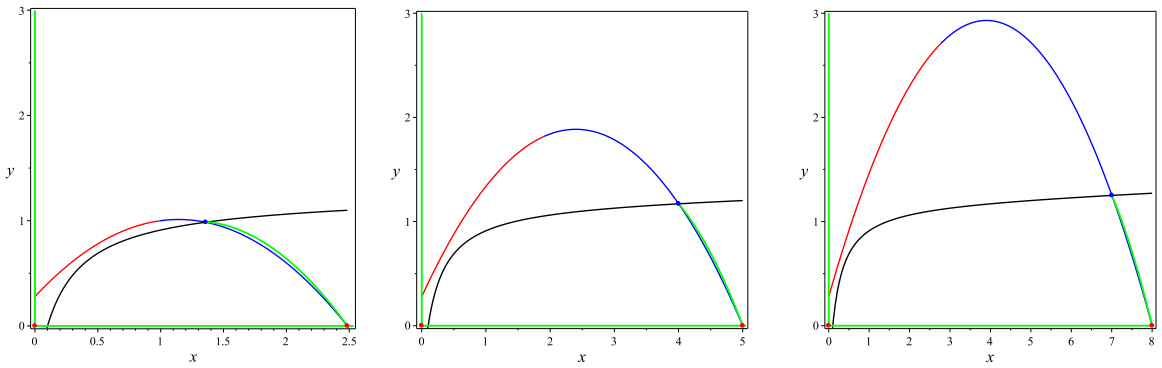

(a) $K = 2.485$ (b) $K = 5$ (c) $K = 8$

Figure 5.7: Environmental enrichment response in terms of prey density in VT model (4.23), with g, p and q given by (4.1). $r = 4.97$, $a = 3.564$, $c = 0.2$, $e = 0.2525$, $\alpha = 40$, $\delta = 80$, $m = 0.3$. The value of K is depicted in each figure.

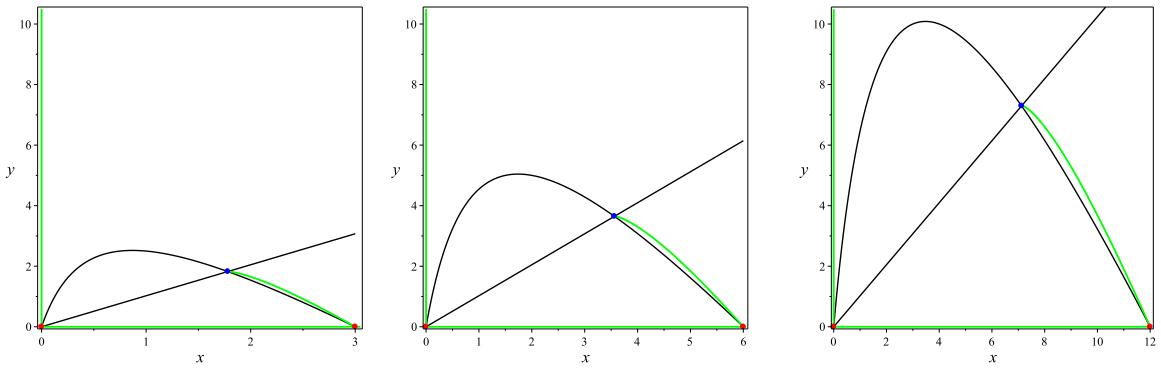

(a) $K = 3$ (b) $K = 6$ (c) $K = 12$

Figure 5.8: Environmental enrichment response in terms of prey density in AG model (5.9). $r = 0.6$, $a_1 = 0.36$, $c = 0.5$, $e = 0.84$, $m = 0.2$. The value of K is depicted in each figure.

Conclusion

In this dissertation, a general predator-prey model (3.3) with a variable mortality rate was considered under hypotheses H_1, H_2, H_3. The qualitative study of model (3.3) shows the possibility of the existence of at least one positive equilibrium point $E^*(x^*, y^*)$ in addition to the boundary equilibria $E_1(0, 0)$ and $E_2(K, 0)$. Under conditions of existence of a positive equilibrium $E^*(x^*, y^*)$, the equilibria $E_1(0, 0)$ and $E_2(K, 0)$ are saddle points. Local stability properties are given in Theorem 3.2. In particular, this theorem shows that conditions (3.15) and (3.16) are necessary and sufficient for the positiveness of the determinant and the negativeness of the trace at $E^*(x^*, y^*)$ respectively. Graphically, condition (3.15) is verified if the slope of the non-trivial prey isocline at $E^*(x^*, y^*)$ is smaller than that of the non-trivial predator isocline. Likewise, Condition (3.16) is verified if $E^*(x^*, y^*)$ is located outside the subset $\mathcal{A}$ of an ascending branch of the prey isocline. These two graphic interpretations give an extension of the Rosenzweig–MacArthur graphical criterion, which was given for a particular type of model with a constant mortality rate. Consequently, the local exponential stability of $E^*(x^*, y^*)$ is determined graphically by Theorem 3.3. This stability can be observed even if the positive equilibrium lies on an ascending branch of the prey isocline, Contrary to RMA-type model (2.9) for which $E^*(x^*, y^*)$ is LES if and only if it is located on a descending branch of this isocline. By using x^* as a bifurcation parameter for the general model (3.3), conditions for the appearance of PAH have been given by Theorem 3.4 in which we calculated the general formula of the first Lyapunov coefficient ρ. Accordingly, the type of each PAH bifurcation is determined by the sign of ρ as indicated in Remark 3.4. At a value $\tilde{x}$ of a PAH bifurcation, the uniqueness of the limit cycle in model (3.3) is not assured. On the order hand, some global asymptotic stability and non-existence of limit cycle conditions are given by different methods in sections 3.5.4 and 3.5.5.
By considering a logistic growth function and Holling II functional response in all examples of Chapter 4, we have applied our extension Rosenzweig–MacArthur criterion to show graphically the exponential stability of a positive equilibrium point. We have shown the possibility to define the subset $\mathcal{A}$ as an arc of the ascending branch of the prey isocline defined by (4.5). By plotting the non-trivial isoclines of models,

Theorem 3.3 offers a graphical method of local stability properties. For all these models, there are at most two critical points of the PAH bifurcation $(x_L, h(x_L))$ and $(x_R, h(x_R))$. In Gause/RMA and Hsu models, x_L and x_R coincide with 0 and $\hat{x}$ respectively and we find that condition (3.16) is verified if and only if $x^* > \hat{x}$. In Bazykin, CF and VT models, when $\alpha \to 0$, then $x_L \to 0$ and $x_R \to \hat{x}$, and we find the result of RMA model. Using formula (3.26), we can deduce the first Lyapunov coefficient for all models. We have found the same formula given in [59, 73] for RMA model. For Bazykin model, when g, p and q are given by equations (4.1), we have found the number ρ indicated in [43]. For the other models, we have given general formulas that do not seem to be known before in the literature. Phase portraits of the different models show the appearance of various local and global bifurcations which illustrate the rich dynamic of the general model (3.3). Not that, the parameter values are chosen just to illustrate our conclusions. For some figures, we have used the same parameter values given in other articles to explain their results with our graphical stability criterion. The reader can find in [22] numerical illustrations for other sets of values of the numerical parameters of Bazykin and VT models.
Under different numerical simulations obtained, here are some ecological interpretations of the stability results. The absence of a positive equilibrium leads to an extinction of the predator and a stabilization of the prey at its carrying capacity. The existence of a stable positive equilibrium point means the coexistence of two populations. In the case of multiple equilibria, this coexistence will depend on initial conditions. Coexistence can be also oscillatory around a stable limit cycle. The transition between coexistence around an equilibrium point and a limit cycle means the existence of a PAH bifurcation. Note that, we have not found a precise explanation of Remark 3.2 concerning the fact of having a stable positive equilibrium on the ascending branch of the prey isocline. In article [9], this stability is interpreted for CF model as an *Allee effect* of the prey.
In Chapter 5 we briefly discussed some properties of the general model (3.3). We presented the slow-fast system (5.1) by including the parameter ε and we applied Tikhonov's Theorem and the singular perturbations theory to describe the behaviour of solutions in this case, at least on bounded time intervals. By using the slow-fast VT model (5.6) as an illustration, numerical simulations in Fig. 5.2 and 5.3 showed the influence of varying the perturbation parameter ε on the asymptotic behaviour of solutions, when the positive equilibrium E^* is located on the ascending branch of the prey isocline. There exists a threshold of ε corresponding to a PAH bifurcation, and for ε tending to 0, the model shows oscillations with relaxations. This sensitivity is also observed for the slow-fast AG model (5.10) in Fig. 5.5. In this case, for decreasing values of ε, a cycle appears by a PAH bifurcation and then disappears when ε crosses a second threshold, probably by a saddle-node bifurcation of cycles. These

phenomena are not observed for the slow-fast RMA model (5.8). We also discussed the *enrichment paradox* observed in RMA model when increasing the carrying capacity K. One way to overcome this paradox is to introduce a variable mortality rate as for the general model (3.3) or by considering a density-dependent functional response as in AG model (5.9). This discussion is based only on simulations and no theoretical study has been made yet.

Appendix A

Preliminary concepts from dynamical systems theory

We recall some concepts and theorems derived from [33, 51, 66, 72]. We consider the following autonomous system

$$\dot{X} = f(X), \quad X = (x_1, ..., x_n), \quad f = (f_1, ..., f_n), \tag{A.1}$$

with the initial value $X(0) =: X_0$. The function f is of class C^1 on an open set $\mathcal{U}$ of $\mathbb{R}^n$ and $X_0 \in \mathcal{U}$.
Note that, system (A.1) and the initial condition X_0 define the so-called Cauchy problem.

A.1 Some Definitions

Flow : the flow of (A.1) is the application ϕ_t defined for all $t \in \mathcal{I} \subset \mathbb{R}$ by

$$\begin{array}{rccc} \phi_t & : & \mathcal{I} \times \mathcal{U} & \to & \mathcal{U} \\ & & (t, X_0) & \mapsto & \phi_t(X_0) = X(t). \end{array}$$

The function ϕ_t associates to all $X_0 \in \mathcal{U}$ the unique solution $X(t)$ of the Cauchy problem.
Orbit : let ϕ_t be the flow of (A.1) on $\mathcal{U}$. For each $u \in \mathcal{U}$, the orbit (or the path) of ϕ_t passing through the point u is the set γ defined by

$$\gamma(u) = \{X \in \mathcal{U} : \exists t \in \mathbb{R}, X = \phi_t(u)\}.$$

Phase portrait : the set of orbits of all $u \in \mathcal{U}$ is called the phase portrait.
Equilibrium point : a point E is called an equilibrium point (or stationary point,

fixed point,...) of (A.1) if $f(E) = 0$. The orbit of an equilibrium point is reduced to the point itself

$$\gamma(E) = \{E\}.$$

Linearized system : the linearized system corresponding to (A.1) at an equilibrium point E is given by

$$\dot{X} = AX, \tag{A.2}$$

where A is the $n \times n$ Jacobian matrix of f calculated at E.
Hyperbolic equilibrium point : E is called a hyperbolic equilibrium point of (A.1) if all of eigenvalues of the matrix A have not a zero real part.
ω-limit (α-limit) point : $\tilde{X} \in \mathcal{U}$ is called an ω-limit point of $u \in \mathcal{U}$ if there exists a sequence $\{t_i\}, t_i \to +\infty$ when $i \to +\infty$, such that $\phi_{t_i}(u) \to \tilde{X}$. Similarly, an α-limit point is defined by taking a sequence $\{t_i\}, t_i \to -\infty$ when $i \to +\infty$.
ω-limit (α-limit) set : the set of all ω-limit (respectively, α-limit) points of the flow is called ω-limit (respectively, α-limit) set which is noted $\omega(\gamma)$ (respectively, $\alpha(\gamma)$) .
Heteroclinic (homoclinic) orbit : an orbit $\gamma(u)$ is said to be heteroclinic if there are two different equilibrium points E_1^* and E_2^* such that

$$\lim_{t \to -\infty} \phi_t(u) = E_1^* \; and \lim_{t \to +\infty} \phi_t(u) = E_2^*.$$

If $E_1^* = E_2^*$, $\gamma(u)$ is called a homoclinic orbit.
Periodic orbit / Limit cycle : an orbit that does not contain any equilibrium point is called a periodic or closed orbit if there exists $T > 0$ such that

$$\forall t \in \mathbb{R}, X(t) = X(t + T). \tag{A.3}$$

An isolated periodic orbit is called a limit cycle, this means that no other closed orbit can be found in its neighbourhood. The minimum value of T for which (A.3) holds is called the period of the closed orbit.
Invariant set : a closed set $\mathcal{M}$ in $\mathcal{U}$ is called an invariant set if

$$\forall u \in \mathcal{M}, \forall t \in \mathbb{R}, \phi_t(u) \in \mathcal{M}.$$

Positively invariant set : a closed set $\mathcal{M}$ in $\mathcal{U}$ is called a positively invariant set if

$$\forall u \in \mathcal{M}, \forall t \geq 0, \phi_t(u) \in \mathcal{M}.$$

Lyapunov function : let E be an equilibrium point of (A.1) and let $V : \mathcal{W} \subset \mathcal{U} \to \mathbb{R}$ be a C^1 function defined on some neighbourhood of E. V is a Lyapunov function if

- $V(E) = 0$ and $V(X) > 0$ if $X \neq E$.
- $\dot{V}(X) \leq 0$ in $\mathcal{W} - \{E\}$ and $\dot{V}(E) = 0$.

Stable (unstable) manifold : stable and unstable manifolds of an equilibrium point E which are noted $W^s(E)$ and $W^u(E)$ respectively, are defined as follows

$$W^u(E) = \{u \in \mathcal{U} : \lim_{t \to -\infty} \phi_t(u) = E\},$$

$$W^s(E) = \{u \in \mathcal{U} : \lim_{t \to +\infty} \phi_t(u) = E\}.$$

A.2 Lyapunov stability

Lyapunov stability deals with the behaviour of trajectories of a system near an equilibrium point. Definitions of this stability are given in the following
Stability : an equilibrium point E of (A.1) is stable if for any $\varepsilon > 0$, there exists a positive scalar $\eta(\varepsilon)$ such that

$$\|X_0 - E\| < \eta \Rightarrow \|X(t) - E\| < \varepsilon, \forall t \geq 0.$$

Otherwise, E is unstable.
Attractivity : an equilibrium point E of (A.1) is attractive if there exists $\eta > 0$ such that

$$\|X_0 - E\| < \eta \Rightarrow X(t) \to E \, as \, t \to +\infty.$$

If $\mathcal{U} = \mathbb{R}^n$ and $\eta = +\infty$, E is globally attractive.
Local asymptotic stability : an equilibrium point E of (A.1) is locally asymptotically stable if it is stable and locally attractive.
Local exponential stability : an equilibrium point E of (A.1) is locally exponentially stable (LES) if there exist positive constants η, $\tilde{a}$, $\tilde{b} > 0$ such that

$$\|X_0 - E\| \leq \eta \Rightarrow \|X(t) - E\| \leq \tilde{a}\|X_0 - E\|e^{-\tilde{b}t}, \forall t \geq 0.$$

Global asymptotic stability : an equilibrium point E of (A.1) is globally asymptotically stable (GAS) if it is stable and globally attractive.
Global exponential stability : the equilibrium point E of (A.1) is globally exponentially stable if there exist positive constants $\tilde{a}$, $\tilde{b}$ such that

$$\|X(t) - E\| \leq \tilde{a}\|X_0 - E\|e^{-\tilde{b}t}, \forall t \geq 0, \forall X_0 \in \mathbb{R}^n.$$

A.3 Classification of equilibria

The local behaviour of (A.1) near an **hyperbolic** equilibrium point E is qualitatively determined by the behaviour of its linearized system (A.2). This leads to establishing the local stability of the hyperbolic equilibrium E according to the signs of the real parts of the eigenvalues λ_j of the matrix A noted $Re(\lambda_j)$, $j = 1, ..., n$. More precisely, E is LES if $Re(\lambda_j) < 0$, it is unstable if $Re(\lambda_j) > 0$ and it is a saddle point if there exist at least two eigenvalues such that one has a positive real part and the other has a negative real part.

The global asymptotic stability of E can be proved by the following theorem.

Theorem A.1. *(**LaSalle's invariance principle**) Suppose that E is an equilibrium point of (A.1). Let V be a Lyapunov function on some neighbourhood $\mathcal{W}$ of E and $\mathcal{M}$ be the largest invariant set of (A.1) in the set S defined by*

$$S = \left\{X \in \mathcal{W} : \dot{V}(X) = 0\right\}.$$

If γ is a bounded orbit of (A.1) which lies in $\mathcal{W}$, then the ω-limit set of γ belongs to $\mathcal{M}$. In particular, if $\mathcal{M} = \{E\}$, then E is GAS.

A.4 Two-dimensional system

In this section, we consider (A.1) with $n = 2$. In the hyperbolic case, the classification of equilibria of the linear model (A.2) (equivalently, model (A.1)) can be determined by the sign of the trace noted tr and the determinant noted det of the matrix A as illustrated by the following theorem.

Theorem A.2. *Let A be the Jacobian matrix at the equilibrium E.*

- *If $det(A) < 0$ then E is a saddle point (repeller).*
- *If $det(A) > 0$ then E is stable (nod or focus) if $trA < 0$, it is unstable (nod or focus) if $trA > 0$.*

The equilibrium point E is a node if A has two real eigenvalues and it is a focus if A has two complex conjugate eigenvalues.

The following theorem is usually applied to determine the existence of a limit cycle in the plane.

Theorem A.3. *(**Poincaré-Bendixson**) Let $\mathcal{M}$ be a positively invariant set containing a finite number of equilibria. Let $u \in \mathcal{M}$, then one of the following possibilities holds.*

- *$\omega(u)$ is an equilibrium point;*
- *$\omega(u)$ is a limit cycle;*
- *$\omega(u)$ consists of finite number of equilibria $E_1, ..., E_k$ and orbits γ such that $\alpha(\gamma) = E_i$ and $\omega(\gamma) = E_j$.*

Now, the non-existence condition of a limit cycle of (A.1) is established in the following theorem

Theorem A.4. *(**Dulac criterion**) Let B be a C^1 function in a simply connected region $D \subset \mathbb{R}^2$. If $\partial(f_1 B)/\partial x_1 + \partial(f_2 B)/\partial x_2$ is not identically zero and does not change the sign in D, then (A.1) has no closed orbit lying entirely in D.*

A.5 Bifurcation theory

Bifurcation means a qualitative change in the phase portrait of system (A.1) with a small change of at least one parameter. Note that, if the behaviour remains unchanged for all nearby vector fields, then the system (A.1) is said to be structurally stable [51]. Bifurcations can be classified according to the minimum number of varying parameters, it is called a bifurcation of codimension-i ($i \in \mathbb{N}^*$) if there are i varying parameters.

A.5.1 Types of bifurcations

Various types of bifurcations [33] can occur in system (A.1), in particular, those of equilibria and limit cycles. A bifurcation is called local if it implies a modification around nonhyperbolic equilibria or periodic orbits by changing its existence (appearance/disappearance) or by modifying its stability properties. Note that, the existence of equilibrium points or limit cycles depends on the direction of the variation of bifurcation parameters. The bifurcation which needs a large region in the phase portrait other than the neighbourhood of the non-hyperbolic equilibrium point or cycles is called global bifurcation. It is a useful method for understanding the global dynamics of system (A.1). In the following, we present some local and global bifurcations of codimension-1 used in this dissertation. For other bifurcations and more details on this theory, the reader is referred to [33, 72].

A.5.2 Some Local bifurcations of codimension-1

Saddle-node bifurcation of equilibria

This bifurcation occurs when an equilibrium point is stable on one side and unstable on the other side. Such a point is called saddle-node since it is neither a saddle nor a node. With this bifurcation, the saddle and node appear (or, disappear) when they separate (or, coalesce).

Poincaré-Andronov-Hopf bifurcation

Such a bifurcation occurs when eigenvalues of the Jacobian matrix become purely imaginary. This bifurcation is characterized by the appearance or disappearance of a limit cycle from an equilibrium point changing its stability. The type of bifurcation is determined by the transition of the stability between the equilibrium and the limit cycle : the appearance or disappearance of a stable (respectively, unstable) limit cycle is referred to a supercritical (respectively, subcritical) Poincaré-Andronov-Hopf bifurcation.

A.5.3 Some Global bifurcations of codimension-1

Some examples of global bifurcations are given, which can occur without any change in the equilibrium point. Moreover, these bifurcations give other scenarios for the appearance or disappearance of limit cycles other than Poincaré-Andronov-Hopf bifurcation.

Saddle-node bifurcation of cycles

This bifurcation occurs when stable and unstable limit cycles coincide and both disappear. At the bifurcation, there exists a periodic orbit which is neither stable nor unstable.

Homoclinic bifurcation

This bifurcation occurs when a limit cycle touches a saddle point. At the bifurcation, the stable and unstable separatrices of the saddle point cross each other creating a loop. The cycle becomes a homoclinic orbit which will disappear after the bifurcation.

Appendix B

Singular perturbation theory

Consider the following slow-fast system

$$\begin{cases} \varepsilon \dfrac{dx}{dt} = G_1(x, y, \varepsilon), \quad x(0) = \alpha_\varepsilon, \\ \dfrac{dy}{dt} = G_2(x, y, \varepsilon), \quad y(0) = \beta_\varepsilon, \end{cases} \tag{B.1}$$

where $(x, y) \in \mathbb{R}^n \times \mathbb{R}^m$ and ε is a small positive parameter. Functions G_1 and G_2 are continuous with respect to their arguments and initial conditions depend continuously on ε. The system (B.1) is said to be singularly perturbed because the continuous dependence theorem with respect to parameters is not applicable. ε is the singular perturbation parameter. Dynamics of (B.1) can be described by the *singular perturbation theory*. This theory separates solutions of (B.1) into fast and slow motions. The fast motion of (B.1) is given by setting the slow variable y to its initial value β_0, it is approximated by the solution of the *boundary layer equation*

$$\frac{dx}{d\tau} = G_1(x, \beta_0, 0), \quad x(0) = \alpha_0, \quad \tau = t/\varepsilon, \tag{B.2}$$

The *fast equation* is given by

$$\frac{dx}{d\tau} = G_1(x, y, 0), \tag{B.3}$$

in which y is considered as a parameter. The asymptotic behaviour of the solution, supposed to be unique, of the fast equation may depend on the initial condition. We are concerned by the case where (B.3) has an isolated asymptotically stable equilibrium $\xi(y)$ uniformly with respect to y in a compact subset Y of $\mathbb{R}^m$, solution of the equation

$$G_1(x, y, 0) = 0. \tag{B.4}$$

The solutions of (B.4) define the *slow manifold* of (B.1). It is the locus of all equilibria of the fast equation, parametrized by y. The component $x = \xi(y)$ of the slow manifold is attractive for all y in Y. The slow motion is approximated by the solution of the *reduced problem*

$$\frac{dy}{d\tau} = G_2(\xi(y), y, 0), \quad y(0) = \beta_0. \tag{B.5}$$

Let $(x(t,\varepsilon), y(t,\varepsilon))$ be the solution[1] of (B.1) and $\bar{y}(t)$ be the solution of the reduced problem (B.5) defined for $0 \leq t \leq T$. Then we have, at least for the slow motion, the following limits given by *Tikhonov's* theorem [41, 63]

$$\lim_{\varepsilon \to 0} x(t,\varepsilon) = \xi(\bar{y}(t)) \quad \textit{for} \quad 0 < t \leq T,$$

$$\lim_{\varepsilon \to 0} y(t,\varepsilon) = \bar{y}(t) \quad \textit{for} \quad 0 \leq t \leq T.$$

More details are given in [41, 63], such as the fast phase approximation or the extension of the previous limits to an unbounded time interval.

[1] In fact, we can have a statement that does not require uniqueness, but this is not the case for our models.

Bibliography

[1] Abrams, P. A. On classifying interactions between populations, *Oecologia* 73, 272–281 (1987). https://doi.org/10.1007/BF00377518

[2] Alabi, T., Patiny, S., Verheggen, F., Francis, F. and Haubruge, É. Origine et évolution du cannibalisme dans les populations animales: pourquoi manger son semblable?, *Biotechnologie, Agronomie, Société et Environnement* 13, (2009).

[3] Arditi, R. and Ginzburg, L. Coupling in predator-prey dynamics: Ratio-dependence, *Journal of Theoretical Biology* 139, 311–326 (1989). https://doi.org/10.1016/s0022-5193(89)80211-5

[4] Arditi, R. and Ginzburg, L. R. How species interact: altering the standard view on trophic ecology, *Oxford University Press (2012)*. https://doi.org/10.1093/acprof:osobl/9780199913831.001.0001

[5] Bazykin, A. D. Nonlinear dynamics of interacting populations, *World Scientific (1998)*. https://doi.org/10.1142/2284

[6] Bazykin, A. D. Volterra's system and the Michaelis-Menten equation, *Problems in mathematical genetics. USSR Academy of Science, Novosibirsk, USSR*, 103–142 (1974).

[7] Beddington, J. R. Mutual interference between parasites or predators and its effect on searching efficiency, *The Journal of Animal Ecology* 44, 331–340 (1975). https://doi.org/10.2307/3866

[8] Boudjellaba, H. and Sari, T. Dynamic transcritical bifurcations in a class of slow–fast predator–prey models, *Journal of Differential Equations* 246, 2205-2225 (2009). https://www.sciencedirect.com/science/article/pii/S0022039609000199

[9] Cavani, M. and Farkas, M. Bifurcations in a predator-prey model with memory and diffusion I: Andronov-Hopf bifurcation, *Acta Mathematica Hungarica*, 63, 213–229 (1994). https://doi.org/10.1007/bf01874129

[10] Cheng, K. S., Hsu, S. B. and Lin, S. S. Some results on global stability of a predator-prey system, *Journal of Mathematical Biology*, 12, 115–126 (1982). https://doi.org/10.1007/BF00275207

[11] Contois, D. E. Kinetics of bacterial growth: relationship between population density and specific growth rate of continuous cultures, *Microbiology*, 21, 40–50 (1959). https://doi.org/10.1099/00221287-21-1-40

[12] Dalziel, B. D., Thomann, E., Medlock, J. and De Leenheer, P. Global analysis of a predator–prey model with variable predator search rate, *Journal of Mathematical Biology*, 81, 159–183 (2020). https://doi.org/10.1007/s00285-020-01504-y

[13] DeAngelis, D. L., Goldstein, R. A. and O'Neill, R. V. A model for tropic interaction, *Ecology*, 56, 881–892 (1975). https://doi.org/10.2307/1936298

[14] Dumortier, F. and Roussarie, R. Bifurcation of relaxation oscillations in dimension two, *Discrete and Continuous Dynamical Systems*, 19, 631–674 (2007). https://doi.org/10.3934/dcds.2007.19.631

[15] Duque, C. and Lizana, M. Partial characterization of the global dynamic of a predator-prey model with non constant mortality rate, *Differential Equations and Dynamical Systems*, 17, 63–75 (2009). https://doi.org/10.1007/s12591-009-0005-y

[16] Egerton, F. N. History of ecological sciences, part 47: Ernst Haeckel's ecology, *Bulletin of the Ecological Society of America*, 94, 222–244 (2013). https://doi.org/10.1890/0012-9623-94.3.222

[17] Freedman, H. I. Deterministic mathematical models in population ecology, Volume 57 of Monographs and textbooks in pure and applied mathematics, M. Dekker (1980).

[18] Gause, G. F., Smaragdova, N. P. and Witt, A. A. Further studies of interaction between predators and prey, *The Journal of Animal Ecology*, 5, 1–18 (1936). https://doi.org/10.2307/1087

[19] Gilad, O. Competition and competition models, *Encyclopedia of Ecology*, 707-712 (2008). https://doi.org/10.1016/B978-008045405-4.00666-2

[20] Guckenheimer, J. and Holmes, P. Nonlinear oscillations, dynamical systems, and bifurcations of vector fields, Springer-Verlag (2002). https://doi.org/10.1007/978-1-4612-1140-2

[21] Hainzl, J. Stability and Hopf bifurcation in a predator-prey system with several parameters, *SIAM Journal on Applied Mathematics*, 48, 170–190 (1988). https://doi.org/10.1137/0148008

[22] Hammoum, A., Sari, T. and Yadi, K. Rosenzweig-MacArthur model with variable disappearance rate. *CARI'2022, Proceedings of the 16th African Conference on Research in Computer Science and Applied Mathematics*, (2022). https://hal.inria.fr/CARI2022/hal-03712243

[23] Hammoum, A., Sari, T. and Yadi, K. The Rosenzweig–MacArthur graphical criterion for a predator-prey model with variable mortality rate, *Qualitative Theory of Dynamical Systems*, 22 (2023). https://doi.org/10.1007/s12346-023-00739-6

[24] Hasík, K. Uniqueness of limit cycle in the predator–prey system with symmetric prey isocline, *Mathematical biosciences*, 164, 203–215 (2000). https://doi.org/10.1016/S0025-5564(00)00007-9

[25] Hassell, M. P. and Varley, G. C. New inductive population model for insect parasites and its bearing on biological control, *Nature*, 223, 1133–1137 (1969). https://doi.org/10.1038/2231133a0

[26] Hofbauer, J. and So, J. W. H. Multiple limit cycles for predator-prey models, *Mathematical Biosciences*, 99, 71-75 (1990). https://doi.org/10.1016/0025-5564(90)90139-P

[27] Holling, C. S. The components of predation as revealed by a study of small-mammal predation of the European Pine Sawfly 1, *The Canadian Entomologist*, 91, 293–320 (1959). https://doi.org/10.4039/Ent91293-5

[28] Holt, R. D. Spatial heterogeneity, indirect interactions, and the coexistence of prey species, *The American Naturalist*, 124, 377–406 (1984). https://doi.org/10.1086/284280

[29] Hsu, S.B. On global stability of a Predator-Prey System, *Mathematical Biosciences*, 39, 1–10 (1978). https://doi.org/10.1016/0025-5564(78)90025-1

[30] Izhikevich, E. M. Dynamical systems in neuroscience, *MIT press* (2007). https://doi.org/10.7551/mitpress/2526.001.0001

[31] Jiang, H. and Wang, L. Analysis of steady state for variable-territory Model with limited self-Limitation, *Acta Applicandae Mathematicae*, 148, 103–120 (2017). https://doi.org/10.1007/s10440-016-0080-3

[32] Kot, M. Elements of mathematical ecology, *Cambridge University Press* (2001). https://doi.org/10.1017/CBO9780511608520

[33] Kuznetsov, Y.A. Elements of applied bifurcation theory, *Applied Mathematical Sciences* (AMS, volume 112), Springer New York, NY (2004). https://doi.org/10.1007/978-1-4757-3978-7

[34] Landry, C. L. Pollinator-mediated competition between two co-flowering Neotropical mangrove species, Avicennia germinans (Avicenniaceae) and Laguncularia racemosa (Combretaceae), *Annals of Botany*, 111, 207–214 (2013). https://doi.org/10.1093/aob/mcs265

[35] Leslie, P. H. Some further notes on the use of matrices in population mathematics, *Biometrika*, 35, 213–245 (1948). https://doi.org/10.2307/2332342

[36] Leslie, P. H. and Gower, J. C. The properties of a stochastic model for the predator-prey type of interaction between two species, *Biometrika*, 47, 219–234 (1960). https://doi.org/10.1093/biomet/47.3-4.219

[37] Liou, L. P. and Cheng, K. S. Global stability of a predator-prey system, *Journal of Mathematical Biology*, 26, 65–71 (1988). https://doi.org/10.1007/BF00280173

[38] Liu, Y. Geometric criteria for the non-existence of cycles in predator–prey systems with group defense, *Mathematical biosciences*, 208, 193–204 (2007). https://doi.org/10.1016/j.mbs.2006.10.003

[39] Liu, Y. Geometric criteria for the nonexistence of cycles in Gause-type predator-prey systems, *Proceedings of the American Mathematical Society*, 133, 3619–3626 (2005). https://doi.org/10.1090/S0002-9939-05-08026-3

[40] Lobry, C. The consumer-resource relationship: Mathematical Modeling, *Wiley-ISTE* (2018). https://doi.org/10.1002/9781119544029

[41] Lobry, C., Sari, T. and Touhami, S. On Tykhonov's theorem for convergence of solutions of slow and fast systems, *Electronic Journal of Differential Equations* (1998).

[42] Lotka, A. J. Elements of physical biology, *Williams and Wilkins* (1925).

[43] Lu, M. and Huang, J. Global analysis in Bazykin's model with Holling II functional response and predator competition, *Journal of Differential Equations*, 280, 99–138 (2021). https://doi.org/10.1016/j.jde.2021.01.025

[44] Malthus, T. R. An essay on the principle of population, *Harmondsworth* (1798).

[45] Michaelis, L. and Menten, M. L. Die kinetik der invertinwirkung, *Biochem. z*, 49, 333–369 (1913).

[46] Minter, E. J., Fenton, A., Cooper, J. and Montagnes, D. J. Prey-dependent mortality rate: a critical parameter in microbial models, *Microbial ecology*, 62, 155-161 (2011). https://doi.org/10.1007/s00248-011-9836-5

[47] Mishra, P., Raw, S. N. and Tiwari, B. On a cannibalistic predator–prey model with prey defense and diffusion, *Applied Mathematical Modelling*, 90, 165–190 (2021). https://doi.org/10.1016/j.apm.2020.08.060

[48] Moghadas, S. and Alexander, M. Bifurcation and numerical analysis of a generalized Gause-type predator-prey model, *Dynamics of Continuous, Discrete and Impulsive Systems Series B: Applications and Algorithms*, 13, (2006).

[49] Monod, J. The growth of bacterial cultures, *Annual review of microbiology*, 3, 371–394 (1949). https://doi.org/10.1146/annurev.mi.03.100149.002103

[50] Morin, P. Community ecology, *John Wiley and Sons* (2009).

[51] Perko, L. Differential equations and dynamical systems, *Springer Science and Business Media* (2013).

[52] Polis, G. A. The evolution and dynamics of intraspecific predation, *Annual Review of Ecology and Systematics*, 12, 225–251 (1981). https://doi.org/10.1146/annurev.es.12.110181.001301

[53] Pruitt, J. N., Berning, A. W., Cusack, B., Shearer, T. A., McGuirk, M., Coleman, A., Eng, R. Y. Y., Armagost, F., Sweeney, K. and Singh, N. Pre-copulatory sexual cannibalism causes increase egg case production, hatching success, and female attractiveness to males, *Ethology*, 120, 453–462 (2014). https://doi.org/10.1111/eth.12216

[54] Rinaldi, S. and Muratori, S. Slow-fast limit cycles in predator-prey models, *Ecological Modelling*, 61, 287–308 (1992). https://doi.org/10.1016/0304-3800(92)90023-8

[55] Rosenzweig, M. L. Paradox of enrichment: destabilization of exploitation ecosystems in ecological time, *Science*, 171, 385–387 (1971). https://doi.org/10.1126/science.171.3969.385

[56] Rosenzweig, M. L. and MacArthur, R. H. Graphical representation and stability conditions of predator-prey interaction, *Amer. Natur.* 47, 209-223 (1963). https://doi.org/10.1086/282272

[57] Rousseu, F., Charette, Y. and Bélisle, M. Resource defense and monopolization in a marked population of ruby-throated hummingbirds (A rchilochus colubris), *Ecology and Evolution* 4, 776–793 (2014). https://doi.org/10.1002/ece3.972

[58] Roy, S. and Chattopadhyay, J. The stability of ecosystems: a brief overview of the paradox of enrichment, *Journal of biosciences* 32, 421–428 (2007). https://doi.org/10.1007/s12038-007-0040-1

[59] Seo, G. and Wolkowicz, G.S.K. Sensitivity of the dynamics of the general Rosenzweig–MacArthur model to the mathematical form of the functional response: a bifurcation theory approach, *Journal of Mathematical Biology*, 76, 1873–1906 (2018). https://doi.org/10.1007/s00285-017-1201-y

[60] Strohm, S. and Tyson, R. The effect of habitat fragmentation on cyclic population dynamics: a numerical study, *Bulletin of Mathematical Biology*, 71, 1323–1348 (2009). https://doi.org/10.1007/s11538-009-9403-0

[61] Sutherland, W. J. From individual behaviour to population ecology, *Oxford University Press on Demand* (1996).

[62] Teixeira Alves, M. Des interactions indirectes entre les proies : modélisation et influence du comportement du prédateur commun, Université Nice Sophia Antipolis (2013). https://theses.hal.science/tel-00833242

[63] Tikhonov, A. N. Systems of differential equations containing small parameters in the derivatives, *Mat. Sb.(NS)*, 31, 575–586 (1952).

[64] Turchin, P. and Batzli, G.O. Availability of food and the population dynamics of arvicoline rodents, *Ecology*, 82, 1521–1534 (2001). https://doi.org/10.1890/0012-9658(2001)082[1521:aofatp]2.0.co;2

[65] Verhulst, P. F. Notice sur la loi que la population suit dans son accroissement, *Correspondence mathematique et physique*, 10, 113–121 (1838).

[66] Vidyasagar, M. Nonlinear systems analysis, Society for Industrial and Applied Mathematics (2002). https://doi.org/10.1137/1.9780898719185

[67] Volterra, V. Fluctuations in the abundance of a species considered mathematically, *Nature*, 118, 558–560 (1926). https://doi.org/10.1038/118558a0

[68] Volterra, V. Variazioni e fluttuazioni del numero di individui in specie animali conviventi, *Atti Reale Accad. Nazionale dei Lincei*, 6, 641–648 (1927).

[69] Wang, S. and Yu, H. Stability and bifurcation analysis of the Bazykin's predator-prey ecosystem with Holling type II functional response, *Math. Biosci. Engin*, 18, 7877–7918 (2021). https://doi.org/10.3934/mbe.2021391

[70] Ward, A. J., Webster, M. M. and Hart, P. J. Intraspecific food competition in fishes, *Fish and Fisheries*, 7, 231–261 (2006). https://doi.org/10.1111/j.1467-2979.2006.00224.x

[71] Wiens, J. A. Overview: the importance of spatial and temporal scale in ecological investigations, *Community ecology*, 145–153 (1986).

[72] Wiggins, S. and Golubitsky, M. Introduction to applied nonlinear dynamical systems and chaos, *Springer*, 2, (2003). https://doi.org/10.1007/b97481

[73] Wolkowicz, G.S.K. Bifurcation analysis of a predator-prey system involving group defence, *SIAM Journal on Applied Mathematics*, 48, 592–606 (1988). https://doi.org/10.1137/0148033

[74] Yadi, K. Averaging on slow and fast cycles of a three time scale system, *Journal of Mathematical Analysis and Applications*, 413, 976–998 (2014). http://dx.doi.org/10.1016/j.jmaa.2013.12.044

Abstract. In this dissertation, we propose a general Gause type model of predation with a variable disappearance rate. This suggestion is based on the fact that many ecological examples have shown the dependence of the predator mortality rate on the prey or the predator densities. We give a graphical criterion for the local asymptotic stability of the positive equilibria. It is an extension of the well-known Rosenzweig–MacArthur graphical criterion for the case of a constant predator mortality rate. Some conditions for the global asymptotic stability of the positive equilibrium, when it is unique and for the non-existence of limit cycles are also given. We study the occurrence of a Poincaré-Andronov-Hopf bifurcation and we give the explicit formula of the first Lyapunov coefficient. We apply our results to different predator-prey models. The phase portraits show the rich dynamics of the model considered, in particular, the existence of some global bifurcations. Moreover, we give an overview of some other important properties of the proposed model, which will be developed in the future.
Keywords: predator-prey model, Rosenzweig–MacArthur graphical criterion, variable disappearance rate, stability, Poincaré-Andronov-Hopf, slow-fast systems.

Résumé. Dans cette thèse, nous proposons un modèle général de prédation de type Gause avec un taux de disparition variable. Cette suggestion est basée sur le fait que de nombreux exemples écologiques ont montré la dépendance du taux de mortalité du prédateur des densités de la proie ou du prédateur. Nous donnons un critère graphique de la stabilité asymptotique locale des équilibres strictement positifs. Il s'agit d'une extension du critère graphique bien connu de Rosenzweig-MacArthur pour le cas d'un taux de mortalité du prédateur constant. Quelques conditions de stabilité asymptotique globale de l'équilibre positif, quand il est unique, et de la non-existence d'un cycle limite sont aussi données. Nous étudions l'apparition d'une bifurcation de Poincaré-Andronov-Hopf et nous donnons la formule explicite du premier coefficient de Lyapunov. Nous appliquons nos résultats à différents modèles de prédation. Les portraits de phase montrent la richesse de la dynamique du modèle considéré, en particulier, l'existence de certaines bifurcations globales. De plus, nous donnons un aperçu de certaines autres propriétés importantes du modèle proposé, qui seront développées dans le futur.
Mots-clés: modèle proie-prédateur, critère graphique de Rosenzweig-MacArthur, taux de disparition variable, stabilité, bifurcation de Poincaré-Andronov-Hopf, systèmes lents-rapides.

ملخص. في هذه الأطروحة ، نقترح نموذجًا عامًا للافتراس من نوع Gause مع معدل اختفاء متغير. يعتمد هذا الاقتراح على حقيقة أن العديد من الأمثلة البيئية أظهرت الترابط بين معدل وفيات الحيوانات المفترسة مع كثافة الفريسة أوالمفترس. نعطي معيارًا بيانيا للاستقرار المحلي لنقط التوازن الموجبة تماما. انه امتداد لمعيارRosenzweig-MacArthur البياني المعروف من اجل حالة معدل وفيات ثابت للمفترس. كما انه يتم إعطاء بعض شروط عن اللاستقرار الشامل لنقطة التوازن الموجبة تماما وعن عدم وجود دورة حد (مسار دوري). ندرس ظهور تشعبPoincaré-Andronov-Hopf ونعطي الصيغة الواضحة لمعاملLyapunovالأول. نطبق نتائجنا على نماذج افتراس مختلفة. تُظهر صور فاز ثراء ديناميكيات النموذج المعتبر، على وجه الخصوص ، وجود بعض التشعبات الشاملة. علاوة على ذلك، نقدم لمحة عامة عن بعض الخصائص المهمة للنموذج المقترح، والتي سيتم تطويرها في المستقبل.
الكلمات المفتاحية: نموذج فريسة-مفترس، معيارRosenzweig-MacArthur البياني، معدل اختفاء متغير،استقرار، تشعبPoincaré-Andronov-Hopf ، أنظمة بطيئة- سريعة.